2-2013

Molecular and Population Level Approaches to Understand Taxus Metabolism in Cell Suspension Cultures

Rohan Anil Patil

University of Massachusetts Amherst, rohan85.patil@gmail.com

MOLECULAR AND POPULATION LEVEL APPROACHES TO UNDERSTAND

TAXUS METABOLISM IN CELL SUSPENSION CULTURES

A Dissertation Presented

by

ROHAN A. PATIL

Submitted to the Graduate School of the

University of Massachusetts Amherst in partial fulfillment

of the requirements for the degree of

DOCTOR OF PHILOSOPHY

FEBRUARY 2013

Department of Chemical Engineering

MOLECULAR AND POPULATION LEVEL APPROACHES TO UNDERSTAND

TAXUS METABOLISM IN CELL SUSPENSION CULTURES

A Dissertation Presented

by

ROHAN A. PATIL

Approved as to style and content by:

_____

Susan C. Roberts, Chair

_____

Elsbeth L. Walker, Member

_____

Neil S. Forbes, Member

_____

T.J. Mountziaris, Department Head

Department of Chemical Engineering

DEDICATION

To my family

ACKNOWLEDGEMENTS

I would like to deeply acknowledge the help and support of my advisor Prof. Susan C. Roberts in shaping my scientific abilities and this dissertation. Sue is an excellent mentor and provides an outstanding research environment in the group for graduate students to work and develop. I would like to thank Prof. Elsbeth Walker and Prof. Jennifer Normanly for their invaluable advice and constructive comments during the Taxol group meetings. I am grateful to Prof. Neil Forbes for being a very helpful committee member. I would like to thank all the past and present Roberts group members – Kyongsik Chin, Kham Vongpaseuth, Vishal Gaurav, Martin Kolewe, Whitney Stoppel, Sarah Wilson and Lisa Leone for being wonderful lab colleagues. In particular, I would like to thank Martin Kolewe for all the enlightening discussions we had within and outside the lab which has taught me a lot about research and kept me in good spirit for majority of my graduate studies. I would like to thank Dr. Lenka for his valuable contributions and collaboration during the last few years of my research. I would also like to thank Shana Passonno for all her useful suggestions and career related advice.

The stay here at Amherst is a significant portion of my life and I would like to thank all the people who I met here at UMass. I would particularly like to thank Naveen, Hitesh, John, Aniruddha, Chandrakant and Bhushan their friendship and making this stay a memorable experience. I would also like to acknowledge all the past and present colleagues in Elab-II for making my graduate life an enjoyable experience. Last but not the least, I would express my gratitude to my parents and family, who have supported me

in all my academic studies so far and have been a continuous source of encouragement and support to me. Their unconditional love has made me the person that I am today.

ABSTRACT

MOLECULAR AND POPULATION LEVEL APPROACHES TO UNDERSTAND

***TAXUS* METABOLISM IN CELL SUSPENSION CULTURES**

FEBRUARY 2013

ROHAN A. PATIL

B.Chem. Engg., THE INSTITUTE OF CHEMICAL TECHNOLOGY, MUMBAI

Ph.D., UNIVERSITY OF MASSACHUSETTS AMHERST

Directed by: Professor Susan C. Roberts

Plant cell culture is an attractive platform technology for production and supply of important plant derived medicinals. A unique characteristic of plant cells is the ability to grow as multicellular aggregates in suspension. The presence of these non-uniform aggregates results in creation of distinct microenvironments, which can induce variations in cellular metabolism (e.g., growth, oxygen consumption and secondary metabolite synthesis). This heterogeneity can lead to unpredictable and suboptimal performance in large scale bioprocesses. One example is the *Taxus* cell culture system, which produces a widely used chemotherapeutic drug – paclitaxel (Taxol ®). Despite extensive process engineering efforts which have led to increased yields of paclitaxel, *Taxus* cells exhibit variability in productivity that is poorly understood. Elicitation of *Taxus* cultures with methyl jasmonate (MeJA) induces the accumulation of paclitaxel, but to varying extents in culture. A significant negative correlation was observed between paclitaxel level and

mean aggregate size of the culture, demonstrating the relevance of measuring, and potentially controlling aggregate size during long term subculture.

Understanding the regulation of gene expression can provide rational engineering strategies to control variability and optimize performance of *Taxus* cell cultures. Biosynthetic pathway gene analyses revealed upregulation of genes upon elicitation with MeJA; results also suggested additional molecular regulatory points outside of the biosynthetic pathway. In order to fully understand *Taxus* molecular regulation and the relationship to paclitaxel production variability, a transcriptome-wide analysis using next generation sequencing (454 and Illumina) methods was performed. Several pathways outside of paclitaxel biosynthesis were found active upon MeJA elicitation. Global comparison of gene expression amongst cultures accumulating different levels of paclitaxel is being performed to completely understand the interactions amongst the paclitaxel biosynthetic pathway and other complimentary and competing pathways to suggest effective targets for metabolic engineering. This work collectively represents the first molecular studies to understand metabolic regulation in *Taxus* cell cultures.

Apart from inducing paclitaxel biosynthesis, MeJA decreases cell growth in *Taxus* cell cultures. The MeJA-mediated repression of cell growth was shown to correlate with inhibition of cell cycle progression as evident both at the culture level through flow cytometric analyses and at the transcriptional level by repression of key cell cycle-associated genes. Results from this study provide valuable insight into the mechanisms governing MeJA perception and subsequent events leading to repression of *Taxus* cell growth.

TABLE OF CONTENTS

LIST OF TABLES

LIST OF FIGURES

Figure   **Page**

CHAPTER 1
INTRODUCTION AND BACKGROUND

1.1 Introduction

1.1.1 Production routes for plant-based products

Traditionally, valuable plant derived phytochemicals, also referred to as secondary metabolites, have been obtained either by natural harvestation or chemical synthesis. Natural harvestation necessitates destroying the whole plant or selectively harvesting specialized organs; this makes the process expensive, time-consuming and environmentally unfriendly (McCoy and O'Connor 2008). These issues are compounded further with slow growing, rare or endangered plants, as well as medicinal plants growing in remote areas (Hawkins 2008). Total or partial chemical synthesis is economically viable only for production of relatively simple structures such as aspirin and ephedrine (Li et al. 2010), but impractical for secondary metabolites with complex structures, such as multiple rings and chiral centers (Chemler and Koffas 2008). Over the past decade, genetic engineering approaches to transfer plant pathways into microbial hosts have provided a competitive alternative for production of certain plant natural products (e.g., artemisinin synthesis in *E. coli* (Martin et al. 2003) and *S. cerevisiae* (Ro et al. 2006). Microbial fermentation processes are well-established and offer the advantages of rapid doubling times, shorter production times, easier extraction of the final product, and inexpensive feed stocks for growth. While a number of plant proteins have been heterologously expressed in microbial hosts (Yesilirmak and Sayers 2009), only a handful of plant natural products have been completely produced in microbes (Alper et al. 2005; Ro et al. 2006). Production of a non-native compound in microbes requires

1

identification and successful transfer of all the relevant plant biosynthetic pathway genes. For a number of plant-derived natural products (e.g., paclitaxel), the metabolic pathways leading to product formation *in planta* are very complex, and are either partially or completely unknown (Croteau et al. 2006). Even after a complete pathway for a particular natural product has been identified, production in prokaryotic hosts is still complicated, as they lack cellular compartmentalization that may be necessary for spatial and temporal partitioning of intermediates en route to final product (Vongpaseuth and Roberts 2007; Wu et al. 2006). Technical drawbacks associated with functional expression of native plant enzymes such as cytochrome P450s (Chemler and Koffas 2008) further impede efficient transfer of a complete biosynthetic pathway for production of a desired compound. Thus, despite the attractiveness of synthesis in microbial hosts, significant engineering challenges remain for more complex secondary metabolites.

The use of plant based *in vitro* systems for production of specific secondary metabolites provides an attractive alternative to natural harvestation, chemistry-based routes, and microbial engineering (Rao and Ravishankar 2002; Kolewe et al. 2008; Wilson and Roberts 2011). *In vitro* culture of plant cells is a mature technology with several decades of success, and can be applied to almost any plant species (Wink et al. 2005). As well as offering a realistic option for large scale production of secondary metabolites, *in vitro* plant cultures offer a controlled and regulated environment for studies of growth, metabolism, cell-environment interactions, and for establishment of superior plant varieties through genetic manipulation.

1.1.2 *In vitro* plant culture

In vitro culture of plants or plant cells can involve various degrees of differentiation. Whole plants or seedlings, organ cultures, or dedifferentiated suspension cultures propagated from callus can be grown aseptically in a defined culture media. These different types of *in vitro* cultures (see Figure 1.1 for *Taxus* species) can be interconverted using established techniques, most of which rely on specific phytohormone concentrations. Differentiated plant cell cultures, specifically organ cultures such as roots and shoots, have been shown to accumulate significant levels of secondary metabolites, often comparable with levels quantified in the whole plant (Roberts and Wink 1998; Matkowski 2008). In particular, hairy root cultures, obtained by transforming root cultures with *Agrobacterium rhizogenes*, have been promising for increased capacity of secondary metabolite production (Srivastava and Srivastava 2007). Several medicinal compounds belonging to the alkaloid, terpenoid and phenolic families have been produced successfully in hairy root cultures. Examples include resveratrol in *Arachis hypogaea*, artemisinin in *Artemisia annua*, indole alkaloids in *Catharanthus roseus*, and camptothecin in *Camptotheca acuminate* and *Ophiorrhiza pumila* (Ono and Tian 2011). Although many promising reactor designs exist at the small scale, it has been difficult to scale-up differentiated cultures to large-sized bioreactors primarily due to issues with nutrient delivery, limiting the wide-spread commercial application of this technology (Mishra and Ranjan 2008; Georgiev et al. 2007).

On the other hand, dedifferentiated suspension cultures can be maintained in batch, semi-continuous or continuous environments, and are more amenable to scale-up than hairy root cultures or other differentiated organ cultures (Kieran et al. 1997). Plant

cell suspension cultures under strictly controlled conditions provide a rapid and flexible means for production of desired compounds and a number of processes have been commercialized for the production of secondary metabolites (reviewed in (Eibl R 2002) and (Kolewe et al. 2008)) including ginseng, shikonin and berberine . The bioprocessing principles applied to the culture of microbial and mammalian cells also apply to dedifferentiated plant suspension cells (Hellwig et al. 2004); although plant cell culture technology has lagged behind equivalent fermentation/culture systems for microbes, yeast and animal cells (Evans et al. 2003; Hellwig et al. 2004).

1.1.3 Challenges to *in vitro* plant culture

Table 1.1 shows comparison of some of the characteristics of microbial, mammalian and plant cells of relevance to bioprocessing. Unlike other cell culture systems, dedifferentiated plant cells grow slower and are more easily damaged by traditional mechanisms for aeration and agitation that are required for culture maintenance and processing. Typically in microbial and mammalian systems, the growth phase and production phase are uncoupled, and hence optimal conditions for growth and production can be established and applied separately to maximize synthesis of the desired compound. For plant cell cultures, product accumulation is sometimes associated with the growth phase, and hence two-phase cultures are not always feasible (Roberts 2007). Plant cell cultures also tend to have poor genetic stability, which has been associated with aneuploidy and polyploidy, intra-chromosomal rearrangements, and single gene mutations (Cassells and Curry 2001; Phillips et al. 1994), hence affecting culture performance. In addition, many secondary metabolic pathways are only active in differentiated organs, leading to no or very low accumulation in dedifferentiated culture.

4

Even in cultures that successfully produce the compound of interest, yields are often low and variable (Ketchum and Gibson 1996; Roberts 2007). A number of strategies including strain improvement, selection of high-producing lines, medium optimization, elicitation with biotic or abiotic compounds, precursor addition, permeabilization, immobilization, and *in situ* extraction have been used with mixed success to increase metabolite yields to suitable levels for commercial production (reviewed in (Bourgaud et al. 2001; Dornenburg and Knorr 1995; Kolewe et al. 2008; Shuler 1999; Smetanska 2008; Verpoorte et al. 1999)). Long term variability in product yield over successive subcultures has often been observed (Deusneumann and Zenk 1984; Kim et al. 2004; Ogino et al. 1978; Qu et al. 2005). Relatively little research has been done to understand and ultimately control this variability in secondary metabolite production, which can have a considerable impact on the success of a commercial plant cell culture process. Plant cell culture bioprocessing and metabolism are complicated by the natural tendency of plant cells to form aggregates (Kieran et al. 1997; Roberts 2007). The causes and effects of cellular aggregation in plant cell cultures and its contribution to heterogeneity of cultures are described herein (see section 1.1.4).

Molecular approaches for engineering biosynthetic pathways within a plant cell offer great promise to enhance accumulation of constitutive compounds. However, such approaches are often infeasible due to i) lack of complete knowledge regarding secondary metabolic pathways and their regulation in most plant systems, ii) incomplete knowledge about global metabolism, such as product transport and degradation, and regulatory elements such as transcription factors for pathway genes or other signaling mechanisms, and iii) lack of metabolic engineering tools, such as reliable genetic transformation

methods. A brief overview on molecular approaches to understand secondary metabolism is described herein (see section 1.1.5). Understanding the reasons behind heterogeneity observed in plant cell cultures at a molecular level and applying targeted molecular approaches can lead to successful strategies to optimize and stabilize production, making plant cell culture a more attractive commercial technology for the supply of valuable plant-derived medicinal compounds.

1.1.4 Aggregation and heterogeneity in plant cell suspension cultures

Plant suspension cultures are initiated by placing pieces of dedifferentiated callus tissue in a liquid suspension, and maintained under suitable conditions of aeration, agitation, and other physical parameters. Depending on the friability of callus tissue, either single cells or small aggregates break off and start growing in the medium containing nutrients and growth hormones (Muir et al. 1954). During cell division, the dividing cells remain connected to each other via cell walls, and as a result, aggregates ranging from two to a few hundred cells exist in the culture.

The presence of aggregates during large scale culture affects mixing, as they tend to sediment and/or stick to the reactor surface, forming extensive wall growth. Moreover, large aggregates cause rheological problems by creating dead zones in the culture vessel, blocking the opening and pipe line of the reactor, and affecting the operation of the probes to monitor culture condition during growth and product formation. Cellular aggregation has also been found to be the primary reason for the high viscosities observed in a number of plant cell suspension systems (Kato et al. 1978; Doran 1999). These problems are further compounded during the later stages of growth, as plant cells

become stickier due to secretion of cell wall extracellular polysaccharides, causing additional clumping of aggregates.

In the context of morphological characteristics, cells within large aggregates are subject to different microenvironments with respect to light, oxygen and nutrient availability, cell to cell signaling, and applied surface shear forces. This often leads to biochemical and morphological heterogeneity in the cultures, with some aggregate populations exhibiting different characteristics.

1.1.4.1 Effect of aggregation on typical culture parameters

1.1.4.1.1 Aggregation and growth

Plant cells grown in batch culture increase in biomass by cell division until the depletion of an essential nutrient sends them into a stationary phase. Multiple analyses of changes in aggregate size distribution in a batch culture indicate that aggregate size increases during the exponential phase of the growth, and decreases during the stationary phase (Capataz-Tafur et al. 2011; Kolewe et al. 2010; Mavituna and Park 1987; Ranch and Giles 1980; Scragg et al. 1987). Formation of aggregates occurs as a result of cell division, and hence aggregation increases during the period of maximal cell division (i.e. exponential phase). On the contrary, in the stationary phase, cells get released from the aggregates and there is reduced cell division, which leads to decrease in mean aggregate sizes.

There is no clear trend in the relation between mean aggregate size in a culture and the growth rate, and is very much species dependent. (Yang et al. 1994) showed that

once separated through sieves, finer (less aggregated) wheat suspension cultures had a higher growth rate than their larger aggregate counterparts. A similar observation was seen with the cultures of *Coffea arabica,* where the growth of cultures inoculated with smaller aggregates was significantly superior to those of large aggregate cultures (Dubuis et al. 1995). In contrast, studies in celery (Watts et al. 1984) and safflower (Hanagata et al. 1993) suspension cultures show that some degree of aggregation was necessary for rapid growth and cell division, and finer suspensions had a slower growth rate as compared to aggregated suspensions. (King et al. 1973) demonstrate that highly dispersed cultures obtained by incubation with enzymes show a growth pattern similar to the aggregated suspensions; indicating that cell aggregation is not essential for high rates of growth and division in cell suspension cultures.

1.1.4.1.2 Aggregation and oxygen consumption

Oxygen requirements in plant cells (typically 1- 4 mmol $l^{-1}h^{-1}$) are comparatively lower than microorganisms ($\sim$ 5-90 mmol $l^{-1}h^{-1}$), due to their lower growth rates (Kobayashi et al. 1989; Taticek et al. 1990; Hellwig et al. 2004). Oxygen supply is known to affect both growth and production of metabolites (Huang and Chou 2000; Linden et al. 2001). A number of bioreactors have been designed to study aeration effects in plant cell cultures, with the primary focus on mass transfer coefficients at the gas-liquid boundary (k_La) (Kieran et al. 1997). However, it has also been suggested that the solid-liquid boundary between an aggregate and the medium is far more constraining for the delivery of oxygen to the cell than the gas-liquid boundary (Curtis and Tuerk 2006). Oxygen enrichment of the gas phase can be used to minimize the oxygen limitation at this solid-liquid interface. In addition, suspension cultured plant cells must have significant oxygen transport within

the aggregate, to maintain aerobic respiration and desired growth rates. Due to these constraints there exists a critical aggregate size, above which oxygen limitation to the centermost cells may result. Relatively few studies have been done to study oxygen transport within aggregates, primarily because experimental measurement within the shear sensitive aggregates is difficult. Most of the work has been based on theoretical models developed to calculate the critical size of the aggregate which use a simple mass balance of oxygen (Hulst et al. 1989; Pepin et al. 1999). These models also assume a zero order reaction with known oxygen uptake rate, diffusion coefficient and dissolved oxygen concentration to calculate the concentration profile within an aggregate. These studies suggest that diffusion of oxygen is moderately restricted in the interior of aggregates of 1mm in diameter, and severe oxygen deficiencies are observed when the aggregates reach about 3 mm size. (Ananta et al. 1995) used diffusion-reaction theory to analyze the experimentally measured oxygen uptake rates in immobilized cultures of *Solanum aviculare*. Direct experimental measurement of the aggregate properties revealed that the critical aggregate size at which oxygen limitation actually occurs was much larger than that predicted by the theory. It was hypothesized that the plasmodesmata which interconnect cells within aggregates and the negative pressures created by the gas-filled cavities within the porous aggregates aids and promotes oxygen transfer, factors which were not accounted for in the theoretical analysis. The effects of oxygen limitation seem to be species dependent, with both increased (Schlatmann et al. 1995) and decreased (Hulst et al. 1989) secondary metabolite synthesis reported in large aggregates.

1.1.4.1.3 Aggregation and secondary metabolite accumulation

For recombinant protein production, cellular aggregation in plant suspension cultures is

usually considered undesirable as it complicates bioreactor operation. However, certain degrees of cell aggregation and cell differentiation seem to be desirable for secondary metabolite production in plant cell cultures (Becker 1970; Zhao et al. 2001). Aggregation causes changes in environmental conditions experienced by each cell in an aggregate, altering cellular metabolism and inducing differential biochemical responses. Activation of certain genes or enzymes involved in biosynthesis, transport or storage of secondary metabolites is possible (Hsu et al. 1993; Lindsey and Yeoman 1983). In some suspension cultures, cells do not just clump together, but form sophisticated differentiated structures in the culture (Ellis et al. 1996; Hoekstra et al. 1990; Kuboi and Yamada 1978; Xu et al. 1998; Zhao et al. 2001), which can often lead to higher levels of secondary metabolite accumulation. (Kuboi and Yamada 1978) showed that all the cells in tobacco suspension cultures had a uniform ability to form aggregates. However, the potential for tracheid differentiation in these studies was higher when the cells were located in the center of the aggregate, indicating that differentiation is a result of environmental circumstances, and not an inherited trait by particular cells.

To date, a number of studies have been attempted to understand the effect of cellular aggregation on secondary metabolite accumulation in cell cultures. However, there is no consensus across plant species, and the results seem to vary depending on the particular species and secondary metabolite. Table 1.2 indicates the relation between secondary metabolite accumulation and aggregate size for some plant cell culture systems. Larger aggregates have been shown to have a positive effect on secondary metabolite production, a positive effect up to a critical size, or a negative effect. This lack of trend in metabolite accumulation with aggregate size is not unexpected, as

10

fundamental differences exist amongst distinct plant species, and their metabolic pathways may be differentially regulated with varying conditions.

1.1.5 Molecular approaches to understand the regulation of secondary metabolism

Research efforts have led to identification of several precursor pathways necessary for the biosynthesis of secondary metabolites, including the polyketide pathways (for synthesis of fatty acids and polyketides), mevalonate and DXP pathways (for synthesis of terpenes), shikimate pathway (for synthesis of aromatic alkaloids, lignins and phenylpropanoids), polyamine pathway (for synthesis of aliphatic alkaloids) and mixed pathways where intermediates of two or more pathways act as substrates for secondary metabolites (e.g., terpene indole alkaloids). However, complete information on all the biosynthetic steps involved in secondary metabolite synthesis, and fundamental understanding concerning the regulation of secondary metabolism is still lacking for the majority of complex biosynthetic pathways. Therefore, optimal design strategies for enhancing productivity through pathway manipulation are presently elusive for most medicinal plant systems.

Genomics and post-genomics approaches can offer opportunities for understanding molecular regulation, ultimately leading to strategies to improve both yield and selectivity of secondary products. However, a lack of genome and transcriptome sequencing information for medicinal plants make the traditional metabolic engineering approaches infeasible for these systems. Efforts have been further thwarted by a lack of reliable transformation methods to introduce foreign genes, silence genes or overexpress constitutively-expressed genes. Nonetheless, progress has been made in recent years to

overcome some of these challenges (Verpoorte and Memelink 2002; Goossens et al. 2003; DellaPenna 2001; Kumar and Gupta 2008).

Identification of key metabolic targets (genes and enzymes) within a biochemical pathway is a prerequisite to manipulate the pathway and enhance constitutive levels of secondary metabolites. Several strategies including precursor feeding, elicitation to induce gene expression, application of metabolic inhibitors, analysis of a variety of strains, and quantification of mRNA expression, enzyme activities and metabolite profiles, have been used to identify unknown genes and characterize a number of secondary metabolic pathways. Recent molecular techniques such as cDNA-AFLP and differential display analysis have also been used to map unknown genes in key secondary pathways and correlate gene expression, enzyme function and metabolite production (Kumar and Gupta 2008). Integrating proteomics and metabolomics with genetic information will allow researchers to map, and subsequently better understand, these complex metabolic networks. Metabolic network information can be integrated into flux models to identify targeted metabolic engineering strategies (Verpoorte and Memelink 2002, Libourel and Shachar-Hill 2008).

Genetic engineering approaches for effective manipulation of secondary metabolite synthesis and accumulation in plants have been used effectively in several species, where stable transformation methods are readily available. Overexpression of genes encoding rate influencing pathway enzymes can improve the yields of native secondary metabolites. Successful examples include *Agrobacterium*-mediated transformation of several plant species to increase constitutive levels of alkaloids, phenylpropanoids and terpenoids (reviewed in (Gomez-Galera et al. 2007)). However,

single gene manipulation does not typically improve yield to appreciable levels, and several novel genetic engineering approaches such as redirecting carbon flux from a common precursor, targeting metabolites to specific cellular compartments, creation of metabolic sinks for storage of high yielding secondary metabolites, and RNA interference (RNAi) technology to silence competing pathway steps, have been developed (Kumar and Gupta 2008; Gomez-Galera et al. 2007). These approaches have been used to engineer a limited number of secondary metabolic pathways in a small number of medicinal plants.

Transcription factors offer much promise for the manipulation of metabolic pathways because of their ability to control multiple pathway steps that are necessary for metabolite accumulation. Key transcription factors for secondary metabolite synthesis have been identified in *Arabidopsis thaliana* and *Catharanthus roseus* (Gigolashvili et al. 2007; van der Fits and Memelink 2000); however, presence of such global transcription factor/s have not been identified for other significant medicinal plant species such as *Taxus*. Although manipulating the expression of specific transcription factors can modulate pathway flux, oftentimes it is important to increase either precursor availability or introduce multiple transcription factors (James 2003; Pierre 2004), indicating differential regulation on separate branches of the pathway.

Sequencing of genomes and transcriptomes of model plant species (Arabidopsis) and major agricultural crops (rice, maize, sorghum, etc.) have considerably improved our understanding of primary metabolic processes of plants. However, these results have not been directly applicable to enhance our understanding of secondary metabolic pathways, primarily because these pathways are active in only a handful of specialized plant

species, and are not very well conserved across the plant kingdom. However, progress is being made to generate resources for understanding the genes, enzymes and complex processes responsible for the biosynthesis of important plant-derived drugs from fourteen medicinal plant species including *Atropa belladonna*, *C. roseus*, *Digitalis purpurea*, *Hypericum perforatum*, *Rosmarinus officinalis*, *Camptotheca acuminata, Cannabis sativa, Ginkgo biloba, Dioscorea villosa, Echinacea purpurea, Hoodia gordonii, Panax quinquefolius, Rauvolfia serpentina* and *Valeriana officinalis* (http://medicinalplantgenomics.msu.edu/). Once available, the Medicinal Plant Genomic and Metabolomic Resource will provide a valuable resource of transcriptomes and associated metabolomes for key plant species. These data will ultimately advance our understanding on several species-specific metabolites and provide novel information about the genes and metabolites of medicinal compound synthesis. Even though these efforts have been initiated with a number of medicinal plant species, the *Taxus* species, which produces a pharmaceutically relevant drug – paclitaxel and which is the subject of the work in this thesis, is not included in this limited list.

1.1.6. Paclitaxel production in *Taxus* suspension cultures

1.1.6.1 Paclitaxel

Paclitaxel, (Taxol®, Bristol-Myers-Squibb) (Figure 1.2) a diterpene found in various tissues of *Taxus* species belongs to a family of plant secondary metabolites known as taxoids. It was discovered during the massive bio-screening program initiated by the National Cancer Institute (NCI) in which more than 110,000 plant derived compounds were examined for anti-cancer activity (Horwitz 2004). In the 1960's, Wall and Wani

isolated this highly substituted ring diterpenoid from extracts of *Taxus brevifolia*, a Pacific yew tree which had demonstrated anti-cancer activity. Subsequently, the chemical structure of paclitaxel was published (Wani et al. 1971). A few years later, the unique cytotoxic mechanism of action of paclitaxel was discovered, which paved the way for paclitaxel to move into clinical trials on humans. Early clinical trials were conducted by the NCI and results were very promising. After several phases of clinical trials, in 1994 Bristol-Myers-Squibb entered into a collaborative arrangement with the NCI to commercialize paclitaxel. Thereafter, it has been used as a potent chemotherapeutic agent and the Food and Drug Administration (FDA) has approved its use in the treatment of breast, ovarian, non-small cell lung cancer and AIDS-related Kaposi's sarcoma (www.fda.gov). It is also under evaluation for the treatment of Alzheimer's and heart disease (Vongpaseuth and Roberts 2007; Kamath et al. 2006).

1.1.6.2. Paclitaxel supply and *Taxus* cell culture

Taxus suspension cell culture is an alternative to stripping bark from *Taxus* trees and extracting paclitaxel and precursors from needles, and has been commercialized by Phyton Biotech. Inc. (Germany) and Samyang Genex Corp. (Korea) for the supply of paclitaxel (Tabata 2004). Total synthesis of paclitaxel has been achieved (Borman 1994), however low yield and non-green chemistry has hindered efforts to produce paclitaxel synthetically. Genetic engineering of paclitaxel biosynthetic pathway into *E. coli* offers advantages such as green chemistry, cheaper sources and larger production scale (Chang et al., 2006). However, to date only two out of 19 paclitaxel biosynthetic enzymatic steps have been successfully engineered in *E. coli* (Ajikumar et al. 2010). A daunting task of transferring all the paclitaxel biosynthetic pathway steps (Figure 1.3), of which some

steps are partially undefined, still remains before this production route can be considered viable for large scale paclitaxel supply.

With the commercial success of paclitaxel production using plant cell culture technology, the feasibility of large scale culture of plant cells for commercial supply of medicinal phytochemicals has been demonstrated. Different strategies have been used to enhance productivity of paclitaxel in plant cell cultures, including: precursor feeding (Fett-Neto et al. 1994), *in situ* extraction (Zhang and Xu 2001), media optimization (Verpoorte and Memelink 2002), and elicitation with biotic and abiotic elicitors (Wu and Lin 2003). In particular, methyl jasmonate (MeJA) elicitation has been particularly effective in enhancing paclitaxel yields in *Taxus* suspension cultures (Mirjalili and Linden 1996; Yukimune et al. 1996; Ketchum et al. 1997), and numerous secondary metabolites in a variety of other plant cell culture systems (Gundlach et al. 1992). However, along with high product yields, a high degree of biochemical and physiological stability is important for development of optimal plant cell culture processes (Morris et al. 1989). Although accumulation of some secondary metabolites has been found to be stable over time (Zenk et al. 1977), there are numerous occasions where variability in product accumulation has been observed (Kim et al. 2004; Qu et al. 2005). Taxane accumulation in *Taxus* cell cultures has been shown to be variable within different species (Kim et al. 2004), and over time within a single cell line (Ketchum and Gibson 1996). Relatively little research has been done to understand and control this variability in secondary metabolite production in cell suspension cultures, which can have a considerable impact on the success of a plant cell-based bioprocess.

1.1.6.3 Previous work on aggregation in *Taxus* cell cultures

Taxus cells like most other plant cell culture systems grow as aggregates in suspension cultures ranging from two to thousands of cells (less than 100 μm to well over 2 mm). Figure 1.4 shows typical aggregates found in *Taxus* suspension cultures. Several methods exist to measure the aggregate size distribution within the culture including, wet sieving and dry weight measurements, image analysis, focused beam reflectance method (FBRM) and coulter counter technique. A study was conducted that tested several different methods for characterizing aggregate size in *Taxus* suspension cell cultures, and it was found that the Coulter counter was just as accurate, if not more accurate at measuring size distributions and total biomass than filtration or image analysis (Kolewe et al. 2010). Over the course of a batch culture, the mean aggregate size of the *Taxus* culture increased during exponential growth phase, but this trend reversed once the culture reached stationary phase. Figure 1.5 shows the general changes in biomass and mean diameter of aggregates during the growth cycle of *Taxus cuspidata* cells in suspension culture.

The majority of studies aimed at investigating the relationship between aggregate size and secondary metabolite accumulation separate differently sized aggregates using a series of sieves or filters, followed by measurement of secondary metabolites. In most cases the cultures were allowed to accumulate secondary metabolites (either by elicitation or through some stress mediated response) and then fractionated to measure cell-associated metabolite levels. Though straightforward, this method of fractionation using sieves neglects the metabolites secreted in the medium. In contrast, some studies including one in *Taxus* cell cultures were done by altering the aggregate size distribution at the time of culture initiation (Kolewe et al. 2011; Hanagata et al. 1993; Kinnersley and

Dougall 1980). In these studies, cultures were fractionated on the day of inoculation and made to grow independently as small and large aggregates, followed by measurements of total metabolite accumulation (cell-associated and secreted in medium) as a function of aggregate size. The results from the *Taxus* suspension culture system indicated that cultures initiated from smaller aggregate cultures had higher levels of paclitaxel than their counterpart large aggregate cultures. The results from these studies thus suggest a possible process optimization strategy, in which rational manipulation of aggregate size at culture initiation can lead to high yielding cell lines, and in due course can facilitate economically viable sources for secondary metabolites.

1.1.6.4 Molecular approaches to understand *Taxus* metabolism

Significant early work to identify paclitaxel biosynthesis enzymes and pathway genes was initiated by Croteau and colleagues at Washington State University using precursor feeding experiments, cell-free enzymology, cDNA library construction and pathway gene cloning (Croteau et al. 2006). Further studies to identify cDNAs encoding the cytochrome P450s in the paclitaxel biosynthetic pathway were done using mRNA differential display methods by comparison of transcripts between MeJA-elicited and unelicited *Taxus* cells (Schoendorf et al. 2001). These studies were supplemented with a homology-based search of a cDNA library from MeJA-elicited cells, as well as random sequencing of the same induced library (Jennewein et al. 2004) to find potential paclitaxel pathway genes. A comprehensive review on the studies used to reveal the steps involved in the biosynthesis of paclitaxel is reported elsewhere (Croteau et al. 2006).

Efforts to understand regulation of the taxane biosynthetic pathway in *Taxus* cultures have been initiated in our laboratory, in collaboration with both the Walker and Normanly groups at UMass Amherst. Research indicates that regulation occurs at the level of mRNA, and upregulation of late pathway genes may be effective in enhancing paclitaxel accumulation in *Taxus* cell suspension cultures (Nims et al. 2006). However *Taxus* suspension cultures are highly heterogeneous, leading to significant variability in metabolite accumulation levels amongst cultures and over time. To fully understand how this variability is controlled, molecular information relevant to both the paclitaxel pathway and general *Taxus* primary and secondary metabolism are necessary. Comparison of gene expression amongst cultures that accumulate paclitaxel/taxanes to varying extents can aid in identification of key pathways responsible for regulating paclitaxel accumulation. Because regulation is likely to occur at least in part outside of the biosynthetic pathway, other metabolic events need to be considered. An integrated approach consisting of gene-to-gene and gene-to-metabolite networks, as developed for terpenoid indole alkaloid metabolism in *C. roseus* cell cultures (Rischer et al. 2006) will provide a basis for better understanding of paclitaxel metabolism in *Taxus* cell cultures.

1.2 Research objectives

The work presented in this dissertation aims to better understand metabolic heterogeneity in *Taxus* suspension cultures from both a molecular and cellular perspective, which can help uncover some of the underlying causes for variability in paclitaxel yields and better understand heterogeneity in *Taxus* cell cultures. Such information can ultimately be used to optimize performance (i.e., promote growth and enhance secondary metabolite

accumulation) of plant cell cultures. Research towards this overarching objective can be categorized as follows:

- ➢ Long term paclitaxel production variability analysis in *Taxus* cell cultures (Chapter 2).

- ➢ Molecular approaches to understand *Taxus* cell cultures exhibiting metabolic heterogeneity

  - - Expression profiling of taxane biosynthetic pathway genes in *Taxus* cell cultures with different bulk paclitaxel accumulation patterns (Chapter 3).

  - - Transcriptome analysis of *Taxus* cell cultures exhibiting differences in paclitaxel accumulation and aggregation patterns using next generation sequencing methods (Chapter 4).

- ➢ Uncovering the link between primary and secondary metabolism in MeJA-elicited *Taxus* cell cultures by studying the effect of MeJA addition on metabolism and cell cycle progression (Chapter 5).

Table 1.1 A comparison of key characteristics of microbial, mammalian and plant cells relevant to bioprocessing.

Characteristic	Bacterial cells	Mammalian cells	Plant cells
Size	~ 1 µm	~ 10 µm	~ 20-50 µm
Doubling time	< 1 hour	~ 1 day	Several days
Shear sensitivity	Insensitive	Sensitive	Sensitive
Oxygen demand	High	Low	Medium
Product accumulation	Typically extracellular	Typically extracellular	Often cell-associated
Production phase	Uncoupled with growth	Uncoupled with growth	Often growth associated
Variability in accumulation	Low	Low	High
Contamination risk	Low	High	Low
Cell line stability	High	Low	Medium
Product yields	High	High	Low
Post translational processing	Simple	Advanced	Advanced
Compartmentalization	None	Compartmentalized	Compartmentalized
Cryopreservation techniques	Well-developed	Well-developed	Immature

Table 1.2 Relationship between aggregate size and secondary metabolite accumulation in various plant cell culture systems.

System	2º Metabolite	Effect of increasing aggregate size on metabolite accumulation	Reference
Fragaria ananassa (strawberry)	Anthocyanin	Increased	(Edahiro and Seki 2006)
Apium graveolens L. (celery)	Phthalides and Terpenoids	Increased	(Watts et al. 1984)
Catharanthus roseus (periwinkle)	Ajmalicine	No clear trend	(Kessler et al. 1999)
Salvia officinalis (sage)	Ursolic acid	Decreased	(Bolta et al. 2003)
Daucus carota (carrot)	Anthocyanin	Decreased	(Kinnersley and Dougall 1980)
Vaccinium pahalae (ohelo)	Anthocyanin	Decreased	(Pepin et al. 1999)
Carthamus tinctorius L. (safflower)	Anthocyanin	Decreased	(Hanagata et al. 1993)
Taxus cuspidata (yew)	Paclitaxel	Decreased	(Kolewe et al. 2011)

Daucus carota (carrot)	Anthocyanin	Increased up to critical diameter, then decreased	(Madhusudhan and Ravishankar 1996)
Saussurea medusa (snow lotus)	Jaceosidin	Increased up to critical diameter, then decreased	(Zhao et al. 2003)
Tagetes patula (marigold)	Anthocyanin	Increased up to critical diameter, then decreased	(Hulst et al. 1989)

Figure 1.1 Three different types of *in vitro* culture for *Taxus*. **(A)** callus culture, **(B)** hairy root culture (Syklowska-Baranek et al. 2009), and **(C)** suspension culture.
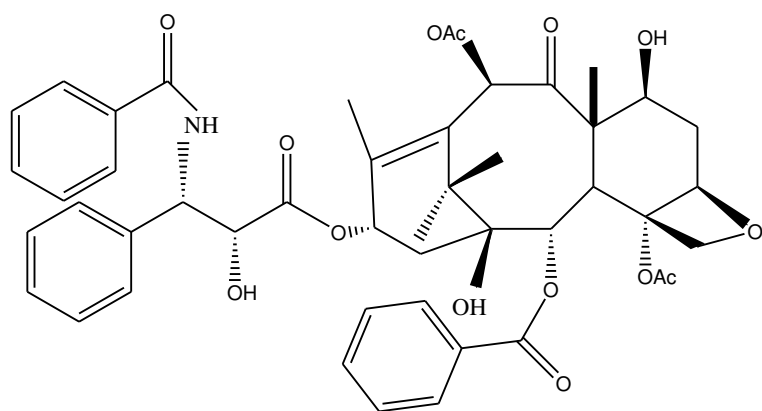
Figure 1.2 Chemical structure of paclitaxel.
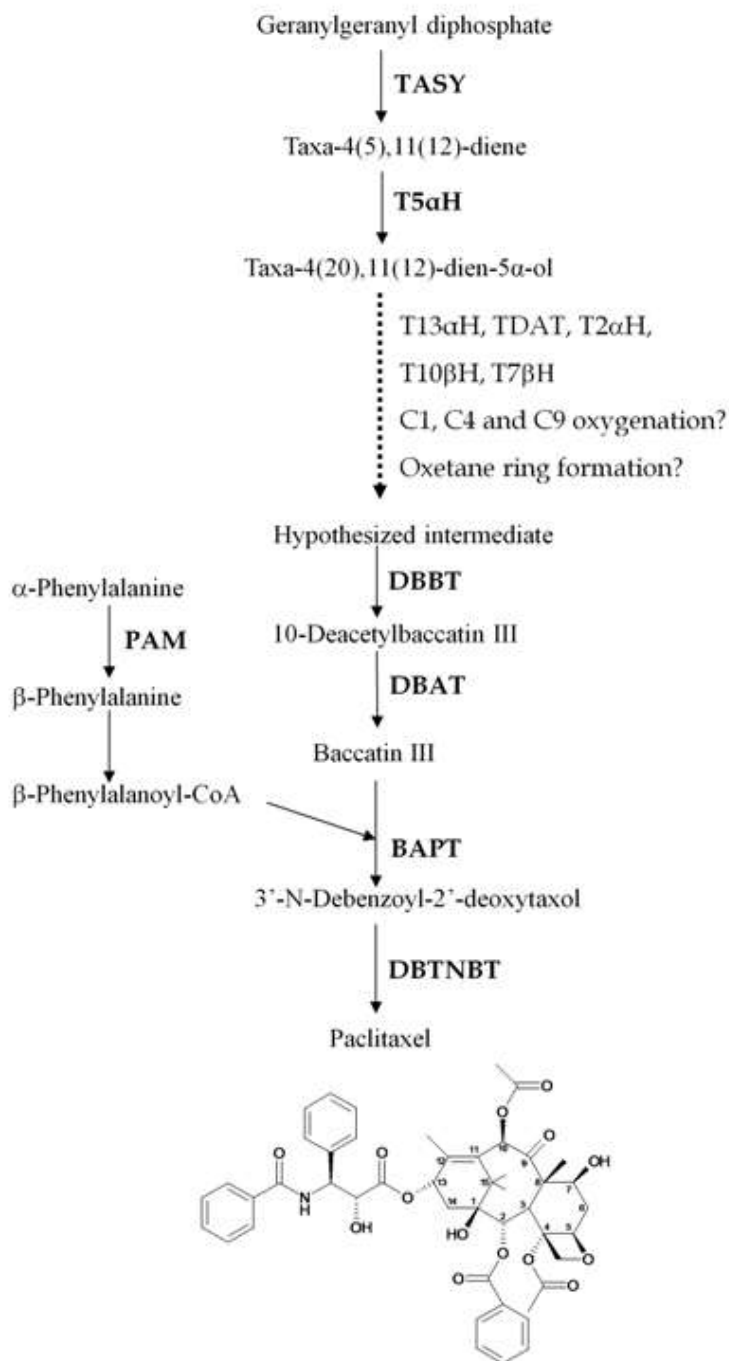
Figure 1.3 Overview of the paclitaxel biosynthetic pathway. Abbreviations indicate enzymes. TASY: taxadiene synthase; T5αH: taxadiene 5α-hydroxylase; T13αH: taxadiene 13α-hydroxylase; TDAT: taxadiene 5α-ol O-acetyltransferase; T2αH: taxane

2α-hydroxylase; T10βH: taxane 10β-hydroxylase; T7βH: taxane 7β-hydroxylase; DBBT: taxane 2α-O-benzoyltransferase; DBAT: 10-deacetylbaccatin III-10-O-acetyltransferase; PAM: phenylalanine aminomutase; BAPT: baccatin III 13-O-(3-amino-3-phenylpropanoyl) transferase; DBTNBT: 3'-N-debenzoyl-2'-deoxytaxol-N-benzoyltransferase. Question marks indicate incompletely known steps.
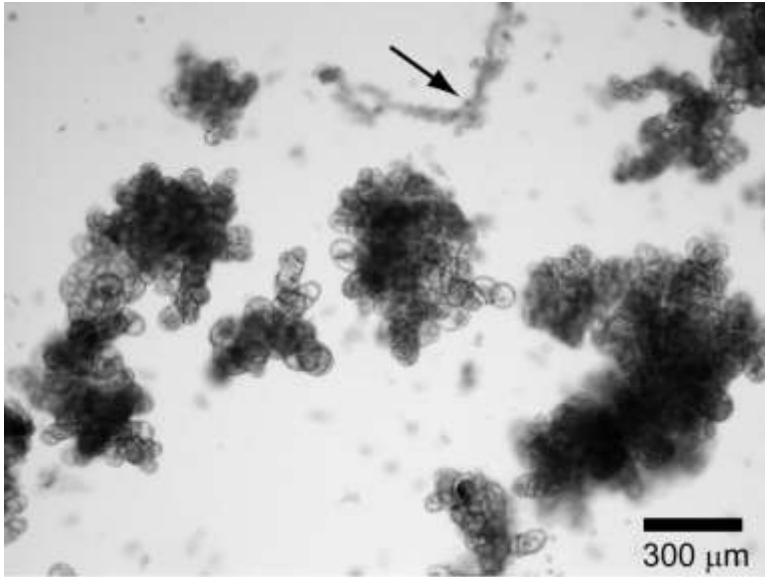
Figure 1.4 Characteristic aggregates observed in *T. cuspidata* P93AF cell suspension cultures. Arrow indicates typical morphology of cellular debris.
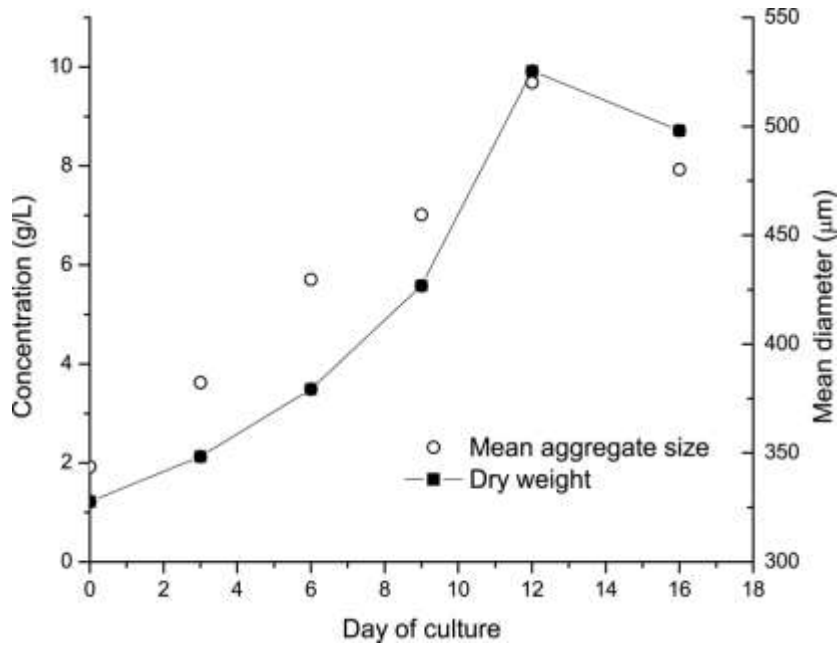
Figure 1.5 Increase in cell biomass and mean aggregate size during exponential growth in *Taxus* cell cultures (Adapted from (Kolewe et al. 2010)).

CHAPTER 2
CELLULAR AGGREGATION IS A KEY PROCESS PARAMETER ASSOCIATED WITH LONG TERM VARIABILITY IN PACLITAXEL ACCUMULATION IN *TAXUS* SUSPENSION CULTURES

2.1 Introduction

In spite of the demonstrated effectiveness and past successes of plant-based natural products, particularly as chemotherapeutics (Cragg et al. 2009), pharmaceutical companies have had a declining interest in screening for natural products over the past couple of decades (McChesney et al. 2007; Harvey 2008). One of the primary reasons for this decline is the issue of drug product supply, including the economic considerations pertaining to commercialization of a particular supply route. Plant suspension cell culture technology has proven successful for the synthesis of natural products in a controlled environment, with several products supplied commercially at a large scale (Eibl and Eibl 2002; Kolewe et al. 2008). Nevertheless, the use of plant cell suspension culture technology has been hampered by the periodic fluctuations in metabolite levels, often observed in suspension cultures over multiple passages (Roberts 2007; Lee et al. 2010). Inconsistent cell culture product titers and flask to flask variations over passages can complicate the development of an economically viable cell culture bioprocess. Freezing and regenerating high-producing plant cell lines using cryopreservation techniques can alleviate such issues created during culture passage, and this approach has been successfully demonstrated for several plant species (Reinhoud et al. 1995; Ishikawa et al. 2006). However, cryopreservation of plant cells is not a widely established technique, because cryopreservation protocols and parameters such as pretreatment/preculture,

freezing and post-thaw/regeneration have to be adapted and optimized for each plant species and cell line (Mustafa et al. 2011). Even if an optimized cryopreservation protocol exists for a species, post-thaw viability, growth and performance, and the issue of preserved cell lines differing from original ones hinder application of such methods (Boisson et al. 2012; Zeliang et al. 2010). Elicitation using abiotic or biotic compounds, such as jasmonic acid, is often used to enhance accumulation of secondary metabolites in suspension cultures (Gundlach et al. 1992; Suzuki et al. 2005; Pauwels et al. 2008; Krzyzanowska et al. 2012). Though elicitation increases culture metabolite yields, fluctuations in metabolite levels of *Taxus* cultures over multiple passages post-elicitation are observed (Kim et al. 2004).

Several studies in a variety of plant cell culture systems have reported fluctuations in secondary metabolite levels over culture passages (Callebaut et al. 1997; Qu et al. 2005; Hirasuna et al. 1991; Morris et al. 1989; Deusneumann and Zenk 1984). Genetic and epigenetic instabilities have generally been suggested as the primary causes for such variability (Qu et al. 2005; Zhao and Verpoorte 2007). Several other hypotheses have emerged to explain the observed variability including, development of heterogeneous populations in cell culture, amongst which only certain productive cells accumulate secondary metabolites (Hall and Yeoman 1986), changes in inter- and intracellular communication amongst cells (Hall and Yeoman 1987), and the influence of environmental factors (e.g., light, temperature, pH) or process parameters (e.g., oxygen levels, agitation) (Yeoman and Yeoman 1996; Saito and Mizukami 2002). Variability in secondary metabolite yield may also be created by inadequate control of factors such as initial cell density and time of inoculation during routine culture passage (Morris et al.

31

1989; Kolewe et al. 2008). Understanding the factors that influence fluctuations in secondary metabolite levels can aid in the design of improved bioprocessing strategies.

The tendency of plant cells to remain connected via cell walls and form aggregates has a considerable effect on bioprocess performance, including growth and metabolite levels (Patil et al. 2012; Capataz-Tafur et al. 2011). *Taxus* cell suspension cultures, which produce the valuable secondary metabolite paclitaxel, consist of aggregates ranging from 100 μm to over 2000 μm (Kolewe et al. 2010) (Fig.1). Recent studies from our laboratory indicate that the degree of cellular aggregation in *Taxus* cultures affects the level of paclitaxel accumulation (Kolewe et al. 2011). These results demonstrated the relationship between aggregate size and paclitaxel accumulation within individual experiments (Kolewe et al. 2011, Patil et al. 2012), but did not address long-term culture passage. Because plant cell cultures are typically maintained by non-selective culture passage over extended periods of time, an explicit relationship between aggregation patterns and corresponding secondary metabolite levels over multiple passages is important and can be used to suggest strategies for superior culture performance.

Inconsistencies during the culture passage procedure can cause changes in growth rate or affect the lag period such that cells in the next passage may be different metabolically with respect to both growth and metabolite production (Morris et al. 1989). Monitoring cell cycle distribution provides a useful means to understand the cell division potential of the cultures (Yanpaisan et al. 1999). Cultures with a high percentage of G2 phase cells have higher frequency of cell division. Secondary metabolite synthesis is often associated with differentiation of plant cells, which occurs after arrest of cells at the

G1 or G2 phase (Bergounioux et al. 1992). Thus, monitoring cell cycle distributions over time can provide information on differentiation characteristics of the cultures. Instability of nuclear DNA content, which is often observed in terms of induced polyploidy or aneuploidy, is frequently observed in plant cell suspensions (Baebler et al. 2005; Creemers-Molenaar et al. 1992). Variable ploidy levels have also been shown to affect secondary metabolite production in seedlings of *Hypericum perforatum* (Kosuth et al. 2003),hairy root cultures of *Artemisia annua* (De Jesus-Gonzalez and Weathers 2003) and *Hyoscyamus muticus* (Dehghan et al. 2012). Studies on genomic stability of *Taxus* cell cultures immediately following culture initiation (two-year timeframe) have been reported (Baebler et al. 2005) and indicate heterogeneity in genomic stability amongst cell lines; however, paclitaxel levels have not been correlated to nuclear DNA content or ploidy levels in well-established *Taxus* suspension cultures.

Here, the variation in aggregate size, extracellular sugar concentration, ploidy, and proportion of cells in particular phases of the cell cycle were quantified and correlated with paclitaxel accumulation over multiple passages (six months). Factors such as media composition, inoculation density, day of culture passage and cultivation temperature, which are known to influence secondary metabolite levels (Zhong et al. 1995; Qu et al. 2006), were kept constant. Determining factors that correlate with variable paclitaxel yields over long-term passage can lead to the development of new bioprocessing strategies to favorably control paclitaxel accumulation in *Taxus* suspension cell cultures.

2.2 Materials and methods

2.2.1 Cell culture maintenance, elicitation and biomass measurements

Taxus cuspidata cell line P93AF was provided by the U.S. Plant Soil and Nutrition Laboratory in Ithaca, NY, and maintained in our laboratory, as described previously (Naill and Roberts 2004). Suspensions were maintained in 250 mL Erlenmeyer flasks capped with Bellco (Vineland, NJ) foam closures at 23 ^{o}C and 125 RPM in gyratory shakers in the dark. For each culture passage, six replicate cultures were generated. Three cultures were sacrificed for analyses and three cultures were passaged to six new flasks for the next cycle. Culture passages were performed by transferring 20 mL of inocula (corresponding to a packed cell volume of 4-5 mL) originating from a 14-day old suspension culture into 80 mL of fresh medium. A Multisizer 3^{TM} Coulter counter equipped with a 2,000 μm aperture (Beckman Coulter, Brea, CA) was used to measure biomass and culture aggregate size distributions, as described previously (Kolewe et al. 2010). For Coulter counter analysis, two x 2 mL samples of well mixed culture broth from each of the three replicate flasks were collected on day 7. Samples for extracellular sucrose and glucose analyses and nuclei isolation were also taken on day 7 (described below). Post-sampling, cultures were treated with 150 μM methyl jasmonate (MeJA), as described previously (Naill and Roberts 2004). Following MeJA elicitation, 1 mL samples of well mixed culture broth containing both cells and media were taken on day 7 post-elicitation (day 14 in the cell culture passage) with a cut pipette tip and stored at -80 ^{o}C prior to taxane analysis (described below).

2.2.2 Glucose and sucrose measurements

The levels of extracellular sucrose and glucose were measured in cell culture media samples using a blood glucose analyzer (YSI 2700 Select Biochemistry Analyzer, YSI Life Sciences, Yellow Springs, OH). For analysis, 500 μl of cell culture media was collected on day 7 post-transfer. Briefly, dextrose (D-glucose) diffuses across a membrane (that contains glucose oxidase) in the analyzer. This reaction oxidizes the dextrose to hydrogen peroxide and D-glucono-δ-lactone. The hydrogen peroxide is amperometrically detected at a platinum electrode surface. The current produced is directly proportional to the hydrogen peroxide and dextrose concentrations in the sample. Sucrose is indirectly measured through enzymatic hydrolysis.

2.2.3 Isolation of intact nuclei for ploidy and nuclear DNA content analyses

Approximately 3-4 mL of well mixed culture broth (corresponding to 0.5 g wet biomass) was filtered over Miracloth (Calbiochem, CA) and used for isolation of intact nuclei (Gaurav et. al 2010). Samples were taken after every two passages. Briefly, one mL of Galbraith buffer (45 mM $MgCl_2$, 30 mM sodium citrate, 20 mM 3-(N-morpholino)-propanesulfonic acid (MOPS), 0.5 % (w/v) Triton X-100, pH 7.0) at 4 ^{o}C was added to the biomass sample on a petri dish (50 mm x 12 mm), and the biomass was chopped with a sharp razor approximately 500 times to disrupt cell walls and allow for the release of intact nuclei. An additional 2 mL of Galbraith buffer was added to resuspend the chopped biomass, and this suspension was successively filtered over 80 μm and 30 μm nylon mesh (SmallParts, Inc., Miramar, FL).

For ploidy and cell cycle analysis, 50 μl of 1 mg/mL RNAse and 50 μl of 1 mg/mL propidium iodide were added to 1 mL of the filtered nuclei solution. Samples were stained for 30-45 min. on ice before flow cytometric analysis (Becton Dickinson (San Jose, CA) LSRII analytical flow cytometer). Forward scatter and side scatter were collected on a logarithmic scale, and PI fluorescence was collected on a linear scale. A minimum of 5000 events was collected in the gated region of a forward scatter and side scatter plot corresponding to nuclei. For cell cycle analysis, Watson Pragmatic Model of FlowJo (v7.6) software (Tree Star, Inc.) was applied to the PI histogram to determine the percentage of cells in G0/G1, S and G2 phases. For nuclear DNA content analysis, 1 mL of the filtered nuclei solution was aliquoted and approximately ten thousand chicken erythrocyte nuclei singlets (Biosure, Grass valley, CA) were added as an internal standard. The mixture of *Taxus* nuclei and chicken nuclei was incubated with 50 μl of 1 mg/mL RNAse and 50 µl of 1 mg/mL PI for 30 minutes on ice, before flow cytometric analysis, as described above, where forward scatter, side scatter and PI fluorescence were collected on a logarithmic scale.

2.2.4 Taxane analysis

Taxanes were identified and quantified using a Waters Acquity UPLC H-Class system. Separation on UPLC was performed using an Acquity (Waters, Milford, MA) BEH C_{18} column (particle size 1.7 μm, 50 mm × 2.1 mm). Samples were prepared for metabolite analysis, as described elsewhere (Naill and Roberts 2004). Paclitaxel and baccatin III authentic standards (Sigma-Aldrich, St. Louis, MO) were used to generate standard

curves for quantification of metabolite content, and as a reference for comparison of sample peak retention times and characteristic taxane UV absorption spectra.

2.3 Results and discussion

2.3.1 Relationship between paclitaxel levels and mean aggregate size

Paclitaxel levels measured in each culture passage (on day 7 post-elicitation with MeJa, day 14 of the cell culture period) varied over the six-month experimental timeframe, showing a 6.9-fold difference between the highest and lowest levels of accumulation (Fig. 2a). Such batch-to-batch variations can have significant economic implications in large scale fermentation systems. As the mean size of the aggregates was shown to affect the level of paclitaxel accumulated in cultures in distinct experiments (Kolewe et al. 2011), we measured the aggregate size distribution during each passage (Fig. 2a). Similar to paclitaxel levels in the culture, a saw-tooth pattern was observed for mean aggregate size when plotted against time (passage number). Both paclitaxel level and mean aggregate size in the cultures followed a distinct relationship: as the mean aggregate size of the culture decreased, the amount of paclitaxel accumulated in that culture passage increased. A significant negative correlation (r = 0.75, p < 0.01) was observed between mean aggregate size and paclitaxel accumulation (Fig. 2b). These results were consistent with previous observations (Kolewe et al. 2011), where in individual experiments, cultures initiated with smaller aggregate size distributions accumulated higher paclitaxel levels than their larger aggregate counterparts. However, the differences in paclitaxel levels observed in this study were over sequential multiple passages without any manipulation of aggregate sizes prior to inoculation. Interestingly, similar variations in

mean aggregate size were observed for cultures that do not accumulate paclitaxel post-elicitation (data not shown),

Since plant cell suspension cultures are inherently heterogeneous, it is not surprising that metabolite levels over time are not consistent. It is possible that unconscious selection of aggregates of a particular size class may occur during subculturing (Kinnersley and Dougall 1980), which in this case could contribute to the observed fluctuations in mean aggregate size, and hence paclitaxel yields. One of the reasons for inconsistent selection of aggregates of a particular size class could be due to the density difference between large and small aggregates present in the culture. Routine transfer of aggregated plant cells is performed by continuous gentle shaking of the parent flask while pipetting a desired volume of culture into fresh media using a wide-mouthed pipet. The tendency of large aggregates to sink faster could cause them to escape the pipette, potentially leading to unintentional exclusion of larger aggregates. In the case of suspension cultures where key secondary metabolites are pigments, the highly pigmented cultures are chosen via simple visualization for passage, which could lead to prolonged higher productivity (Yamada and Hashimoto 1990; Yeoman and Yeoman 1996). However, in suspension cell systems such as *Taxus*, secondary metabolites are not fluorescent or colored, preventing screening and selective subculturing via simple visualization. The data presented here suggest that selection of aggregates of a particular size class during subculturing could be a simple method for plant suspension systems such as *Taxus* to maintain high and stable producing cell lines.

2.3.2 Relationship between sucrose consumption, paclitaxel levels and mean aggregate size

There may be differential utilization of sugars from the media amongst culture passages, which could influence growth, aggregate size distribution, and ultimately paclitaxel accumulation. During each passage, the concentration of both glucose and sucrose was measured in the extracellular medium on day 7 post-inoculation. Extracellular sugar concentration ranged from 8.5 to 5.6 g/L on day 7 (initial value on day 0 is 20 g/L) and did not correlate with either paclitaxel level or culture mean aggregate size (data not shown). Thus, by day 7, cells in each passage utilized similar levels of sugar, irrespective of the mean aggregate size of the culture. This result was not completely unexpected as a similar amount of inocula was used to initiate cultures in each passage to avoid the effect of varying inoculation density on metabolite levels (Morris 1986). This result also suggests that for the range of aggregate sizes in these *Taxus* cultures, diffusion limitations for simple sugars are likely not present, as sugar consumption normalized by biomass was found to be independent of aggregate size.

2.3.3 Cell cycle, DNA content and ploidy analyses

Flow cytometry offers a rapid and accurate method for determining ploidy content, assessing DNA content and analyzing cell cycle participation. Monitoring the pattern of cell cycle distribution over culture passages provides information on cell division potential and differentiation characteristics at each passage (Neumann et al. 2009; Yanpaisan et al. 1999). For example, an increased proportion of cells in G0/G1 phase would indicate potential differentiation of cells into organized tissues (Yanpaisan et al.

1999). To examine the cell cycle activity for *Taxus* cells during each passage, the proportion of cells in each phase of the cell cycle, G0/G1, S and G2 were determined using flow cytometry. A similar percentage of cells remained in each cell cycle phase on day 7 of each passage (Fig. 3). Throughout the study, on day 7 of each passage, 72-78% cells were found in G0/G1-phase, 14-17% cells in S-phase, and 7-11% cells in G2-phase. These results suggest that prior to MeJA elicitation, no cell cycle inhibition or arrest occurs with repeated culture passage. Nonetheless, it is important to realize that this analysis was uni-variate, and does not distinguish between non-cycling G0 cells and cycling G1 cells, as both have 2C DNA content. A multi-parametric analysis with a cellular marker such as RNA (Bergounioux et al. 1988) or protein content (Citterio et al. 1992), or using thymidine analogs such as BrDU (Yanpaisan et al. 1998) or EdU (Kotogany et al. 2010), must be used to distinguish between cycling and non-cycling cells. Previous data illustrate that a significant portion of *Taxus* cells (~65 %) reside in G0 phase (Naill and Roberts 2005).

Nuclear DNA content correlates with ploidy level, and its estimation in relative units can be used to detect changes in ploidy levels amongst passages (Dolezel et al. 2007). Using chicken nuclei as a standard (2C DNA content = 2.33 picograms (pg)), the 2C DNA content of the *Taxus* P93AF cell line measured with flow cytometry was found to be ~ 36 pg (Fig. 4a). The nuclear DNA content measured on day 7 (mid-exponential phase) did not vary from one passage to another. Previous work has shown heterogeneity in nuclear DNA content amongst cell lines over a two-year timeframe following culture initiation, where some cell lines exhibit stable genome size (four of nine evaluated) and others (five of nine evaluated) show variation. (Baebler et al. 2005). During each passage,

only two peaks were observed, corresponding most likely to 2C and 4C DNA (G1 and G2) content (Fig. 4b). Thus, no changes in ploidy and nuclear DNA content were detected throughout the six-month timeframe investigated here, implying orderly progression through mitosis. Changes in ploidy levels are often observed once suspension cultures are established (Maciejewska et al. 1999; Creemers-Molenaar et al. 1992), and in most cases an increased ploidy is seen as the culture ages. Varying the concentration of growth hormones has also been shown to induce changes in culture ploidy levels (Mishiba et al. 2001). However, the cell line examined here was maintained with the same concentration of growth hormones over time (Gibson et al. 1993). Constant ploidy levels and nuclear DNA content over the six-month timeframe indicate that ploidy levels in our mature *Taxus* cultures do not vary on the same time scale as metabolite production patterns, and are most likely not a cause of this relatively short term variability in yield. Other genetic factors such as structural changes in nuclear DNA, gene mutations and translocation of chromosomes to new segments, and/or epigenetic factors such as gene silencing by DNA methylation, may contribute to the observed differences in paclitaxel accumulation amongst passages, and require further study.

2.4 Conclusions

Uncertainty in product levels and limited success of plant cell cryopreservation techniques necessitates studies into understanding the reasons for variability in secondary metabolite accumulation in plant suspension cultures. *Taxus* cell cultures consist of a heterogeneous population of cells, with aggregates of varying sizes present in the culture. Here, we have shown that culture mean aggregate size is an important process parameter that correlates with variable paclitaxel accumulation during long term suspension culture

maintenance. Sugar utilization, nuclear DNA content (i.e., ploidy levels) and cell cycle participation did not differ significantly amongst passages. Information regarding aggregation size distributions during a batch culture could be incorporated into kinetic models to more accurately predict culture growth, metabolism and product formation (Kolewe et al. 2012). This study further emphasizes the importance of rational manipulation of aggregate sizes during routine culture passage for optimization of plant cell culture bioprocesses (Hanagata et al. 1993; Kinnersley and Dougall 1980; Kolewe et al. 2011). This is particularly relevant in suspension systems where major secondary metabolite products are often not pigmented, and a simple visual selection of high metabolite producing cells is not always possible.
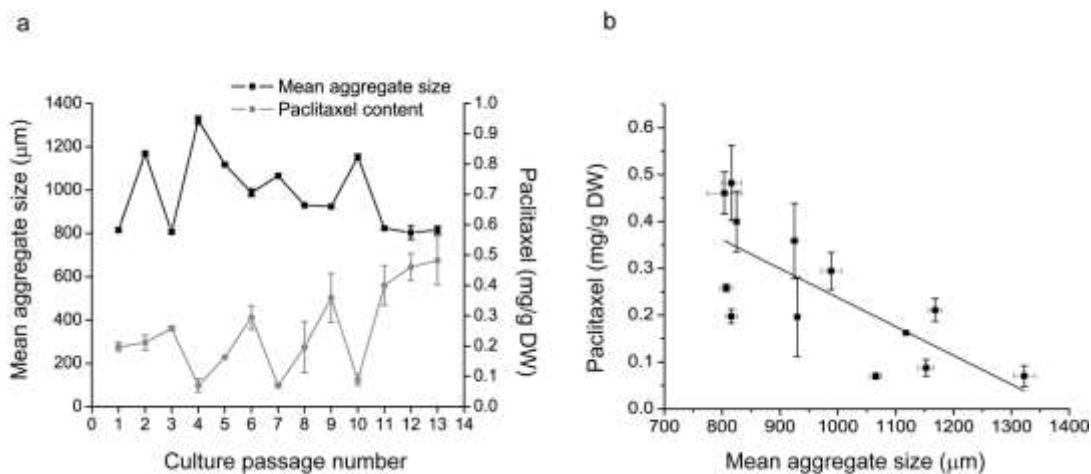
Figure 2.1 Fluctuations in mean aggregate size and paclitaxel levels over multiple passages of *T. cuspidata* P93AF cell suspension cultures. Passage is done every 14 days. **(A)** Squares represent the mean aggregate size of the culture obtained through Coulter counter measurements. Circles represent paclitaxel content in the culture as measured through UPLC. **(B)** Relationship between culture mean aggregate size and paclitaxel level. The Pearson correlation coefficient (r) is -0.75 ($p < 0.05$ as determined using a two-tailed test), indicating a statistically significant negative linear relationship. Data points represent three biological replicates. Horizontal bars represent standard errors of the mean aggregate size and vertical bars represent standard errors of the culture paclitaxel level.
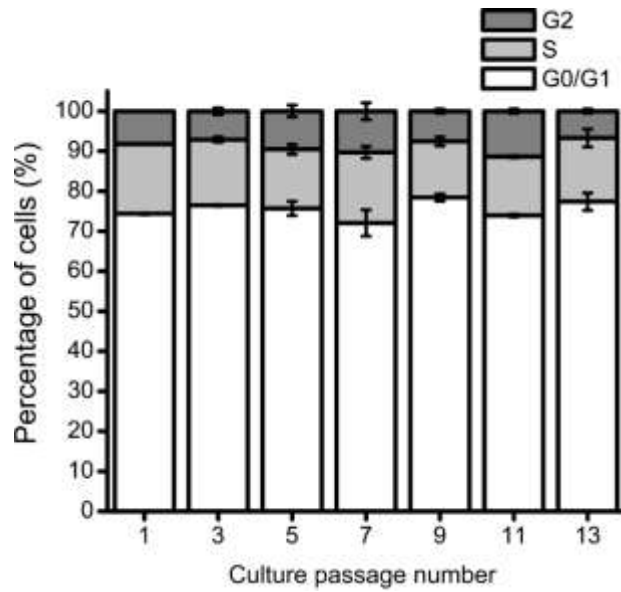
Figure 2.2 Cell cycle analysis of *T.cuspidata* P93AF cell line over multiple subcultures.

FlowJo (Treestar, Inc.) cell cycle analysis algorithm was applied to the propidium iodide

histograms to differentiate cell cycle phases.
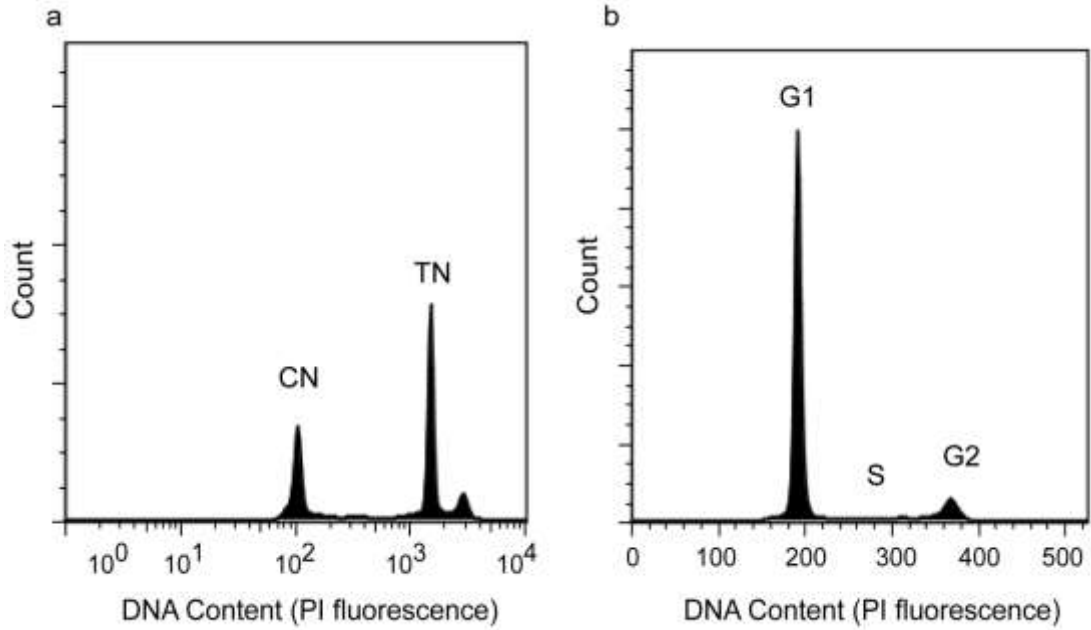
Figure 2.3 Flow cytometric DNA histograms. **(A)** Semi-log plot of DNA content in chicken nuclei (CN) singlets (2.33 pg 2C DNA content) and *Taxus* nuclei (TN), stained with 50 µg/ml propidium iodide. The first peak is for chicken nuclei singlets (CN) and the next two peaks are for *Taxus* nuclei (TN). **(B)** Linear plot of DNA content for *Taxus* nuclei stained with 50 µg/ ml propidium iodide. Cell cycle phase is indicated on the figure. Coefficients of variation were below 4% for all measurements.

2.5 Additional information (not included in paper)

i) Relationship between aggregate size and extracellular sugar consumption

The sucrose consumption data for P93AF cell line, which was not statistically significantly related to aggregate size, is shown in Figure 2.4.
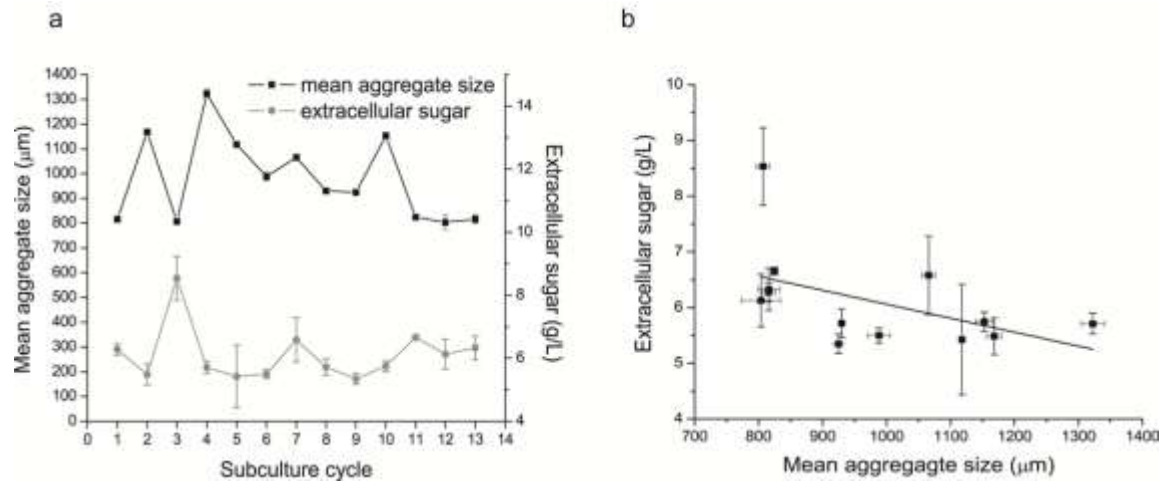
Figure 2.4 (A) Fluctuations in mean aggregate size and extracellular sugar levels over subculture cycles. **(B)** Relationship between mean aggregate size of the culture and extracellular sucrose level in the culture. The Pearson correlation coefficient (r) is -0.5 (p > 0.1) indicating a non-significant moderate negative linear relationship between mean aggregate size and extracellular sugar levels in the cultures. The level of significance was determined using a two-tailed test. Error bars represent SEM.

ii) Long term study with *T. cuspidata* P991C cell line

A similar experiment was performed with another cell line, *T. cuspidata* P991C by Martin Kolewe (Roberts Lab). Similar to the P93AF cell line, fluctuations in aggregate

size were observed over subcultures (Figure 2.5).   However, these cultures did not produce detectable levels of paclitaxel, as measured by HPLC. Hence a correlation between aggregate size and paclitaxel levels during the subculture period was not possible.
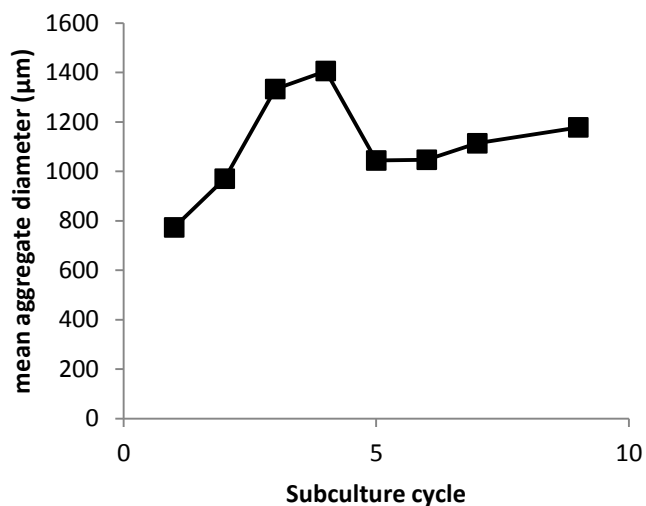
Figure 2.5 Fluctuations in mean aggregate size over subculture cycles in *T. cuspidata* P991C cell line. Mean aggregate size of the culture was obtained using the Coulter counter.

iii) Effect of dilution of Coulter counter solution

For all the Coulter counter analysis in this dissertation and in previous studies in the Roberts laboratory, 2 x 2 mL samples of well-mixed culture broth from each culture flask were added to 380 mL of diluent consisting of 65:35 Isoton (1% NaCl with preservatives, Beckman Coulter):Glycerol. Following each set of samples, the diluent was vacuum filtered over a series of 3.5 and 2.0 μm depth filters and recycled for further use (Kolewe

et al. 2010). However, the recycled diluent becomes diluted over time by the addition of cell culture media during sampling, and hence it becomes necessary to determine the reliability of data acquired from Coulter counter after a certain number of samples are analyzed.

To quantify the effect of dilution, several different diluent concentrations were tested. Two 250 mL *Taxus* culture flasks were combined and samples of well-mixed culture broth were analyzed in each of the diluent solutions evaluated. Mean aggregate size, volume (measured by the Coulter counter), and the amount of diluent solution remaining in the Coulter counter flask after a 60 second analysis, were measured to compare different diluents; results are shown in Table 2.1. In each case, 2 x 2 mL of well-mixed culture were added to 450 mL of Coulter counter solution. A higher volume (450 mL) of diluent was used for these experiments as opposed to 380 mL, which was originally specified (Kolewe et al. 2010). If sufficient diluent is not present in the Coulter counter flask, air bubbles can pass through the Coulter counter aperture, adversely affecting the measurements. In a 60 second analysis with a constant flow rate of 5.1 mL/s (Kolewe et al., 2010), the Coulter counter will withdraw more solution if the diluent is of lower viscosity. As a variety of glycerol concentrations (i.e., diluents with different viscosity) were tested, a higher volume of diluent was used to avoid the potential formation of air bubbles.

Results in Table 2.1 indicate that as the diluent becomes more diluted, or as the concentration of glycerol in the diluent decreases, both the mean cell aggregate size and culture biomass concentration increases. For example, when the glycerol concentration in the diluent was decreased from 35% to 15%, the mean aggregate size measured changed

from 349 μm to 438 μm. Similar results were observed over time (one month-old vs. five month-old vs. one year-old diluent). As the diluent gets recycled, it becomes more diluted, leading to increased aggregate size and biomass readings. Ideally, if there was no effect on diluent concentration over time, results for each diluent should have been identical, as samples were analyzed from the same culture. Also, the decrease in viscosity of the diluent (due to addition of media) leads to more solution being used for the analysis. This is evident from the amount of diluent remaining in the Coulter counter flask after each analysis (Table 2.1).

This study illustrates that dilution of the Coulter counter solution over time affects aggregate and biomass readings and therefore diluents should be changed frequently to ensure reliable results. The basis for changing the diluent should be the number of samples that are analyzed with the same diluent or the number of times the diluent has been recycled. Further in depth studies to evaluate the approximate number of samples that can be analyzed with the same diluent need to be performed if the diluent recycle process is used. Results from such studies are especially important for collecting reliable data for long term studies, e.g., aggregate size fluctuations over time.

As mentioned above, the total number of samples analyzed with the same diluent will influence the mean aggregate size and volume measured. If a small number of samples are analyzed over a certain time period, then the diluent properties would not change drastically and the Coulter counter data are very reliable. Accordingly, during the time frame where the Coulter counter data for this chapter were collected (Figure 2.1, Fig 2.5), there was infrequent analysis of samples using the recycled Coulter counter diluent, indicating confidence in the collected data. The reliability of the data is also evident from

49

the results (Figure 2.1, 2.5), where the aggregate size fluctuated over time. If there were significant effects due to diluent dilution, then a steady increase in the aggregate size would have been observed.

Table 2.1 Effect of Coulter counter solution on sample analyses. Regular diluent (one month-old, freshly made, five-month old and one year-old) refers to 65:35 Isoton (1% NaCl with preservatives):Glycerol. Data represent the average of 2 x 2 mL samples for each "treatment." Mean aggregate size and volume are the values obtained directly from the Coulter counter (without using conversion factors to provide a more accurate number for aggregate size)

Solution	Mean aggregate size μm	Volume $* 10^9 \, \mu m^3$	Diluent remaining (mL)
Freshly made diluent (65% NaCl-35% glycerol	349	25.42	170
75 % NaCl-25 % glycerol	384	33.97	138
85% NaCl-15% glycerol	438.3	54.13	110
65% NaCl-35% glycerol + 500 ml B5 media	373.4	35.82	138
One month-old diluent	354	28.89	150
Five month-old diluent	419.7	40.72	122
One year-old diluent	431.4	45.5	115

iv) Effect of inoculation density on mean aggregate size of the culture

Process parameters such as inoculation density and day of subculture can affect secondary metabolite accumulation in plant cell cultures (Qu et al. 2006). To test the effect of inoculation density on aggregation patterns of *Taxus* cell cultures, triplicate flasks of control cultures (normal inoculation density, 1.4 g/L), low inoculation density cultures (0.6 g/L) and high inoculation density cultures (2.8 g/L) were made, and growth and aggregate size were measured over time using the Coulter counter method. Figures 2.6A and 2.6B show the biomass content and mean aggregate size for high, normal and low inoculated cultures, respectively. Biomass was consistently higher in the high inoculation density cultures as compared to normal and low inoculation density cultures until day 14 of the culture period. High inoculation density cultures had consistently smaller aggregates than normal and low inoculation density cultures. Results from this experiment suggest altering inoculation density as a means of producing smaller aggregates, and potentially higher paclitaxel yields. However, additional experiments need to be conducted to investigate if these effects are observed over multiple subculture cycles and should be correlated to paclitaxel levels.
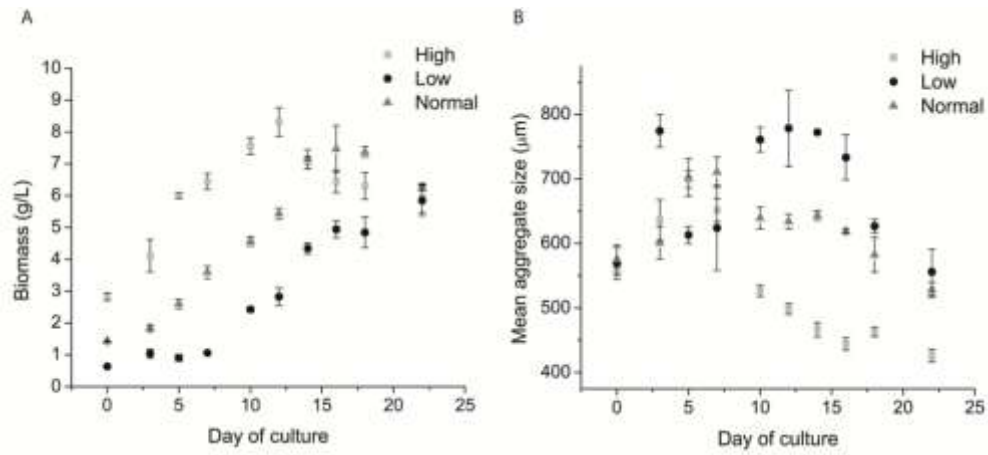
Figure 2.6 Effect of inoculation density on biomass and mean aggregate size of *T. cuspidata* P93AF cultures. **(A)** Biomass, **(B)** Mean aggregate size as measured by the Coulter counter method. Reported values are the average of three replicate flasks and error bars represent standard error of the mean.

CHAPTER 3
CONTRIBUTION OF TAXANE BIOSYNTHETIC PATHWAY GENE EXPRESSION TO OBSERVED VARIABILITY IN PACLITAXEL ACCUMULATION IN *TAXUS* SUSPENSION CULTURES

3.1 Introduction

Natural products represent many of the most effective drugs currently available for the treatment of a variety of diseases, and are particularly useful as anti-cancer and anti-infectious agents (Li and Vederas 2009). Paclitaxel (Taxol®), a taxane diterpenoid produced by *Taxus* genus is a potent chemotherapeutic widely used in the treatment of breast, ovarian and non-small cell lung cancers as well as AIDS-related Kaposi's sarcoma (Colegate and Molyneux 2008). Paclitaxel is also being investigated for use in the treatment of neurological disorders, additional cancers and in post-surgery heart patients (Vongpaseuth and Roberts 2007). Large scale commercial synthesis of plant natural products via cell culture has proven to be challenging due to low yields and instability in productivities (Lee et al. 2010; Roberts 2007). Despite these limitations, plant cell culture has emerged as a sustainable source for paclitaxel supply, being commercially produced by Phyton Biotech Inc. and Samyang Genex Corp. using large scale fermentation. The successes of large scale industrial plant cell culture in the U.S. and world-wide with paclitaxel (Fett-Neto et al. 1992; Srinivasan et al. 1995; Yukimune et al. 1996; Wickremesinhe and Arteca 1994) and several other plant-derived compounds such as ginseng (Ushiyama 1991), shikonin (Fujita et al. 1982), and berberine (Sato and Yamada 1984), have clearly demonstrated both the feasibility of this technology, and broad applicability across a range of plant species and products.

The primary difficulties associated with establishment of plant cell culture bioprocesses are the low and variable yields in secondary metabolite accumulation (Kolewe et al. 2008). To overcome low yields, a variety of traditional optimization strategies have been effective, including elicitation with methyl jasmonate (MeJA) (Yukimune et al. 1996; Gundlach et al. 1992; Mirjalili and Linden 1996). By combining media and process optimization strategies with MeJA elicitation, paclitaxel accumulation of 110-120 mg/L have been reported in academic laboratories (Yukimune et al. 1996; Ketchum et al. 1999) and up to 295 mg/L (Tabata 2004) and 900 mg/L (Bringi et al. 2007) have been achieved in industrial environments. Along with high product yields, development of cell lines and processes with a high degree of biochemical and physiological stability is critical for the ultimate success of this technology platform (Roberts 2007; Morris et al. 1989). Variability in product accumulation has been observed in suspension cultures that are maintained over long periods of time (Qu et al. 2005; Deusneumann and Zenk 1984), including paclitaxel accumulation in *Taxus* cultures (Ketchum and Gibson 1996; Kim et al. 2004). Though production instabilities have been attributed to epigenetic and/or genetic causes (Baebler et al. 2005; Bonfill et al. 2006), few molecular studies have been performed (Hefner et al. 1998; Nims et al. 2006) to gain a mechanistic understanding of paclitaxel accumulation variability in *Taxus* cell cultures, and hence no rational engineering strategies have emerged to control or leverage favorable variability to optimize performance.

Understanding regulation of gene expression is critical to the design of targeted metabolic engineering approaches. To probe regulation of paclitaxel accumulation, expression patterns of known paclitaxel biosynthetic pathway genes can be quantified.

Paclitaxel biosynthesis consists of 19 putative enzymatic steps (Jennewein et al. 2004) and has only been partially elucidated (see Figure 1.3 for paclitaxel biosynthetic pathway). Regulation of paclitaxel/taxane biosynthetic pathway genes has been examined through RNA gel blot analysis and semi-quantitative RT-PCR in MeJA-elicited *T. cuspidata* suspension cultures (Nims et al. 2006). Similar studies using qRT-PCR have been reported for *T. chinensis* suspension cultures where the elicitation strategy focused on increasing Taxuyunnanine C, a 14β-hydroxy taxoid, generated through an early branch of the paclitaxel biosynthetic pathway (Gao et al. 2011). For the majority of known pathway steps, mRNA abundance increased following elicitation, indicating substantial regulation of the pathway at the level of mRNA. . However, these studies focused on comparison of cultures with and without elicitation. Variability in paclitaxel accumulation is often observed amongst cultures elicited with MeJA (Kim et al. 2004). Therefore, to link variability fully to gene expression, comparison of multiple culture states with different biosynthetic capabilities is necessary.

Plant cells in suspension culture remain connected to each other after cell division, resulting in the formation of cellular aggregates of various sizes. In *Taxus* suspension cultures, aggregates ranging from less than 100 μm to well over 2 mm have been observed (Kolewe et al. 2010). Cells within these aggregates are subject to different microenvironments, leading to cell-cell differences in morphology (Wallner and Nevins 1973) and metabolism (Verma and Van Huystee 1970). Recently, we have developed an approach to assess the effect of aggregate size as a process variable on paclitaxel accumulation, and have demonstrated that cultures with smaller aggregates accumulate significantly more paclitaxel upon elicitation with MeJA than cultures with larger

aggregates (Kolewe et al. 2011). Using this approach, it is possible to predictably and rapidly obtain cultures with different biosynthetic capabilities upon MeJA elicitation.

In this paper, we use this approach to quantify expression of paclitaxel biosynthetic pathway genes in cultures with varying levels of paclitaxel accumulation, to clarify the underlying causes of production variability that have been observed at the process scale. Using qRT-PCR, we first compared expression profiles in cultures elicited with MeJA that produce detectable levels of paclitaxel and unelicited cultures that do not produce detectable levels of paclitaxel, to elucidate the on/off state of paclitaxel accumulation. Next, we established cultures with small and large aggregate distributions (Kolewe et al. 2011) that exhibit variable paclitaxel accumulation patterns upon elicitation with MeJA, to enable comparison of gene expression between cultures in which taxane accumulation is positive but significantly different. Using this method we were able to examine cultures that had 15-fold and 2-fold differences in paclitaxel accumulation after MeJA elicitation, respectively. This is the first study to compare gene expression in cultures with variable levels of paclitaxel accumulation, providing valuable information regarding the regulation of paclitaxel synthesis.

3.2 Materials and methods

3.2.1 Cell culture maintenance, elicitation and biomass measurements

The *Taxus cuspidata* P93AF cell line was provided by the United States Plant Soil and Nutrition Laboratory (Ithaca, NY) and was used in all experiments. All chemicals were obtained from Sigma-Aldrich Co. (St. Louis, MO), unless otherwise noted. Cell cultures were maintained, as described previously (Kolewe et al. 2011). For elicitation, 200 µM

methyl jasmonate (MeJA) was added on day 7 post-transfer during the mid-exponential phase of growth, as described previously (Naill and Roberts 2004). A Multisizer 3^{TM} Coulter counter equipped with a 2,000 μm aperture (Beckman Coulter, Brea, CA) was used to measure culture aggregate size distributions, as described previously (Kolewe et al. 2010). As the total aggregate volume was previously shown to correlate directly with biomass (Kolewe et al. 2010), this measurement was also used to determine dry weight (DW), and all DW data presented here were based on this correlation. For analysis, two x 2 mL samples of well-mixed culture broth from each flask were taken at each time point.

3.2.2 Initiation of cultures with different aggregate size distributions and sampling for growth, RNA and metabolite analyses

Three 14-day old suspension flasks were combined into one culture and its aggregate size distribution and mean aggregate size were determined using the Multisizer 3^{TM} Coulter counter. This culture was aseptically separated into two cultures (one "small aggregate culture" and one "large aggregate culture") using a filter corresponding to its mean aggregate size, based on correlations developed in previous work (Kolewe et al. 2010). Three biological replicates each of small aggregate culture and large aggregate culture were initiated and maintained as 200 mL cultures in 500 mL shake flasks, as described previously (Kolewe et al. 2011). Measurements for biomass were taken on the day of inoculation (day zero) and on the day of elicitation with MeJA (day seven). Prior to MeJA elicitation and 15 hours post-elicitation, samples for total RNA extraction were collected. Cell suspensions (3-4 mL of well mixed cultures) were filtered through Miracloth® (Calbiochem, La Jolla, CA) to yield ~500 mg fresh cell weight, thoroughly ground in liquid nitrogen and stored at -80 °C in polypropylene tubes prior to RNA

analysis (see below). Following MeJA elicitation, 1 mL samples of well mixed culture broth containing both cells and media were taken every 2-3 days with a cut pipette tip and stored at -80 $^{\circ}$C prior to metabolite analysis (see below).

3.2.3 Metabolite analysis

Taxanes were identified and quantified using a Waters (Milford, MA) Alliance 2690 HPLC with a 996 photodiode detector (Naill and Roberts 2004) or a Waters Acquity UPLC H-Class system. Separation on the HPLC was accomplished on a Taxsil (Varian, Inc., Torrance, CA) column (particle size 5 µm, 250 × 4.6 mm). The UPLC separation was performed using Acquity (Waters, Milford, MA) BEH C_{18} column (particle size 1.7 µm, 50 × 2.1 mm). Samples were prepared for taxane analysis, as described elsewhere (Naill and Roberts 2004), and analyzed on either the HPLC or UPLC system. Baccatin III and paclitaxel authentic standards (Sigma-Aldrich, St. Louis, MO) were used to generate standard curves for quantification of taxane content.

3.2.4 Gene expression analysis

3.2.4.1 RNA isolation and reverse transcription

Total RNA was extracted using RNeasy Plant Mini Kit (Qiagen, Valencia, CA) following the manufacturer's instructions. Genomic DNA was eliminated by treating each sample with Ambion's Turbo DNA-free DNase I (Applied Biosystems, Foster City, CA) according to the manufacturer's instructions. The concentration of total RNA was estimated using a Nanodrop 1000 spectrophotometer (Thermo Scientific, Wilmington, DE). RNA quality was further assessed by denaturing gel electrophoresis. 1 µg of total

RNA was subjected to reverse transcription using the Affinity Script cDNA synthesis kit (Agilent Technologies, Santa Clara, CA) with oligo dTs as primers. Reactions were performed according to the manufacturer's protocol in a total volume of 40 µL. For use as templates for qRT-PCR, cDNA samples were diluted five-fold in sterile water.

3.2.4.2 Primer design

Primer pairs for qRT-PCR amplification were designed based on selected sequences using Primer3 software (http://frodo.wi.mit.edu/primer3/) with the following criteria: melting temperature of 63 ± 3 °C, primer sequences of length between 20 – 25 bp, and GC content of 40 % to 60 %. Amplicon lengths were optimized to 100 – 250 bp to ensure maximal polymerization efficiency for qRT-PCR. Specificity of the primer pairs was evaluated by melting-curve analysis (*Mx3000P* real-time PCR instrument software, version 2.0) after 40 amplification cycles. Table 1 lists the primers used in this study.

3.2.4.3 Quantitative real time RT-PCR (qRT-PCR)

qRT-PCR reactions were performed in a 96-well plate with a Mx3000P Real-time PCR system (Stratagene, La Jolla, CA), using SYBR Green to monitor dsDNA synthesis. A 25 µL PCR reaction was prepared containing 12.5 µL of Brilliant 2× SYBR green master mix (Agilent Technologies, Santa Clara, CA), 2 µL of template cDNA (or water for no template control), 100 nM of each primer, and 50 nM of diluted ROX dye (to compensate for non-PCR related variations in fluorescence, Agilent Technologies). The SYBR Green fluorescence data were collected with the following thermocycler conditions: initial denaturation at 95 °C for 10 min followed by 40 cycles at 95 °C for 30 s, 60 °C for 1 min, and 72 °C for 1 min. Melting-curve analysis was performed at the end of the

amplification procedure to check the specificity of the PCR reaction. Mean PCR efficiency for each gene was calculated by LinRegPCR (Ramakers et al. 2003) by using 4 − 6 points and the best correlation coefficient. The reported fold induction is the geometric mean of the relative fold induction values for target genes normalized to each of the endogenous controls, actin (GenBank accession NO: JF735995) and GAPDH (GenBank accession NO: L26922). The use of actin and GAPDH as internal reference genes was validated by ensuring that the relative expression of each gene remained constant in both small aggregate cultures and large aggregate cultures before and after elicitation with MeJA. The expression ratio results were tested for significance by a randomization test using the Relative Expression Software Tool (REST©) (Pfaffl et al. 2002). The statistical model used by this software is a pair-wise fixed reallocation randomization test. The software returns the probability of the alternative hypothesis (P(H1)), which is that the difference between sample and control groups is due only to chance. A P value of less than 0.05 was considered significant.

3.3 Results and discussion

3.3.1 Analysis of paclitaxel/taxane biosynthetic pathway gene expression in unelicited and MeJA-elicited cultures

Cultures accumulated paclitaxel/taxanes only upon elicitation with MeJA (Figure 3.1A and 3.1B), and therefore this experiment was designed to investigate gene expression in the on/off state of paclitaxel/taxane accumulation. Expression of seven known taxane biosynthetic pathway genes was quantified and compared between MeJA-elicited and unelicited cultures (Figure 3.1C). Most genes were significantly up-regulated in MeJA-

elicited cultures relative to unelicited cultures (1.5 – 160 fold). These data concur with previous reports on different *Taxus* cell lines that show increased steady state mRNA levels of biosynthetic pathway genes upon MeJA-elicitation using Northern gel blot analysis (Hefner et al. 1998; Nims et al. 2006; Hu et al. 2006; Kai et al. 2005), RT-PCR (Nims et al. 2006) and qRT-PCR (Gao et al. 2011; Exposito et al. 2010). In this study, the fold change in T5αH expression upon elicitation with MeJA was lower than that quantified for most other pathway genes, which agrees with previous results (Nims et al. 2006; Wheeler et al. 2001). In a time course study using Northern gel blot analysis, T5αH expression was shown to be higher at 6h relative to 18h, after which transcripts were not detected (Nims et al. 2006). Figure 3.1C shows results at 15 hours post-elicitation, and therefore T5αH transcript abundance was significantly lower by this time point, resulting in a lower observed expression ratio. In addition, BAPT expression was relatively weakly induced with MeJA elicitation as compared to the other pathway genes, agreeing with previous data (Nims et al. 2006). Thus, these data again support the hypothesis that BAPT may be a critical rate influencing step in the paclitaxel biosynthetic pathway and a primary target for metabolic engineering. Once the qRT-PCR technique was successfully established and induction of gene expression was confirmed with MeJA elicitation, we examined cultures that produced paclitaxel at different levels, enabling a more detailed understanding of metabolic differences amongst *Taxus* cultures with varying bulk paclitaxel/taxane production capabilities.

3.3.2 Analysis of cultures that exhibit high variability in paclitaxel/taxane accumulation

A comparison of gene expression in cultures that exhibit variations in paclitaxel/taxane accumulation after MeJA elicitation (i.e., higher-accumulating cultures vs. lower-accumulating cultures) has not previously been reported, but since variability in product synthesis is common amongst cultures, such a comparison is therefore of great practical interest. To obtain such differences in paclitaxel/taxane accumulation, we initiated cultures with different aggregate size profiles but the same initial biomass, and analyzed paclitaxel/taxane accumulation as well as pathway gene expression. Size distributions taken from small aggregate cultures and large aggregate cultures following inoculation on day 0 and prior to elicitation on day 7 indicated that once established, cultures maintained disparate aggregate size profiles (Figure 3.2A, 3.2B). Growth is typically retarded upon elicitation with MeJA (Kim et al. 2004; Yukimune et al. 1996) and small and large aggregate cultures maintain similar growth patterns post-elicitation (Kolewe et al. 2011). Throughout the production period of the cell culture batch, small aggregate cultures accumulated higher levels of both baccatin III and paclitaxel in comparison to large aggregate cultures (Figure 3.2C, 3.2D). The total baccatin III and paclitaxel levels were up to 120-fold and 15-fold higher, respectively, in small aggregate cultures as compared to large aggregate cultures, indicating substantial difference in metabolite accumulation.

Five of the seven genes investigated were up-regulated in MeJA-elicited small aggregate cultures as compared to MeJA-elicited large aggregate cultures (P < 0.05), but the level of up-regulation varied amongst the genes (Figure 3.2E). The relative transcript levels of early and middle pathway genes (T5αH, DBBT and DBAT) showed a minor

63

(1.4, 2 and 1.8 – fold, respectively) increase in small aggregate cultures relative to large aggregate cultures. A more substantial increase for the later pathway genes, PAM and DBTNBT (12-fold and 7-fold respectively), was observed in small aggregate cultures. The relative expression levels of TASY and BAPT were not significantly different between the cultures. One possibility for suppressed secondary metabolism in large aggregate cultures is that MeJA elicitation is not uniform in larger aggregates, where transport limitations exist, and therefore MeJA may not effectively penetrate into the interior of all aggregates (Yuan et al. 2002). These effects may be amplified since MeJA is produced endogenously by cells in response to external stimuli (Gundlach et al. 1992), as jasmonic acid biosynthesis is regulated by a positive feedback loop (Wasternack 2007; Pauwels et al. 2008). Overall, these data demonstrate some differences in pathway gene expression between cultures that accumulate substantially different paclitaxel levels (in this case 15-fold), but suggest there are additional factors that regulate paclitaxel accumulation. Interestingly, when the relative expression levels of the same pathway genes were compared in unelicited small and large aggregate cultures, higher mRNA levels for most pathway genes (six of the seven evaluated; $P < 0.05$) were observed in the small aggregate cultures (Figure 3.2F). Up-regulation of greater than 2-fold was observed for four genes, DBBT, PAM, BAPT and DBTNBT, suggesting a difference in initial metabolic state prior to MeJA elicitation. However, no differences were observed in paclitaxel accumulation in unelicited cultures, as the levels of paclitaxel produced were below the limit of quantification of UPLC. These data indicate there are bottlenecks to product accumulation in unelicited cultures that are overcome through elicitation.

3.3.3 Analysis of cultures with smaller differences in paclitaxel/taxane accumulation but higher levels of production

A second experiment was conducted with the same *T. cuspidata* cell line, in which the aggregate sizes for both small aggregate cultures and large aggregate cultures were slightly larger (Figure 3.3A, 3.3B). Like the previous experiment, a similar metabolite trend was observed, with small aggregate cultures accumulating higher levels of baccatin III and paclitaxel (Figure 3.3C, 3.3D). However, there were two important differences: 1) the relative change in metabolite accumulation between small and large aggregate cultures maximally was only 4.6-fold for baccatin III and 1.7-fold for paclitaxel, compared to 120-fold for baccatin III and 15-fold for paclitaxel in the previous experiment; and 2) the large aggregate cultures in this experiment accumulated a relatively high level of paclitaxel (1.6 mg/g DW), which was 13-fold higher than large aggregate cultures and on the same order as small aggregate cultures from the previous experiment. Aggregate size is not the only factor influencing variability in paclitaxel accumulation amongst cultures, and it is not uncommon to observe varying differentials in paclitaxel accumulation (Kolewe et al. 2011). Additional genetic and epigenetic factors not explicitly measured or controlled for likely contribute to the variability observed amongst *Taxus* cultures between experiments.

In this case, qRT-PCR analysis revealed no differences in the expression levels of pathway genes between small and large aggregate cultures after elicitation with MeJA (Figure 3.3E). Both small and large aggregate cultures accumulated high levels of paclitaxel, indicating that pathway genes were up-regulated by MeJA, but the differences

in baccatin III and paclitaxel accumulation between small and large aggregate cultures could not be attributed to additional increases in mRNA abundance of pathway genes.

While this work collectively shows that some degree of variability in secondary metabolism can be linked to changes in biosynthetic pathway gene expression, there are clearly contributions from other factors. Metabolite levels are not only determined by pathway gene expression levels, but also by post-transcriptional and/or post-translational regulation of enzyme activity (Verpoorte and Memelink 2002). For example, discrepancies in post-transcriptional and/or post-translational regulation were hypothesized for the lack of resveratrol production in *Vitis vinifera* cell cultures even after high induction of one of the key pathway genes (Lijavetzky et al. 2008). Primary metabolism is known to provide critical substrates for secondary metabolic pathways and hence, precursor pool availability can also affect product accumulation. For example, phenylalanine addition to *T. cuspidata* cultures resulted in an increase in paclitaxel accumulation (Fett-Neto et al. 1994). In addition to paclitaxel biosynthesis, post-biosynthetic events such as storage and degradation of paclitaxel and its precursors may be important (Roberts 2007; Siegler 1998; Zhang et al. 2002). The paclitaxel biosynthetic pathway originates in the plastid and involves hydroxylation in the endoplasmic reticulum and acylation in the cytosol (Croteau et al. 2006). Knowledge about subcellular trafficking and transport of paclitaxel and precursors, mechanisms for extracellular secretion and *in vivo* degradation will help suggest additional potential regulators of paclitaxel/taxane accumulation.

3.4 Conclusions

Significant variability is observed in paclitaxel accumulation amongst cultures of different *Taxus* species and over time within a single species. In this paper, we studied the relationship between paclitaxel biosynthetic pathway gene expression and the varying bulk levels of paclitaxel observed amongst cultures. Through qRT-PCR, we demonstrated induction of paclitaxel biosynthetic pathway genes through elicitation with MeJA, which is necessary for paclitaxel accumulation. By analyzing MeJA-elicited cultures with varying levels of paclitaxel accumulation, we observed additional up-regulation of paclitaxel biosynthetic pathway gene expression between cultures with significant differences in paclitaxel accumulation capabilities (15-fold). In particular, increased expression of late pathway genes, such as PAM and DBTNBT, was observed when there were substantial differences in bulk paclitaxel accumulation levels. However, when paclitaxel accumulation levels are only moderately different (2-fold), no differences in pathway gene expression were measured, suggesting that other factors affect the bulk paclitaxel accumulation patterns. This is the first study to address the relationship between gene expression and variability in paclitaxel accumulation through generating cultures with different paclitaxel accumulation potentials upon elicitation with MeJA. A systems-wide genomics approach along with consideration of post-biosynthetic pathway events such as transport and degradation are necessary to fully understand the factors that regulate paclitaxel accumulation in cell culture.

Table 3.1 Sequences for forward and reverse primers of the paclitaxel biosynthetic pathway genes used in qRT-PCR

Gene	Genbank Accession	Primer Pair (5'-forward-3'/5'-reverse-3')	Product size (bp)
TASY	U48796	TGCAGCGCTGAAGATGAACG AGTGCCAGTGCTGCTGCTCA	181
T5αH	AY289209	GCAACAGCCACGCAGGATCT TTGGCGAAGTGGTGGTGTCA	136
DBBT	JF735996	CATGGCGGACAACGACCTTT CCCACAACAAATCCCCCACA	159
DBAT	AF193765	CCTGCAGCTCTCCACCCTTG CGCCCTGCAAAAGGGGAATA	162
PAM	AY582743	GAGGTCATGGAAGCGCTGGA CAATGTAGGCGAGCGGGATG	109
BAPT	AY082804	GCCTTCGCCCAAAACAATCC ACACCCTGCCCTGTGCACTC	228
DBTNBT	AF466397	GGAGTGCACAGGGGATGGTG GGCAATGCCCCCACATGTAA	190
GAPDH	L26922	TTCCCTGGGGTGAGGTTGGT GCCAAAGGAGCCAGGCAGTT	229
Actin	JF735995	GCGTGAAATTGTCCGCGATG CCGTTCTGCACCAATCGTGA	148
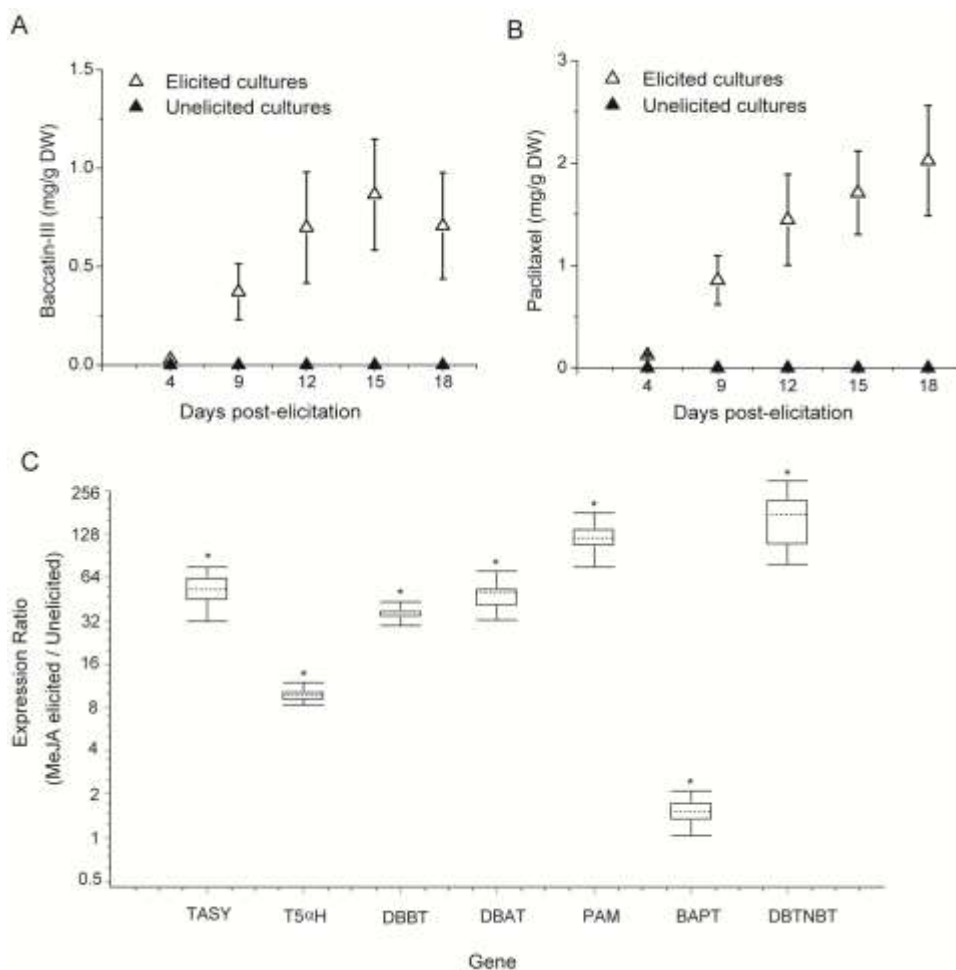
Figure 3.1 Effect of methyl jasmonate elicitation on taxane accumulation and expression of taxane biosynthetic pathway genes. **(A)** Baccatin III accumulation in MeJA-elicited and unelicited cultures. **(B)** Paclitaxel accumulation in MeJA-elicited and unelicited cultures. **(C)** Relative gene expression ratio of seven known paclitaxel biosynthetic pathway genes determined with qRT-PCR, calculated using REST 2009 software. Expression ratio represents the median fold change in MeJA-elicited samples relative to unelicited samples at 15 hours post-elicitation, normalized by actin and GAPDH reference gene expressions. The box represents the middle 50% of observations. The dotted line within the box represents the median expression ratio. Whiskers represent the

minimum and maximum observations. *p<0.05, as determined by randomization tests using REST software. Reported values are the average of three biological replicates.
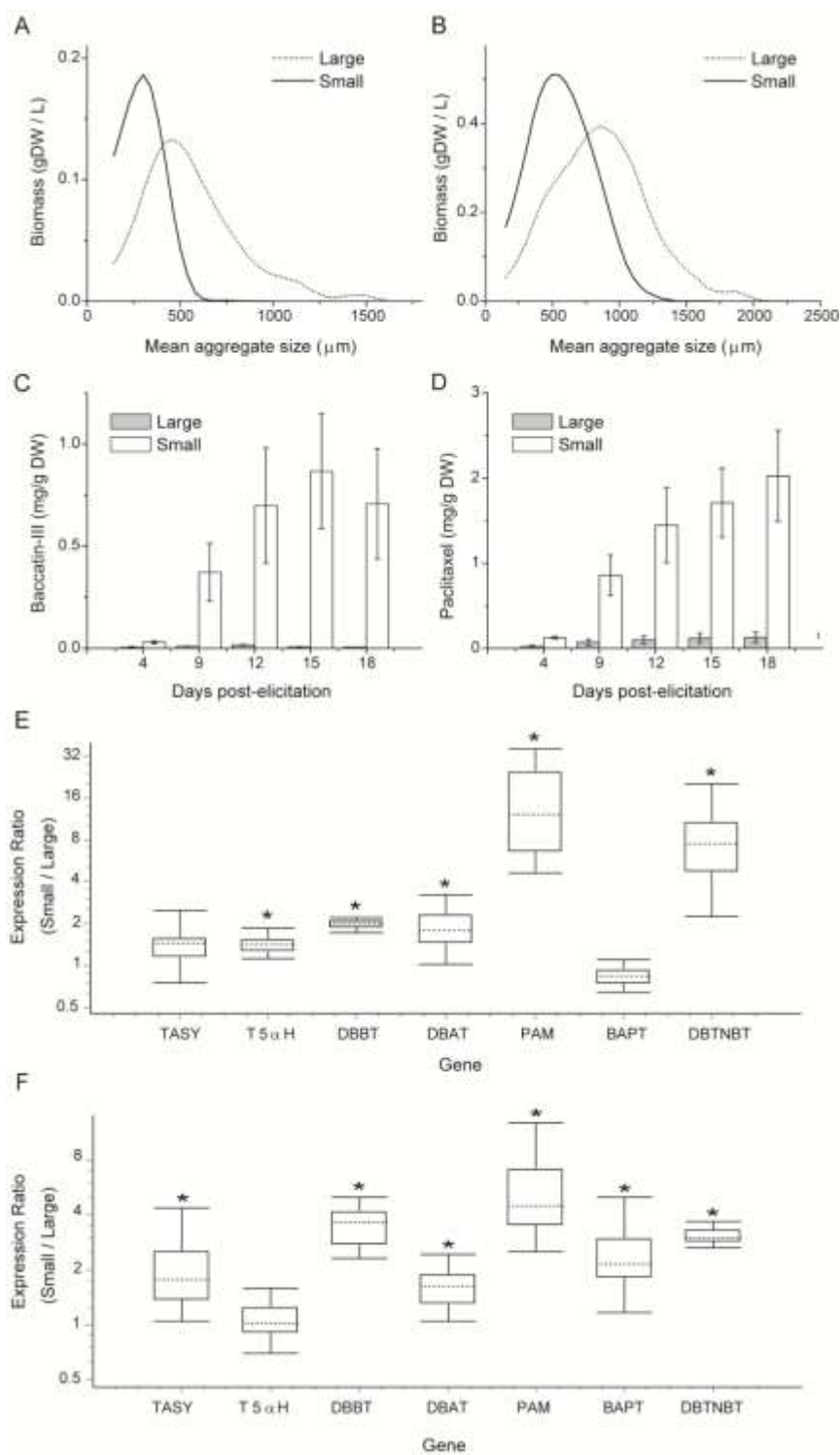
Figure 3.2 Profiles of aggregate size distributions, taxane accumulation and gene expression patterns in cultures exhibiting a large difference in paclitaxel accumulation.

(A, B) Aggregate size distribution at culture initiation and prior to elicitation, respectively. **(C, D)** Baccatin III and paclitaxel accumulation over a three-week period, respectively. **(E, F)** Relative gene expression ratio of seven known paclitaxel biosynthetic pathway genes determined with qRT-PCR, calculated using REST 2009 software. Expression ratio represents the median fold change in small aggregate cultures relative to large aggregate cultures at 15 hours post-elicitation **(E)** and just prior to elicitation **(F)**, normalized to actin and GAPDH reference gene expressions. The box represents the middle 50% of observations. The dotted line within the box represents the median expression ratio. Whiskers represent the minimum and maximum observations. *$p<0.05$, as determined by randomization tests using REST software. Reported values are the average of three biological replicates.
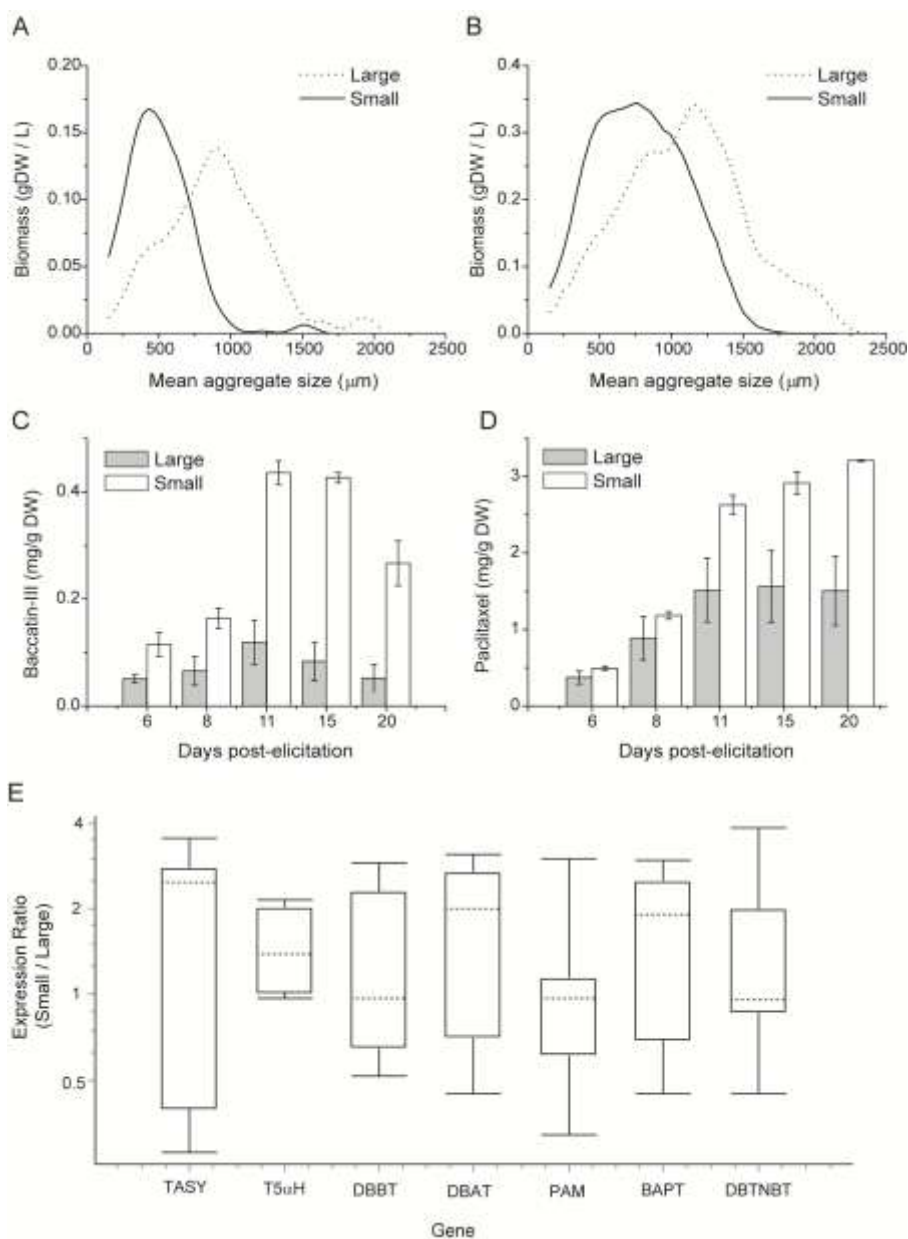
Figure 3.3 Profiles of aggregate size distributions, taxane accumulation and gene expression patterns in cultures accumulating high levels of paclitaxel with a relatively small difference in paclitaxel accumulation. **(A, B)** Aggregate size distribution at culture initiation and prior to elicitation, respectively. **(C, D)** Baccatin III and paclitaxel accumulation over a three-week period, respectively. **(E)** Relative gene expression ratio of seven known paclitaxel biosynthetic pathway genes determined with qRT-PCR,

73

calculated using REST 2009 software. Expression ratio represents the median fold change in small aggregate cultures relative to large aggregate cultures at 15 hours post-elicitation, normalized using actin and GAPDH reference gene expressions. The box represents the middle 50% of observations. The dotted line within the box represents the median expression ratio. Whiskers represent the minimum and maximum observations. Results are statistically similar for all genes ($p>0.05$) as determined by randomization tests using REST software. Reported values are the average of three biological replicates.

3.5 Additional information (not included in the paper)

i) Cloning the *Taxus* actin gene

The sequence for one of the most commonly used reference genes, actin, was not known for *Taxus*. In order to design qRT-PCR primers for actin, we cloned out a partial sequence of actin from our cultured cells. RNA was isolated from cells, and converted to cDNA as described in the Material and methods section. The primers for cloning *Taxus* actin were designed based on the sequence for Picea Abies (Norway Spruce), Genbank ID: FJ869869. PCR reaction was performed with Ex *Taq* DNA polymerase (Takara). The PCR product was integrated into the pCR®/GW/TOPO® plasmid, using the TOPO TA cloning kit (Catalog Number: K250020, Invitrogen). The pCR®/GW/TOPO® contains two thymine overhangs, allowing for incorporation of the PCR product directly into the plasmid and a spectinomycin resistance for screening. The plasmid was then transformed into a chemically competent strain of *E. coli* (DH5α) and plated on LB plates containing spectinomycin. Plasmids were isolated from *E. coli* colonies that grew. M13F (20) and M13R primers on the pCR®/GW/TOPO® plasmid were used for sequencing the product. The resulting sequenced gene was submitted to Genbank (Accession ID: JF735995).

ii) Cloning the full length DBBT gene from the *Taxus* P93AF cell line

Full length *Taxus* DBBT gene (Genbank Accession ID: JF735996) was cloned using the same procedure as described above for the *Taxus* actin gene.

iii) RNA isolation from intact *Taxus* single cells

Sorting of *Taxus* cells based on paclitaxel accumulation can be used for both development of higher accumulating cell lines and characterization of production variability through gene expression analyses, which could ultimately lead to identification of rational strategies to enhance paclitaxel accumulation (Gaurav 2011).

A protocol for isolation of live intact single cells from aggregated *Taxus* suspension cultures was previously developed in the Roberts laboratory (Naill and Roberts 2004) and used to investigate cell specific paclitaxel accumulation (Naill and Roberts 2005b). An osmoticum of 0.5 M mannitol was prepared in nanopure water. 0.3 % dextran sulfate (DS) was added to the mannitol solution to enhance single cell release (Takebe et al., 1968). The enzymes pectolyase Y-23 (0.5 % (w/v), MP biomedicals, catalog no..320952) and cellulase (0.04 % (w/v), Sigma, catalog no. C1794) were dissolved in the osmoticum mixture. Cultured cells were vacuum-filtered through Miracloth® (Calbiochem, San Diego, CA) and transferred into the enzyme solution. Ratios were maintained at approximately 1 g cell weight per 5 mL of solution for consistency. Digestion was carried out for the desired time period (typically 4 hours) at standard culture conditions ($23 - 24$ ^{o}C and 125 rpm in the dark).

When the research presented in this chapter was initiated, we planned on sorting intact *Taxus* cells based on accumulation of paclitaxel using flow cytometry, and examining gene expression in the sorted populations. The previously successfully used procedure was attempted to isolate single cells from *T. cuspidata* P991C and P93AF cell suspensions for gene expression experiments. However, this line of research became

stalled when the process for isolation of viable single cells could not be performed reliably, and hence isolation of RNA from single cells was not possible. Here, some of the research conducted to try and overcome difficulties in isolating viable single cells is summarized.

Intact RNA can only be isolated, and subsequently detected, from viable cells when RNA does not undergo significant degradation post-isolation. Figure 3.4 indicates a denaturing gel electrophoresis for RNA isolated from P93AF *T. cuspidata* aggregated suspension cultures (both MeJA-elicited and unelicited), single cells (SC) and protoplasts (PP) isolated using previously established protocols (Naill et al. 2004, Roberts et al. 2003). Intact total RNA run on a denaturing gel will generally have sharp, clear 28S (~ 5300 bp) and 18S (~ 2000 bp) rRNA bands. The 28S rRNA band should be approximately twice as intense as the 18S rRNA band, as indicated by the RNA ladder. As seen in Figure 3.4, MeJA-elicited cultures, unelicited cultures and protoplasts had intact RNA. However, RNA isolated from single cells exhibited a large smear on the gel, indicating degraded RNA. Viability of cells was verified by fluorescein diacetate (FDA) and propidium iodide (PI) staining, as described in Section 5.2.3. Single cell viability was very low post-enzymatic procedure (< 10 % viable). On the other hand, protoplasts had relatively high viability (up to ~ 90%), which made intact RNA isolation possible. Viability staining of single cells and protoplasts is shown in Figure 3.5.
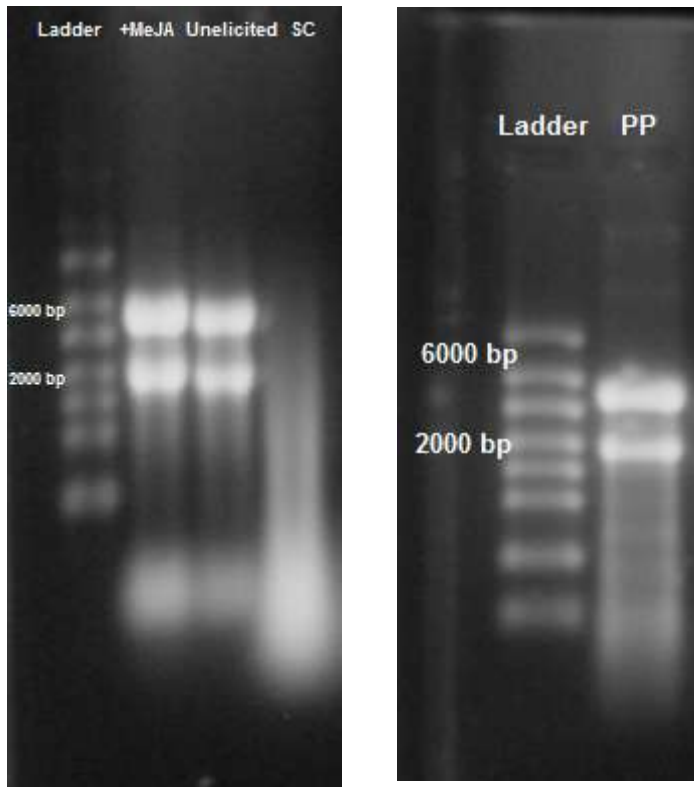
Figure 3.4 Denaturing gel electrophoresis of RNA isolated from aggregated *Taxus* cell cultures (*T. cuspidata* P991C), single cells and protoplasts. Intact and degraded RNA are shown on a 1.5 % denaturing agarose gel. RNA isolated from MeJA-elicited (+MeJA) (day 3 post-elicitation, day 10 of culture period) and unelicited cell cultures (day 10 of culture period), intact single cells (SC) (isolated from day 7 post-transfer cultures), and protoplasts (PP) (isolated from day 7 post-transfer cultures). The 18S and 28S ribosomal RNA bands are clearly visible in the intact RNA samples. The degraded RNA appears as a lower molecular weight smear.
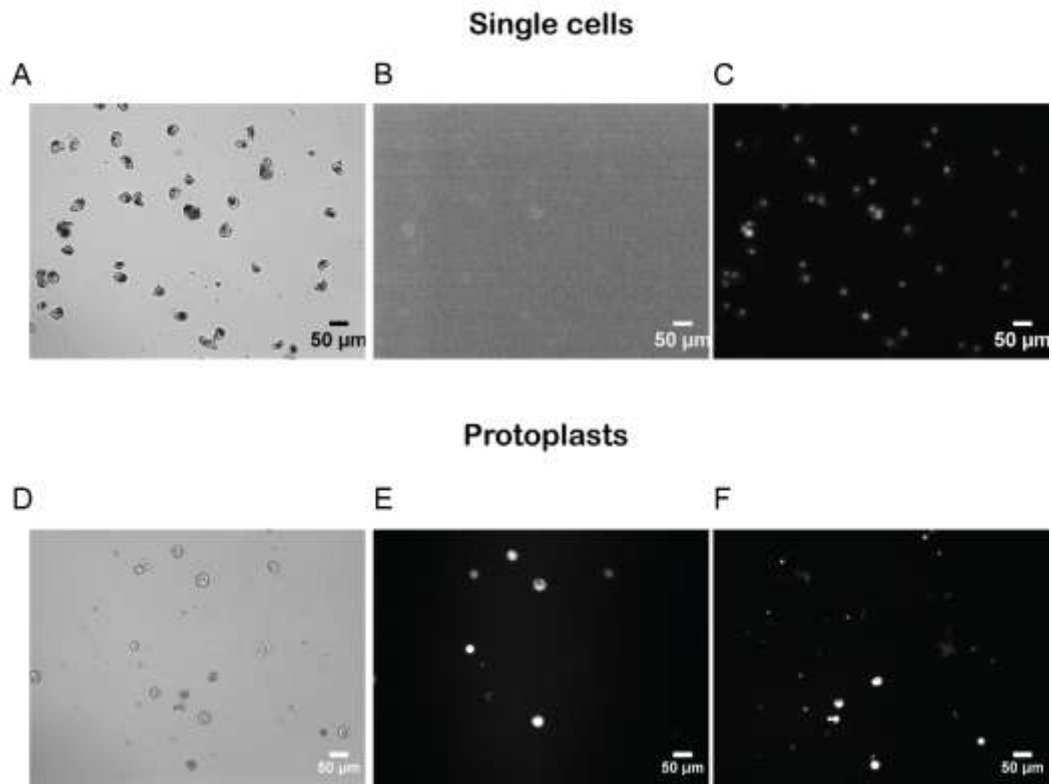
Figure 3.5 Viability staining of single cells and protoplasts isolated from *Taxus cuspidata* P93AF cell line on day 7 of culture period. **(A)**, **(D)** are brightfield images, **(B)** and **(E)** are FDA stained (live) images, **(C)** and **(F)** are PI stained (dead) images. The high background of FDA stain image **(B)** and staining of all the nuclei in PI stain image **(C)** indicate cell death in single cells. In contrast, protoplasts stain positive with FDA **(E)**, with minimal dead protoplasts **(F)**. Bright white spots in (E) and (F) indicate live and dead protoplasts, respectively.

To increase cell viability in the single cell isolation procedure, modifications were made to both the components of the osmoticum solution and the digestion conditions. These experiments were performed in collaboration with Sarah Wilson. Note that the viability of aggregated cultures is always high (~ 95 %) during the timeframes investigated (day 7 – day 14 of the culture period).

1) Varying osmoticum conditions

Aim: To determine the effect of various osmoticum components and osmoticum sterilization conditions on single cell yield and viability.

a) Autoclaving the osmoticum – The osmoticum (0.5 M mannitol and 0.3 % dextran sulfate (DS)), was sterilized either by autoclaving with liquid cycle conditions (121 $^{\circ}$C, 15 min) or filter-sterilizing (using a 0.22 μm filter).

Table 3.2 Effect of varying osmoticum sterilization conditions on single cell isolation in *T. cuspidata* P93AF cell line, using the procedure described above. Cultures ranging from day 7 to day 10 of the culture period were tested. In all cases, viability was measured using FDA and PI staining.

Osmoticum (0.5 M mannitol + 0.3 % DS)	Effect on pH of solution	Single cell yield	Viability of single cells
Autoclave	pH drops from 5.5 to ~ 2	High	All cells are inviable
Filter sterilize	pH remains ~ 5.5	Very low, mostly debris	Very few viable cells (< 5%)

b) Dextran sulfate was removed from the osmoticum.

Table 3.3 Effect of removing dextran sulfate from the osmoticum solution on single cell isolation in *T. cuspidata* P93AF cell line. Cultures ranging from day 7 to day 10 of culture period were tested. In all cases, viability was measured using FDA and PI staining.

Osmoticum (0.5 M mannitol)	Effect on pH of solution	Single cell yield	Viability of single cells
Autoclave	pH changes from 5.5 to ~ 4.6	Very low, mostly cell debris	Very few viable single cells (< 5%)
Filter sterilize	pH remains ~ 5.5	Very low, mostly cell debris	Very few viable single cells (< 5%)

2) Varying the pH of the osmoticum solution

In the previous experiment, it was observed that the pH of the osmoticum affected both cell viability and enzyme activity. At low pH, aggregates were digested to single cells but the cells were not viable. At high pH, the aggregates were completely digested and mostly cell debris was observed, with few viable single cells. In order to create optimal digestion conditions, pH of the regular osmoticum (0.5 M mannitol with 0.3 % DS) was adjusted to an intermediate value. Also, to see the general effect of osmoticum pH on cell viability, cell aggregates were incubated in regular osmoticum (without enzymes) at pH 2, 3, 4, and 6 for four hours and then resuspended in conditioned media (obtained from day 7 post transfer cells) for 12 hours. Both *T. cuspidata* P93AF and P991C cell lines

were used in this study with similar results. Table 3.4 shows the results for the P93AF cell line.

Table 3.4 Effect of varying osmoticum pH on single cell isolation and aggregated culture viability.

Experimental conditions	Results
• 0.5 M mannitol + 0.3 % DS + enzymes • pH adjusted to 3.3	Mostly cell debris and a few viable protoplasts were observed
• 0.5 M mannitol + 0.3 % DS • pH adjusted to 2, 3, 4 and 6 • Cells kept in respective osmoticum for four hours, followed by resuspension in conditioned medium at a concentration of 1 g wet cell mass per 5 mL conditioned medium	• pH 3, 4 and 6 - The cells remained aggregated and were red (stressed) after 12 hours incubation in conditioned medium • pH 2 – Cell aggregates were pale white, but cells were 0 % viable. This result suggests that cell death occurs immediately upon transfer to the osmoticum solution (no time for cells to become stressed and red)

From these experiments, it was determined that the pH of the osmoticum solution has a drastic effect on cell viability and single cell yield. While single cells are obtained when the pH is low (< 3), viability is severely compromised. As the pH is raised to approximately 3, the enzyme activity is possibly increased, resulting in high levels of cell debris, likely due to significant digestion of primary cell walls. In these experiments, single cell viability is very low, but protoplasts that are released from the aggregates remain viable.

Despite all the modifications attempted, a successful balance between single cell yield and cell viability was not attained. One of the possible reasons that the viability of

isolated single cells was considerably lower than that previously reported (Naill and Roberts 2005b) is the variability in *Taxus* cell lines over time. Future studies should consider the results from the above experiments in designing a reliable single cell preparation method that yields viable cells.

CHAPTER 4
TRANSCRIPTOME ANALYSIS OF *TAXUS* CULTURES EXHIBITING METABOLIC AND MORPHOLOGICAL HETEROGENEITY

4.1 Introduction

Transcriptome, or expressed sequence tag (EST), sequencing is an efficient route to generate comprehensive sequence collections that represent expressed genes for a particular cell type in an organism. Transcriptome sequencing of eukaryotic organisms is a more attractive alternative than whole genome sequencing, as the majority of a eukaryotic genome is noncoding and consists of repetitive DNA. Because EST sequences lack introns and intergenic regions, information content can be handled more efficiently and promote a better interpretation of the data. Moreover, whole genome sequencing approaches are expensive and time-consuming, and are currently not feasible in academic laboratories for organisms with large genomes (*e.g.,* plant species like *Taxus*). EST sequencing data can be readily used for gene annotation and discovery, as well as comparative genomics. In plants, a genome- or transcriptome-based analysis can provide valuable insight into important plant metabolic processes. Secondary metabolic processes, which produce a variety of medicinal compounds for human health, are not as well conserved as primary metabolic processes across the plant kingdom. Therefore, even though some plant genomes have been sequenced, understanding, and ultimately manipulating, species-specific secondary metabolic pathways is limited.

For transcriptome sequencing, mRNA is isolated from one or several cell types of an organism or tissue culture and reverse transcribed into cDNA. The cDNA is then

fragmented and sequenced either using traditional Sanger sequencing or next generation sequencing. Use of Sanger sequencing requires fragmented DNA to be subcloned into vectors, followed by amplification in bacterial or viral hosts and then sequenced using the Sanger chain termination method. With the advent of next generation sequencing approaches (e.g., 454, Illumina, SOLiD, etc.), transcriptome sequencing can be completed at a lower cost and in reduced time, as it alleviates the need for cloning, cDNA library construction and labor-intensive Sanger sequencing runs. Amongst the next generation sequencing methods, 454 (Roche) technology offers longer read lengths (about 300 bp), which makes it easier to assemble a transcriptome. Read lengths generated by other next generation sequencing methods such as Illumina and SOLiD are comparatively shorter and can be challenging for *de novo* assembly of a transcriptome, although some algorithms for assembly of such short reads have been developed (Morozova et al. 2009; Garg et al. 2011; Zerbino and Birney 2008). 454 sequencing technology has been used for both assembly of EST data of model plant organisms whose draft genomes are available (Cheung et al. 2006; Weber et al. 2007), and for *de novo* assembly of EST data for organisms where no prior genomic resources are present (Parchman et al. 2010).

With the introduction of low-cost, high-throughput next generation sequencing platforms, genetic information for the *Taxus* species has begun to emerge. Transcriptome sequencing of *Taxus* organs such as needles (Wu et al. 2011), stem and roots (Hao et al. 2011), and cambial meristematic cells (Lee et al. 2010) have been established. However, a transcriptome of cultured *Taxus* cells, which offer the most promising route for sustainable production of paclitaxel and related taxoids at an industrial scale, has not been

generated. A differentially-regulated transcriptome of paclitaxel-accumulating cultured cells including response to secondary metabolite elicitors like MeJA will greatly improve our understanding of global networks affecting paclitaxel biosynthesis. In this work, we used both 454 and Illumina sequencing technologies to generate a base transcriptome for cultured *Taxus* cells (in both paclitaxel-accumulating and nonpaclitaxel-accumulating states). This annotated transcriptome allows for the identification of up-and downregulated transcripts in *Taxus* cultures with variable metabolic patterns. My role in this work was to provide the cell cultures, design the experiments to generate cultures with different treatments, and perform all the metabolite analysis, while Dr. Lenka (Walker Lab) performed the functional annotation and bioinformatics analyses.

The global gene expression profiles of cultures with different metabolic patterns were compared using Illumina sequencing. This global expression study indicated that, along with the paclitaxel biosynthetic pathway, other secondary metabolic pathways were active in MeJA-elicited *Taxus* cultures. Key metabolites from these pathways were also identified in MeJA-elicited cultures, which positively correlated with the gene expression results. For example, along with the paclitaxel biosynthesis pathway, several genes in the phenylpropanoid pathway were upregulated in MeJA-elicited cultures. Lignin and flavonoids, the key metabolites of the phenylpropanoid pathway, were also present in higher quantities in MeJA-elicited cultures as compared to mock-elicited cultures. Activation of the phenylpropanoid pathway and presence of lignin partly explained the observation of increased mean aggregate size of *Taxus* cultures upon MeJA elicitation, as described herein. Though complete analysis of the cultures with different metabolic phenotypes is still ongoing in the paclitaxel collaborative group, preliminary results show

a number of differentially regulated transcripts in each culture-specific state. Such culture-specific global transcript profiling will allow identification of genes involved in global pathway control, including potential paclitaxel biosynthetic genes, and genes that may be involved in other complimentary and competing pathways, to ultimately suggest effective targets for metabolic engineering.

4.2 Materials and methods

4.2.1 Cell culture maintenance, MeJA elicitation and Coulter counter analysis

The *Taxus cuspidata* cell line P93AF was provided by the U.S. Plant Soil and Nutrition Laboratory in Ithaca, NY, and maintained in our laboratory, as described previously (Naill and Roberts 2004). Suspensions were maintained in 500 mL Erlenmeyer flasks capped with Bellco (Vineland, NJ) foam closures at 23 $^{\circ}$C and 125 RPM in gyratory shakers in the dark. Subculture transfers were performed by transferring 40 mL of inocula (corresponding to a packed cell volume of 4-5 mL) originating from a 14-day old suspension culture into 160 mL of fresh medium. For elicitation, cultures were treated with 150 μM methyl jasmonate (MeJA), as described previously (Naill and Roberts 2004). Mock-elicited, or control cultures, were generated by using equivalent amounts of sterile water instead of MeJA. A Multisizer 3^{TM} Coulter counter equipped with a 2,000 μm aperture (Beckman Coulter, Brea, CA) was used to measure biomass and culture aggregate size distributions, as described previously (Kolewe et al. 2010). For Coulter counter analysis, two x 2 mL samples of well mixed culture broth from each of the three replicate flasks were run.

4.2.2 RNA isolation for 454 sequencing

Biological duplicates of MeJA-elicited and mock-elicited cultures were used for RNA isolation and taxane analysis. RNA was isolated at 12h, 36h, 60h, 84h, 108h, 132h, 156h, 180h, 204h, 228h, 252h, 276h, 300h, 324h, and 348h time points spanning 15 days post-elicitation, as described in 3.2.4.1. Equal amounts of total RNA were pooled from each time point for 454 sequencing. After rRNA depletion and fragmentation, a transcriptome library was prepared by sequencing the pooled RNA sample on one full Picotiter Plate (PTP) using the 454 Genome Sequencer FLX Titanium System™ following manufacturer's instructions (Roche, Branford, CT).

4.2.3 Initiation of cultures with different aggregate size distributions and sampling for RNA isolation for Illumina sequencing

Small and large aggregate cultures were generated by altering the aggregate size distribution at the time of culture initiation, as described in 3.2.2. Measurements for biomass and mean aggregate size were taken on the day of inoculation (day 0) and on the day of elicitation with MeJA (day 7). RNA was isolated at both 18 hour and 72 hour time points post MeJA-elicitation, as described in 3.2.4.1. 50 bp paired end mRNA sequencing libraries were prepared from both MeJA-elicited and mock elicited *T cuspidata* P93AF cells at both the 18 and 72 hour time points using Illumina HiSeq 2000 platform (Illumina, Inc. San Diego, CA).

4.2.4 Contig generation, annotation and expression analyses

Reads from both 454 and Illumina sequencing libraries were used in *de novo* assembly to generate contigs using CLC genomics workbench (CLC Bio, Aarhus, Denmark) by setting A, C, G, T voting method for conflict resolution. A total of 48,614 contigs were generated (>200 bp, avg. >100 reads/contig, > 50X coverage) with N50 contig length of 873 bp. These contigs were annotated and assigned gene ontology (GO) terms using Blast2GO default parameters (Conesa et al. 2005). Paired end reads from each Illumina library were mapped onto the contigs using CLC Genomics Workbench software. Gene expression for both MeJA-elicited and mock-elicited cultures at both 18 and 72 hour time points were calculated using RPKM (Reads per kb per million reads) method (Mortazavi et al. 2008). To identify the differentially expressed genes, the proportions-based test was used between any two RNA-seq libraries under comparison with p-value <0.05 (Kal et al. 1999). To calculate the fold change between any two conditions, quantile normalization of the RPKM values was used.

4.2.5 Taxane analysis

Samples for taxane analysis were collected at several time points post-elicitation and analyzed using UPLC, as described in 3.1.7.

4.2.6 Lignin content analysis

For qualitative lignin analysis, MeJA-elicited and mock-elicited cultures were stained with phloroglucinol (Sigma Aldrich). The staining solution was 16 % (v/v) ethanol, 13.5 % (v/v) HCl and 20 mg/mL phloroglucinol. 1 mL of well mixed culture was taken on a

microscope slide, media was removed with a Kimwipe, and the remaining cells were incubated for 3 min in dark, with the phloroglucinol stain solution. The cells were directly photographed using a digital color camera. The cinnamaldehyde end groups of lignin react with the phloroglucinol-HCl to yield a temporary red-violet color (Leple et al. 2007).

For quantitative lignin analysis, acetyl bromide soluble lignin (ABSL) method was used (Foster et al. 2010; Fukushima and Hatfield 2001). This analysis was done in Samuel Hazen's laboratory in UMass, Amherst. Two mg of dried cells (dried in oven overnight at 60 ^{o}C) were dissolved in 100 μl acetyl bromide solution (25% v/v acetyl bromide in glacial acetic acid). The contents were heated at 50 ^{o}C for two hours with occasional mixing by inversion. After cooling the sample to room temperature, 400 μL of 2 M NaOH and 70 μL of 0.5 M hydroxylamine hydrochloride were added. After vortexing the sample, the volume was raised to 2 mL with glacial acetic acid. Optical density at 280 nm was measured using a spectrophotometer. Spectrophotometric readings for MeJA-elicited and mock-elicited cultures were compared to obtain a fold difference in the amount of lignin.

4.2.7 Estimation of total flavonoid content

Flavonoids were extracted and determined using the aluminum chloride (AlCl$_3$) method, as described in (Zhishen et al. 1999). Briefly, 250 mg of dried cells (dried overnight in oven at 60 ^{o}C) were extracted with 1 mL of 80% methanol using sonication in water bath for 30 min. Samples were then centrifuged at 10,000 x g and supernatants collected. 1 mL of distilled water was added to 250 μL of methanol extract, followed by addition of 75

µL of 5% NaNO$_2$ (sodium nitrite). The sample was divided into two parts with equal volumes of approximately 660 µL each. After 5 min. 37.5 µl of 10 % AlCl$_3$ were added to one aliquot, and 37.5 µl of distilled water were added to the other (blank). After one minute, 250 µL of NaOH were added to each aliquot and the total volume was raised to 1.25 mL with distilled water. The solution was well mixed and the absorbance was measured against the blank at 510 nm using a spectrophotometer.

4.3 Results and discussion

4.3.1 Generation of a base transcriptome for *Taxus* cultured cells

A base transcriptome of *Taxus* cell cultures (*T. cuspidata* P93AF cell line) in paclitaxel-accumulating (with MeJA elicitation) and nonaccumulating (without MeJA elicitation) states by *de novo* assembly of 454 and Illumina sequencing reads was generated. A total of 48,614 contigs were generated with N50 contig length of 873 bp. Contig assembly, annotation and gene ontology analysis was done as described in Materials and Methods. The base transcriptome consists of all the genes expressed in *Taxus* cultures through a time period spanning 15 days post elicitation. Corresponding metabolic profiles for baccatin III and paclitaxel are shown in Figure 4.1. Detectable levels of baccatin III were seen after four days post-elicitation. Accumulation peaked at day 10 and then decreased, concurring with previous reports (Nims et al. 2006). Paclitaxel accumulation was detected after five days post-elicitation, increased until day 12, and then leveled off.

4.3.2 MeJA-mediated upregulation of taxane biosynthetic pathway

Cultures with different aggregation characteristics (small and large aggregate cultures, Figure 4.2 A) in both the MeJA-elicited and mock-elicited state were used to generate cultures with varying biosynthetic capabilities (Patil et al. 2012). RNA was isolated at 18 and 72 hours post-elicitation from these cultures (hereafter referred to as Small +MeJA, Small mock, Large +MeJA, and Large mock) to understand which genes and pathways were influenced by MeJA elicitation. As taxane biosynthetic pathway genes peak at approximately 18 hours post elicitation (Patil et al. 2012; Nims et al. 2006), we chose this time point to analyze global gene expression profiles between the MeJA-elicited and mock-elicited small and large aggregate cultures. The 72 hour time point was chosen to uncover genes involved when paclitaxel accumulation begins (Figure 4.1 and (Nims et al. 2006)). This time point allows examination of global expression patterns of genes involved in events such as transport and degradation. Analysis revealed approximately 489 contigs that were annotated as "paclitaxel biosynthetic process (GO: 0042617)" genes. Multiple contigs can represent an individual taxane pathway gene, and therefore far fewer than 489 unique "paclitaxel biosynthetic process" genes are expressed in our cultures. Addition of MeJA induced expression of most paclitaxel biosynthetic process contigs (Figure 4.3). As indicated in the heat map (Figure 4.3), multiple individual contigs form clusters with similar expression patterns. These clusters may reflect individual genes that are represented by multiple contigs, or may represent multiple genes with similar expression patterns. Figure 4.2 shows the time course of taxane metabolite accumulation (10-deacetylbaccatin III, baccatin III and paclitaxel) in both small and large aggregate cultures post MeJA elicitation. Throughout the culture period, mock-elicited

cultures did not produce taxanes at detectable levels via UPLC. These taxane metabolite data positively correlate with the taxane biosynthetic pathway gene expression profiles.

4.3.3 MeJA-mediated upregulation of phenylpropanoid pathway

Along with the paclitaxel biosynthesis pathway, MeJA elicitation upregulated the phenylpropanoid pathway (Figure 4.4) in *T. cuspidata* P93AF cell cultures. Contigs representing genes involved in all steps of the phenylpropanoid pathway were significantly upregulated (data not shown). MeJA is known to induce multiple secondary metabolic pathways within the same culture, e.g., phenylpropanoid and triterpene pathway gene transcripts in *Medicago truncula* cells (Suzuki et al. 2005), and nicotine and phenylpropanoid pathway gene transcripts in tobacco cells (Galis et al. 2006). To validate the upregulation of phenylpropanoid pathway gene expression, relevant metabolites such as lignin and total flavonoids were measured in these cultures. Significant lignin accumulated in MeJA-elicited *Taxus* cultures, as indicated by a positive phloroglucinol-HCl test (Figure 4.5B, C, D, and E). A quantitative acetyl bromide assay revealed that MeJA-elicited cultures accumulate ~ 23% more lignin than mock-elicited cultures (Figure 4.5A). The absolute value of lignin content in the cultures was determined by the % ABSL method described in Foster et al. (2010), using a conversion factor for *Arabidopsis*. The lignin content values in mock-elicited cultures was ~ 190 mg/g biomass, whereas MeJA-elicited cultures had ~ 234 mg/g biomass (~ 23 % increase). These values are well within the range observed for other plant species (39.1 – 312.7 mg lignin/g biomass) as determined by % ABSL method (Fukushima and Hatfield 2001). An increase in lignin content from 19 mg/g (control cultures) to 74 mg/g (elicitor-treated cultures) was observed in spruce cell cultures treated with a fungal elicitor, using

the thioacidolysis method to determine lignin (Lange et al. 1995). The total flavonoid content, quantified by a spectrophotometric method, was considerably higher (~ 122 %) in MeJA-elicited cultures as compared to mock-elicited cultures (Fig 4.5A). These data confirm an increase in flux through phenylpropanoid pathways upon MeJA addition, a result which was not previously observed in cultured *Taxus* cells. Phenylalanine is a precursor to both the taxane and phenylpropanoid pathways. Increasing the precursor pools of phenylalanine, and redirecting carbon flux towards taxane biosynthesis by silencing target genes in the phenylpropanoid pathway (Figure 4.6) may allow for greater availability of phenylalanine for paclitaxel biosynthesis.

4.3.4 Increased mean aggregate size upon MeJA elicitation potentially linked to upregulation of phenylpropanoid metabolism

The mean aggregate size of the MeJA-elicited cultures increased after elicitation and remained higher throughout the course of the experiment in comparison to mock-elicited cultures (Figure 4.7). Jasmonic acid (JA) and MeJA have been shown to cause cell swelling and expansion in mature tuber discs (Takahashi et al. 1994), tuber buds (Abdala et al. 1999) and polyphenolic parenchyma (PP) cells in conifer trees (Hudgins and Franceschi 2004). One mechanism suggested was that MeJA may disrupt cortical microtubules, which leads to cell expansion; however such disruption was seen only in small fraction of MeJA-treated cells (Matsuki et al. 1992; Abe et al. 1990). Another possible mechanism is an increase in the amount of cell wall polysaccharides, which has been observed in potato cells in response to JA (Takahashi et al. 1995). Lignin incorporation leading to thickened cell walls has also been observed in fungal-elicited cell cultures (Eberhardt et al. 1993; Campbell and Ellis 1992). Similarly, increases in

94

production of monolignols and oligolignols, building blocks of lignin (through upregulation of the phenylpropanoid pathway), has been documented in MeJA-elicited Arabidopsis cultures; however, changes in cellular morphology were not reported (Pauwels et al. 2008). Lignins and ferulic acids, which are also derivatives of the phenylpropanoid pathway, are known to form ferulate-polysaccharide-lignin complexes, which cross-link the cell wall (reviewed in (de O. Buanafina 2009)). It has been observed that during stationary phase, cells get released from aggregates and there is reduced cell division, which leads to a decrease in mean aggregate size (Capataz-Tafur et al. 2011; Mavituna and Park 1987; Kolewe et al. 2010). The presence of cross-linking within the cell wall can cause stiffening, which may inhibit cell release. Upregulation of phenylpropanoid pathway genes and some of the metabolites can result in generation of such ferulate-polysaccharide-lignin complexes in MeJA-elicted *Taxus* cultures, resulting in stronger cell aggregates. Mock-elicited cultures would lack such complexes, resulting in cellular release from aggregates at stationary phase, leading to smaller culture mean aggregate size.

4.3.5 Further analysis of transcriptional patterns in cultures with different morphological and metabolic patterns

In order to improve our understanding about the pathways that affect paclitaxel levels within *Taxus* cultured cells, we are further investigating the transcriptional difference between the large and small aggregate cultures. Preliminary global gene expression results indicate that a number of transcripts are differentially upregulated (Figure 4.8A) and downregulated (Figure 4.8B) in these cultures at 18 and 72 hours post-elicitation. The differential transcripts obtained from these cultured cells can be linked to available

pathway databases (e.g., KEGG or MetaCyc) to draw conclusions as to which pathways are active during a particular phenotypic state; this work is ongoing by Dr. Lenka. Such a global comparison of cultures with different bulk paclitaxel/taxane accumulation patterns will provide a superior understanding of *Taxus* cultures at the level of transcription and will certainly provide new targets for metabolic engineering, as evidenced by the phenylpropanoid example described above.

4.4 Conclusions

The transcriptome of cultured *Taxus* cells has been sequenced, *de novo* assembled and characterized, providing a valuable resource for developing a better understanding of the *Taxus* genome. Along with the paclitaxel biosynthetic pathway, the phenylpropanoid pathway is also upregulated upon elicitation with MeJA, supported by increased lignin and flavonoid accumulation in MeJA-elicited cultures as compared to mock-elicited cultures. Although detailed analysis of cultures with differential metabolic and aggregation phenotypes is still pending, preliminary results indicate several transcripts which are differentially regulated in these phenotypes. The annotated transcriptome sequences and culture-specific gene expression profiles will illuminate our understanding of global transcriptional control of paclitaxel biosynthesis, and its cooperating and competing pathways in *Taxus* cultures for enabling targeted metabolic engineering.
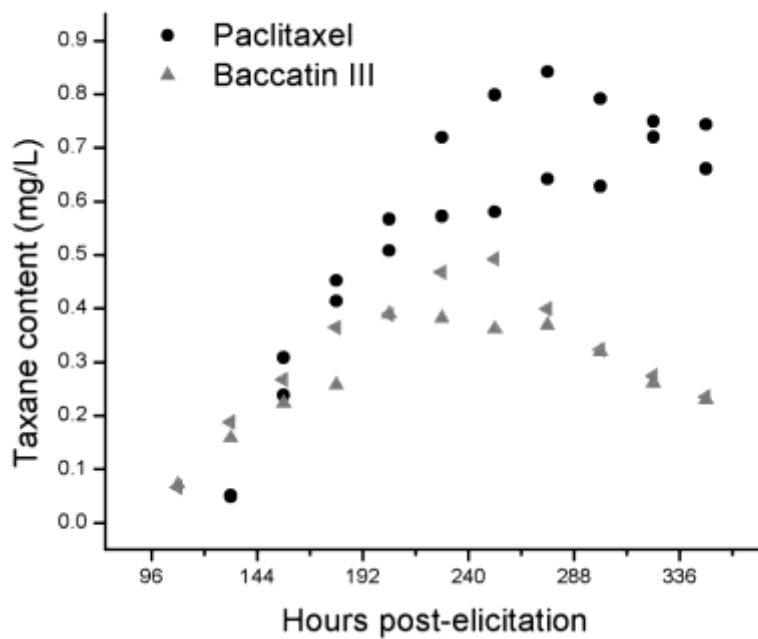
Figure 4.1 Time course of taxane accumulation after MeJA elicitation in *T. cuspidata* P93AF cultures. Cultures were either elicited with 150μm MeJA or mock-elicited on day 7 of the culture period. The data represent two biological replicates for each taxane at each timepoint. Circles represent paclitaxel. Triangles represent baccatin III.
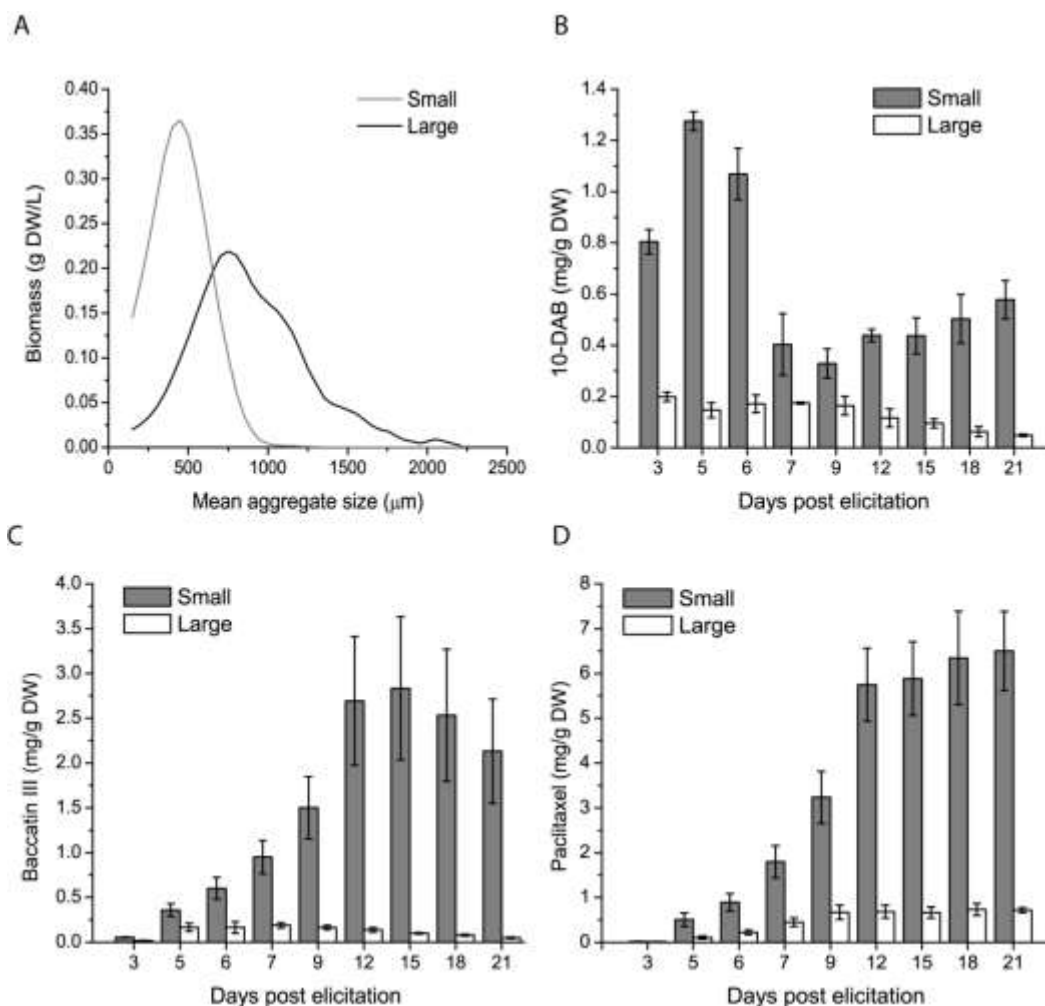
Figure 4.2 Profiles of taxane accumulation in small and large aggregate cultures over a three-week period post MeJA-elicitation. **(A)** Distributions for small aggregate cultures and large aggregate cultures on day 7, prior to MeJA elicitation. Each distribution curve represents the average distribution measured using a Coulter counter for three replicate flasks. Time course of 10-deacetylbaccatin III **(B)**, baccatin III **(C)**, and paclitaxel **(D)** accumulation in small and large aggregate cultures post MeJA elicitation. Reported values are the average of three replicate flasks and error bars represent standard error of the mean. Throughout the culture period, mock-elicited cultures did not produce taxanes at detectable levels.
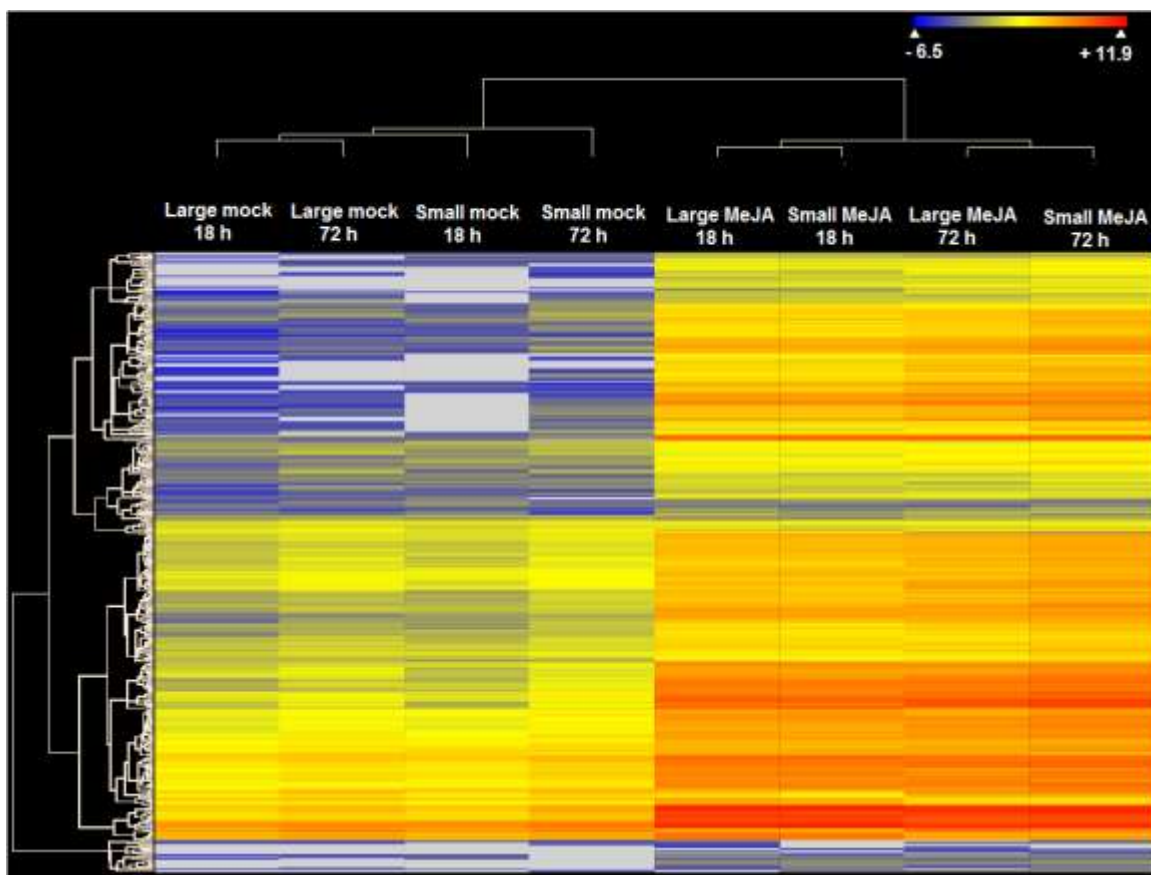
Figure 4.3 Heat map showing the hierarchical clustering of differentially expressed paclitaxel biosynthesis genes displayed by average linkage and Euclidean distance as a measurement of similarity. The heat map was generated by Dr. Lenka using the CIMminer software (http://discover.nci.nih.gov/cimminer/).
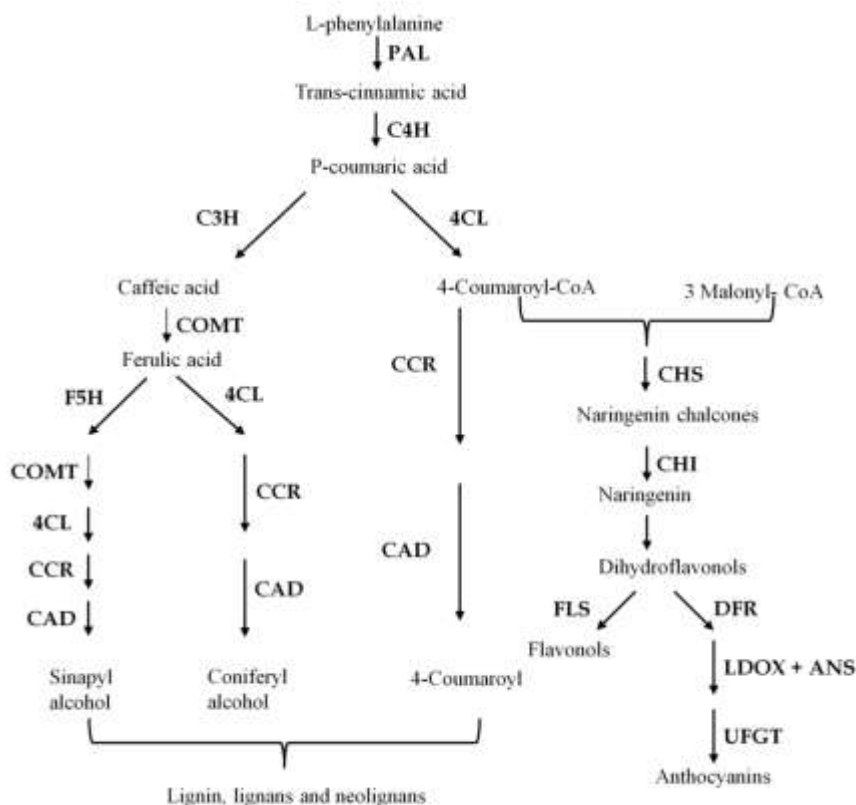
Figure 4.4 Outline of phenylpropanoid biosynthesis pathways. Enzymes are reported with a three letter code: PAL, phenylalanine ammonia lyase; C4H, cinnamate 4-hydroxylase; 4CL, 4-coumarate CoA ligase; C3H, p-coumaroyl shikimate/quinate 3-hydroxylase; COMT, caffeic acid/5-hydroxyferulic acid O-methyltransferase; F5H ferulate 5-hydroxylase; CCR, (hydroxy)cinnamoyl CoA reductase; CAD, (hydroxy) cinnamyl alcohol dehydrogenase; CHS, chalcone synthase; CHI, chalcone isomerase; FLS, flavonol synthase; DFR, dihydroflavonol 4-reductase; ANS, anthocyanidin synthase; LDOX, leucoanthocyanidin dioxygenase; UFGT, UDP glucose-flavonoid 3-o-glucosyl transferase. Contigs representing all the genes of this pathway were upregulated in MeJA-elicited condition.
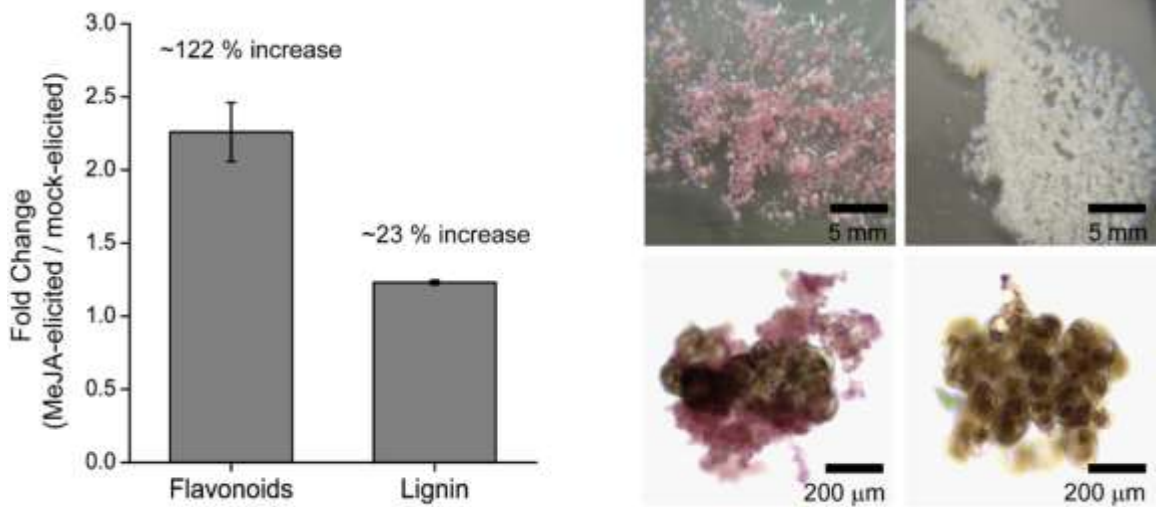
Figure 4.5 Increased phenylpropanoids upon elicitation with MeJA. **(A)** Total flavonoid content was measured using the aluminum chloride method, and lignin was measured using the acetyl bromide soluble lignin method. Fold change represents the percentage increase in MeJA-elicited samples relative to mock-elicited samples at day 13 of the culture period (6 days post-elicitation). Reported values are the average of three replicate flasks and error bars represent standard error of the mean. Phloroglucinol-HCl staining of MeJA-elicited cultures, **(B)** and **(D)**; and control cultures, **(C)** and **(E)**. Pink/red color indicates the presence of lignin as measured by phloroglucinol-HCl staining.
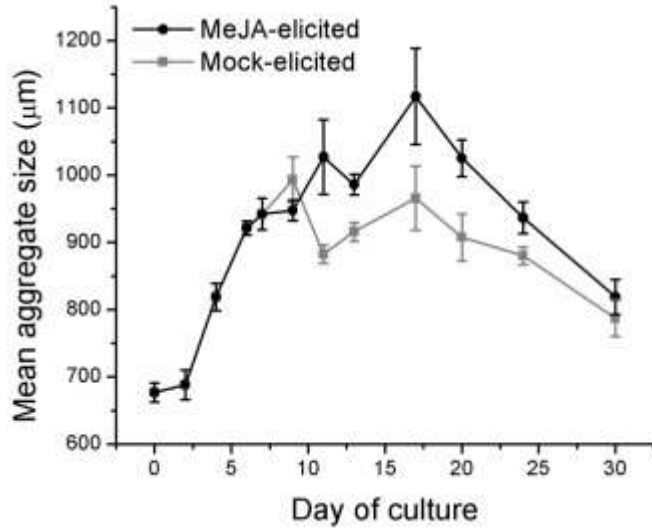
Figure 4.6 Effect of MeJA addition on mean aggregate size of the culture. Cultures were either elicited with 150 μM MeJA or mock-elicited on day 7 of the culture period. Reported values are the average of three replicate flasks and error bars represent standard error of the mean.
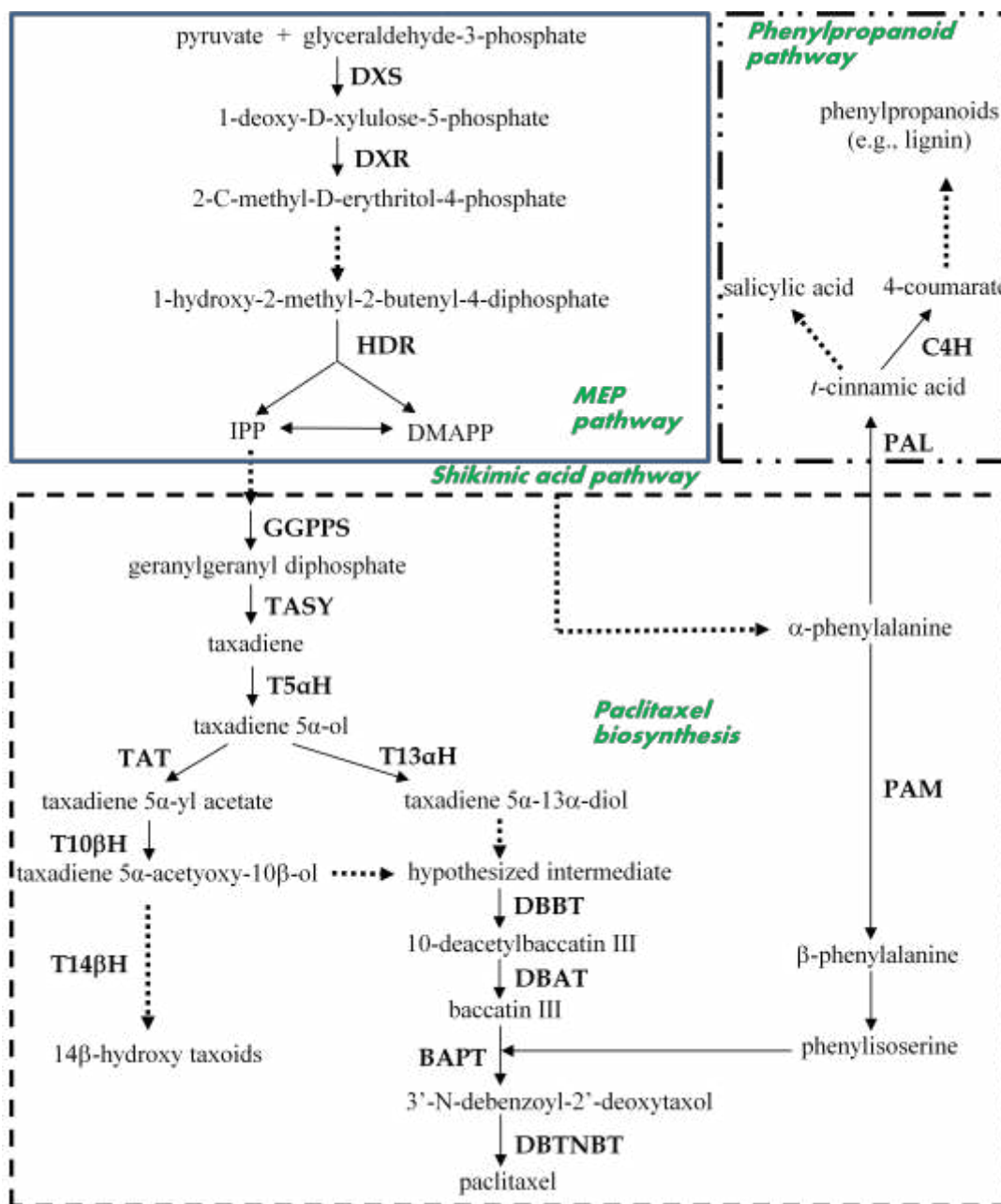
Figure 4.7 Overview of paclitaxel biosynthesis and interacting pathways. Dotted arrows represent multiple steps. Thick arrows represent multiple steps, with some unknown reactions. DXS:1-deoxy-D-xylulose-5-phosphate (DXP) synthase, DXR: DXP reductoisomerase, HDR: 1-hydroxy-2-methyl-butenyl 4- diphosphate reductase, IPP: isopentenyl pyrophosphate, DMAPP: dimethylallyl pyrophosphate, GGPPS:

geranylgeranyl diphosphate synthase, TASY: taxadiene synthase, T5αH: taxadiene 5α hydroxylase, TAT: taxadienol acetyl transferase, T13αH: taxadienol 13α hydroxylase, T10βH: taxane 10β hydroxylase, T14βH: taxoid 14β-hydroxylase, DBBT: taxane 2α-O-benzoyl transferase, DBAT: 10 deacetylbaccatin III-10-O-acetyltransferase, BAPT: baccatin III: 3-amino, 3-phenylpropanoyltransferase, DBTNBT: 3'-N-debenzoyl-2-deoxytaxol-N-benzoyltransferase, C4H:cinnamate-4- hydroxylase, PAL: phenylalanine ammonia lyase, PAM: phenylalanine aminomutase.
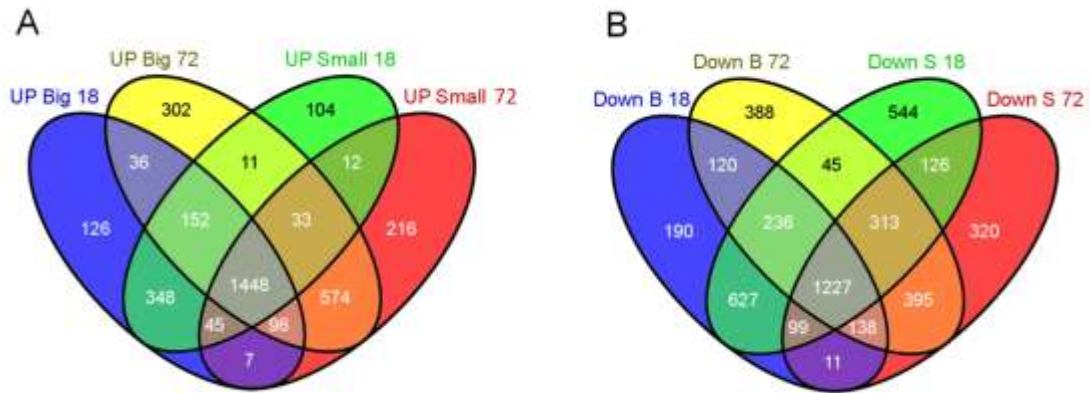
Figure 4.8 Venn diagrams representing overlap between upregulated genes upon elicitation with MeJA. **(A)** and downregulated **(B)** in the different conditions (Small MeJA 18h, Small mock 18h, Small MeJA 72h, Small mock 72h, Big MeJA 18h, Big mock 18h, Big MeJA 72h, Big mock 72h). The large aggregate cultures have been referred to as big aggregate cultures in this figure. Venn diagrams were generated by Dr. Lenka using the ASAP-utilities add on for Excel (http://www.asap-utilities.com/).

CHAPTER 5
METHYL JASMONATE REPRESSES GROWTH AND AFFECTS CELL CYCLE PROGRESSION IN CULTURED *TAXUS* CELLS

5.1 Introduction

Dedifferentiated plant cell suspension cultures provide a regulated environment independent of geographical and external environmental factors for the synthesis of plant-based secondary metabolites. Cell suspension culture offers a distinct advantage over tissue or organ culture as existing bioprocess technology developed for microbial and mammalian cells can be easily adapted to plant cells (Kieran et al. 1997). The use of elicitors in plant cell suspension culture can both increase product yields and consequently decrease the long fermentation times, facilitating the use of plant cell culture technology in commercial applications. Jasmonic acid (JA) and its methyl ester, methyl jasmonate (MeJA) have been widely used as elicitors to induce secondary metabolite production in a variety of plant cell culture systems (Gundlach et al. 1992; Lijavetzky et al. 2008; Pauwels et al. 2008; Yazaki et al. 1997). In particular, jasmonates have been effective at enhancing production of the anticancer drug paclitaxel (Taxol®) in a variety of *Taxus* species and cell cultures (Ketchum et al. 1999; Yukimune et al. 1996; Bonfill et al. 2006). Paclitaxel is widely used for treatment of breast, ovarian and lung cancers as well as AIDS-related Kaposi's sarcoma, and is being investigated for use in the treatment of neurological disorders and in post-surgery heart patients (Vongpaseuth and Roberts 2007). Paclitaxel titers of up to 900 mg/L have been achieved in industrial environments using a combination of MeJA elicitation and cell culture optimization strategies (Bringi V 2007).

Increased secondary metabolite accumulation upon MeJA elicitation is often accompanied with concurrent decreases in culture growth (Thanh et al. 2005; Kim et al. 2005; Zhang and Turner 2008). MeJA has been shown to broadly induce defense responses and secondary metabolism in plants (Reymond and Farmer 1998; Seo et al. 2001; Farmer and Ryan 1990), which diverts carbon resource allocation from primary metabolism (Logemann et al. 1995; Pauwels et al. 2009). Recent studies indicate that MeJA-mediated growth inhibition is associated with perturbations in mitochondrial membrane integrity along with decreases in the biosynthesis of ATP (Ruiz-May et al. 2011) and proteins related to energy metabolism (Cho et al. 2007).

At a mechanistic level, MeJA has demonstrated an inhibitory effect on growth at the level of the cell cycle (Pauwels et al. 2008; Swiatek et al. 2002). Most studies to understand the effect of jasmonates on the cell cycle have been done in angiosperms, such as *Arabidopsis thaliana* and tobacco BY-2 cell suspension cultures (Pauwels et al. 2008; Swiatek et al. 2002). Exogenously applied MeJA blocks the G1/S and G2/M transitions in the cell cycle of cultured tobacco BY-2 cells (Swiatek et al. 2002). Micromolar concentrations of MeJA added to *A. thaliana* suspension cultures repressed the activation of M phase genes, arresting cells in G2 phase (Pauwels et al. 2008). Genomic information and established protocols for synchronizing cell cultures (Kumagai-Sano et al. 2006; Menges et al. 2002) to understand cell cycle events are readily available for these plant species, facilitating mechanistic studies. In contrast, gymnosperms such as *Taxus* have not been as well studied with regard to cell cycle progression and the mechanism of MeJA-repressed growth.

While a number of studies have reported increased taxane biosynthetic pathway gene products upon MeJA elicitation (Nims et al. 2006; Patil et al. 2012; Jennewein et al. 2004), there have been few reports regarding the role of MeJA on growth inhibition and cell cycle progression in *Taxus* cultures (Kim et al. 2005; Naill and Roberts 2005a). In the present study we investigate the influence of MeJA on both cell growth and viability of *Taxus* cells in batch culture. The effect of MeJA on cell cycle progression was determined using asynchronous *Taxus cuspidata* cells. Actively dividing cells were quantified and cell cycle kinetics were determined by cumulative and pulse-labeling using 5-ethynyl-2'-deoxyuridine (EdU), a nucleoside analog of thymidine. Recently obtained 454 and Illumina transcriptome sequencing data for both MeJA-elicited and mock-elicited cultures were used to obtain the expression status of cell cycle-associated genes in the asynchronous *T. cuspidata* cultured cells. There is currently no sequence information on cell cycle regulated genes derived from this division of the plant kingdom, and hence these studies provide the first insight into cell cycle control upon elicitation with MeJA. Because the mechanism of action of MeJA has not been investigated to date for gymnosperms such as *Taxus*, strategies to promote growth, while still enhancing secondary metabolite synthesis for bioprocessing, have not been identified or tested. The results here show that MeJA-induced growth repression in *Taxus* growth occurs at the level of cell cycle, providing important mechanistic information on the influence of MeJA on *Taxus* cell proliferation.

5.2 Materials and methods

5.2.1 Cell culture maintenance and MeJA elicitation

The *T. cuspidata* P93AF cell line was provided by the U.S. Plant Soil and Nutrition Laboratory (Ithaca, NY), and maintained in our laboratory on gyratory shakers in the dark at 125 rpm and 23 ^{0}C. Cell cultures were maintained in 125 mL, 250 mL or 500 mL glass Erlenmeyer flasks with Bellco (Vineland, NJ) foam closures. Every two weeks, cells were subcultured into growth medium, which consisted of Gamborg's B5 basal salts with 20 g/L sucrose, supplemented with 2.7 μM naphthalene acetic acid (NAA) and 0.1 μM benzyladenine (BA). 150 mg/L of citric acid, 150 mg/L ascorbic acid, and 6.0 mM glutamine were filter-sterilized and added post-autoclave. For elicitation, 40 μL of 100% methyl jasmonate (MeJA) was added to 460 μL of 95% (v/v) ethanol and 500 μL nanopure water. This solution was vortexed and then filtered through a 0.2 μm Gelman PVDF filter into a sterile container. This solution was then added to the cultures on day 7 post-transfer to yield a final concentration of 150 μM. The foam closures were covered with aluminum foil to prevent evaporation. Mock-elicited cultures were generated by using equivalent amounts of sterile water instead of MeJA. All chemicals were purchased from Sigma-Aldrich unless otherwise specified.

5.2.2 Biomass and taxane content measurements

A Multisizer 3™ Coulter counter equipped with a 2000 μm aperture (Beckman Coulter, Brea, CA, USA) was used to determine total biomass dry weight based on previously published correlations (Kolewe et al. 2010). For analysis, two x 2 mL samples of well-

mixed culture broth (cells plus media) were taken from each flask. Taxane content in mock-elicited and MeJA-elicited cultures were analyzed at several time points post-elicitation using Ultra Performance Liquid Chromatography (UPLC), as described previously (Patil et al. 2012).

5.2.3 Viability analysis

Qualitative analysis of viability was performed by staining with fluorescein diacetate (FDA) and propidium iodide (PI). 500 μL of well-mixed culture was sampled, to which 10 μL of a 0.5 mg/mL FDA stock solution and 4 μL of a 1 mg/mL PI stock solution was added. After a 10 min incubation in the dark, supernatant was removed, and 500 μL of fresh Gamborg's B5 medium was added. 100 μL of cell suspension was observed under a fluorescence microscope. A Zeiss Axiovert 200 inverted microscope fitted with a blue filter set (excitation at 450–490 nm and emission above 515 nm) for FDA fluorescence and a green filter set (excitation at 530–560 nm and emission above 580 nm) for PI fluorescence was used. FDA detects living cells, whereas PI detects non-viable cells. FDA is a non-fluorescent molecule that is able to diffuse into a cell. Once in a viable cell, intercellular esterases hydrolyse FDA to fluorescein, a highly fluorescent molecule. Viable cells retain the fluorescein and emit fluorescence, whereas dead cells do not fluoresce (Skehan P. 2002; Widholm 1972). Esterases released from unviable cells can result in background fluorescence. PI is a hydrophilic dye that cannot penetrate intact cell membranes. However, it can diffuse into cells with compromised membranes and intercalate with DNA, causing cells to fluoresce, indicating cell death.

5.2.4. DNA laddering assay

Total genomic DNA was extracted following the method of Dellaporta et al. (1983) with a slight modification. Fresh cells (0.2 g) were ground in liquid nitrogen with mortar and pestle. Grinded cells were transferred to a sterilized Eppendorf tube and dissolved in 600 µL buffer (pH 8.0) consisting of NaCl (100 mM), Tris/HCl (50 mM), EDTA (25 mM), sodium dodecyl sulfate (1%, w/v), and β-mercaptoethanol (10 mM). The mixture was shaken vigorously through inversion and incubated in a water bath at 65 ^{o}C for 10 min. 250 µl of potassium acetate (5 M) was added to the mixture, which was incubated on ice for 30 min followed by centrifugation at 10,000g for 10 min at 4 ^{o}C. The supernatant was collected and mixed with equal volume of 100% isopropanol (approximately 600 µL). The precipitate formed was centrifuged, washed with 70% (v/v) ethanol, and redissolved in 200 µl of buffer (10 mM Tris/HCl, 5 mM EDTA, pH 8.0). Further precipitation was achieved by addition of 20 µL sodium acetate (3 M, pH 5.2), followed by 500 µL of 100% (v/v) ethanol and gentle inversion to completely mix the two phases. Precipitates were centrifuged, washed with 70% (v/v) ethanol and then dried at room temperature. Pellets were resuspended in 40 µL buffer (10 mM Tris/HCL, 1 mM EDTA, pH 8.0). RNAse A (100 µg/mL) was added to digest RNA at 37 ^{o}C for 30 min. DNA concentrations were quantified using a Nanodrop 1000 spectrophotometer (Thermo Scientific, Wilmington, DE, USA). For analysis of DNA laddering, equal amounts of DNA were run on a 1.5 % (w/v) agarose gel stained with ethidium bromide (0.5 µg/mL), and observed under a UV transilluminator. 1 kbp and 100 bp DNA ladders (New England Biolabs) were used as molecular weight markers.

5.2.5 Isolation and fixation of intact nuclei

Approximately 0.5 g of biomass (about 3-4 ml of well mixed culture broth) were filtered through Miracloth® (Calbiochem, La Jolla, CA), and transferred to a petri dish to isolate nuclei (Galbraith et al. 1983; Gaurav et al. 2010). 1 mL of Galbraith buffer [45 mM $MgCl_2$, 30 mM sodium citrate, 20 mM 3-(N-morpholino)-propanesulfonic acid (MOPS), 0.3 % (w/v) Triton X-100, pH 7.0] at 4 ^{o}C was added to the biomass sample, and the biomass was chopped approximately 500 times with a sharp razor blade to disrupt cell walls and allow nuclei to be released. An additional 2 mL of Galbraith buffer was added to resuspend the chopped biomass, and this suspension was successively filtered over 80 μm and 30 μm nylon mesh (SmallParts, Inc., Miramar, FL). Post-filtration, nuclei were fixed with 1% paraformaldehyde (dissolved in Galbraith's buffer) at 4 ^{o}C for 30 min. Fixed nuclei were washed twice with Galbraith's buffer by centrifuging at 700 g for 4 min at 4 ^{o}C. After washing, nuclei were resuspended in 1 mL of Galbraith's buffer and stored at 4 ^{o}C until further analysis.

5.2.6 Distribution of cells in different phases of the cell cycle

Triplicate samples of MeJA-elicited and mock-elicited cultures were sampled and nuclei were isolated at several time points post-elicitation as described above. 1 mL of the nuclei solution were aliquoted, and 50 μL of 1 mg/mL RNAse and 50 μL of 1 mg/mL PI were added. Samples were stained for at least 30 min on ice before flow cytometric analysis (see below).

5.2.7 EdU incorporation assay

MeJA-elicited and mock-elicited *Taxus* cell cultures were maintained in medium containing 10 μM EdU for the required incubation period (see cumulative and pulse labeling below). Nuclei were isolated from the EdU-labeled cultures, fixed and incubated with 250 μL EdU detection cocktail (Click-iT EdU Alexa Fluor 488 Flow Cytometry Assay kit, cat no: C35002, Invitrogen, Carlsbad, CA) at room temperature for 30 min as per manufacturer's protocol, with slight modifications. For one sample reaction (250 μL), the following amounts of kit components were used: 219 μL of 1X Click-iT Reaction buffer (Component G, diluted to 1X in Galbraith's buffer), 5 μL Copper (II) sulfate solution (Component H, 100 mM aqueous CuSO4), 1.25 μL Alexa Fluor 488 azide (Component B) and 25 μL 1X buffer additive (component I, diluted to 1X in Galbraith's buffer). Post incubation, 2 mL of Galbraith's buffer were added to the samples as a wash; samples were centrifuged at 700 g and 4 ºC for 4 min, and resuspended in 0.5 mL Galbraith's buffer for subsequent staining and analysis. 1 mg/mL of RNAse A was added followed by 1 mg/mL 7-aminoactinomycin D (7-AAD) (Invitrogen, Carlsbad, CA). Samples were incubated for 60 min at room temperature before flow cytometric analysis (see below).

5.2.8 Pulse labeling of MeJA-elicited and mock-elicited cultures

MeJA-elicited and mock-elicited cultures on day 5 of the culture period were pulse-labeled for 4 hours with 10 μM EdU. Cells were collected by centrifugation at 800 g for 5 min, and washed with conditioned medium. Conditioned medium was obtained by decanting settled MeJA-elicited and mock-elicited cell suspensions incubated without

EdU under the same conditions. The wash procedure was repeated two more times to eliminate excess EdU. The volume was then adjusted with conditioned medium to that before washing, and cultures were continued in the absence of EdU. Samples of pulse-labeled cells were taken periodically over 48 hours and processed for EdU analysis. A series of bivariate DNA-EdU distributions at various times after pulse-labeling was obtained using flow cytometry (see below).

5.2.9 Cumulative labeling of MeJA-elicited and mock-elicited cultures

MeJA-elicited and mock-elicited cultures on day 7 of the culture period were incubated with 10 µM EdU. After EdU addition, nuclei were isolated and fixed every 24 hours for the following 5 days. Isolated nuclei were stained for EdU (Alexa Fluor 488) and DNA content (7-AAD) (see above) and analyzed via flow cytometry (see below).

5.2.10 Flow cytometry

For nuclei analysis, a Becton Dickinson (San Jose, CA) LSRII analytical flow cytometer equipped with an argon laser tuned to 488 nm with the standard filter set-up was used. A minimum of 5000 events were collected in the gated region of a forward scatter and side scatter plot corresponding to nuclei. The scatter plots were manually gated to exclude debris and doublets. For cell cycle analysis, forward scatter and side scatter were collected on a logarithmic scale, and PI fluorescence was collected on a linear scale. For cumulative- and pulse-EdU labeling analysis, a bivariate plot of DNA-EdU was obtained. Alexa Fluor 488 EdU intensity was detected between 515-545 nm. For detection of 7-AAD intensity (DNA content) the 663-677 nm emission range was used with the standard filter sets available on the LSRII. The boundary of EdU-labeled nuclei in

biparametric plots was obtained by subtracting the background using a non-EdU treated culture.

5.2.11Cell cycle-associated contig generation, annotation and expression analysis

RNA was isolated from *T. cuspidata* P93AF cells (MeJA-elicited and mock-elicited) every 24 hours post-elicitation over a time period spanning 22 days of the culture period. Equal amounts of total RNA from each culture were pooled from each time point for 454 sequencing. After rRNA depletion and fragmentation, a transcriptome library was generated by sequencing the pooled RNA sample on one full PicoTiterPlate (PTP) using the 454 Genome Sequencer FLX Titanium System™, following the manufacturer's instructions (Roche, Branford, CT). In addition, 50 bp paired end mRNA-sequencing libraries were prepared from both MeJA-elicited and mock-elicited *T. cuspidata* P93AF cells at 18 and 72 hour time points using the Illumina HiSeq 2000 platform (Illumina, Inc. San Diego, CA). Reads from both 454 and Illumina sequencing libraries were used in *de novo* assembly to generate contigs using CLC genomics workbench (CLC Bio, Aarhus, Denmark) by setting A, C, G, T voting method for conflict resolution. A total of 48,614 contigs were generated (>200 bp, avg. >100 reads/contig, >50X coverage) with N50 contig length of 873 bp. These contigs were annotated using Blast2GO default parameters (Conesa et al. 2005). Based on the Blast2GO annotation, 149 contigs representing known cell cycle-associated genes were identified (Table S1). Paired end reads from each Illumina library were mapped onto the contigs using CLC Genomics Workbench software. Gene expression for both MeJA-elicited and mock-elicited P93AF cells at the 18 and 72 hour post-elicitation time points were calculated by using the RPKM (Reads per kb per million reads) method (Mortazavi et al. 2008). To identify

differentially expressed genes, the proportions-based test was used between any two RNA-seq libraries under comparison with a *p*-value <0 .05 (Kal et al. 1999). To calculate the fold change between any two conditions, quantile normalization of the RPKM values was used.

5.3 Results

5.3.1 MeJA represses cell growth without significant changes in necrosis and apoptosis

Inhibition of growth after MeJA elicitation has been observed in a variety of *Taxus* species and cell lines (Laskaris et al. 1999; Kim et al. 2004; Yukimune et al. 1996; Bonfill et al. 2006), as well as other plant cell culture systems (Goossens et al. 2003; Thanh et al. 2005). Although most reports indicate a decrease in *Taxus* cell growth upon MeJA elicitation, some data show no difference in cell growth between MeJA-elicited and non-elicited *Taxus* cell lines (Bonfill et al. 2007; Ketchum et al. 1999). Upon addition of MeJA on day 7 of the culture period, *T. cuspidata* P93AF cell cultures clearly demonstrate repressed growth (Figure 5.1A) and increased taxane production (Figure 5.1B) as compared to mock-elicited cultures.

Subsequently, we examined the viability of cultures using fluorescein diacetate (FDA) and propidium iodide (PI), to indicate both viable and non-viable cells, respectively. Eight time points were examined spanning 24 days of the culture period; representative data are shown in Figures 1c and 1d. Both MeJA-elicited and mock-elicited cultures exhibited approximately 90% to 95% viability until day 16 of the culture period (9d post-elicitation) (Figure 5.1C and 5.1D). At later time points, the FDA

116

fluorescence intensity decreased in both MeJA-elicited and mock-elicited cultures, implying a decrease in metabolic activity for all cultures (Li et al. 2011). More PI fluorescent cells were observed in MeJA-elicited cultures as compared to mock-elicited cultures on days 21 and 24 of the culture period (14d and 17d post-elicitation) (Figures 1c and 1d), indicating compromised cell membrane integrity and the beginning of cell necrosis in MeJA-elicited cultures. There was a time lag between evidence of reduced viability and a measurable decrease in biomass (dry weight), as has been observed with other *Taxus* cell lines (Kim et al. 2005; Naill and Roberts 2005a).

A hallmark feature of apoptotic cell death is the fragmentation of DNA into oligonucleosomal fragments of approximately 180-200 bp or multiples thereof, giving rise to a ladder during gel electrophoresis of genomic DNA (Yuan et al. 2002; Ryerson and Heath 1996). Genomic DNA was isolated from MeJA-elicited and mock-elicited cultures on day 11, day 24 and day 30 of the culture period. A DNA laddering pattern was not observed until day 30 of the culture period (23d post-elicitation) in mock-elicited and MeJA-elicited cultures (Figure 5.2), indicating that apoptosis is not a direct consequence of MeJA elicitation. Repression of cell growth thus occurs before significant necrosis and apoptosis begins in MeJA-elicited *Taxus* cultures, which necessitates further investigation into the cell cycle to understand the role of MeJA in growth inhibition.

5.3.2 MeJA causes a transient increase in G2 phase cells and a decrease in S phase cells, followed by an arrest at G0/G1 in asynchronous *Taxus* suspension cultures

Nuclei were isolated from mock-elicited and MeJA-elicited cultures and stained with PI for flow cytometric-based DNA quantification. A flow cytometric DNA histogram of

117

Taxus nuclei is shown in Figure 5.3D for reference. All data presented were extracted from similar histograms. The percentage of cells in the different cell cycle phases were calculated using the Watson Pragmatic Model of FlowJo software (v 7.6, Tree Star, Inc.). The proportion of cells in each cell cycle phase in mock-elicited and MeJA-elicited cultures is shown in Figure 5.3 (A-C). Within the first 24 hours post-elicitation, MeJA-elicited cultures had more cells in G2 phase (18% in MeJA-elicited, 13% in mock-elicited cultures) and fewer cells in S phase (10% in MeJA-elicited, 14.5% in mock-elicited cultures) when compared to mock-elicited cultures. This trend was confirmed by further analyzing cultures at shorter time increments before 24 hours post-elicitation (Additional information, Figure 5.7). After 72 hours post-elicitation the percentage of cells in both G2 and S phases decreased and the distributions shifted towards a higher percentage of cells in G0/G1. An increased G0/G1 cell population post-MeJA-elicitation has also been observed with another *Taxus* cell suspension line (Naill and Roberts 2005a).

5.3.3 MeJA slows down the cell cycle

5-ethynyl-2'-deoxyuridine (EdU) pulse labeling was used to investigate the effect of MeJA on cell cycle kinetics. A four-hour EdU pulse was provided to both MeJA-elicited and mock-elicited cultures. As cells only in S-phase are able to incorporate EdU, labeled cells were quantified as they pass through different phases of the cell cycle (S to G2/M to G0/G1) using the bivariate DNA-EdU distributions obtained with flow cytometry. Approximately 10% EdU incorporation was used for pulse labeling, which allows enough cells to be labeled for accurate quantification using flow cytometry. A similar percentage of 5-bromo-2'-deoxyuridine (BrDU) incorporation was used successfully in pulse labeling studies of *Solanum aviculare* cells (Yanpaisan et al. 1998). The G0/G1 peak in

118

mock-elicited cultures appeared 9 hours after the EdU pulse; whereas it took 24 hours after the EdU pulse to observe the G0/G1 peak in MeJA-elicited cultures (Figure 5.4). This later appearance of the G0/G1 peak in MeJA-elicited cultures clearly demonstrates that MeJA repressed cell cycle progression in *Taxus* cultures. However, the appearance of the G0/G1 peak in MeJA-elicited cultures indicates that the cell cycle is not arrested at the G2/M transition.

5.3.4 MeJA decreases the number of cycling cells

Cumulative EdU incorporation in MeJA-elicited and mock-elicited *Taxus* cultures is shown in Figure 5.5. Five days after incubation with EdU, the number of cells incorporating EdU in mock-elicited cultures was approximately 45% of the total cell population, whereas in MeJA-elicited cultures it was only 12% of the total cell population. These data indicate that MeJA addition results in fewer cells participating in DNA synthesis, hence a lower number of actively cycling cells in culture. Repression of DNA synthesis and blockage of cells in G1 and G2 phases of the cell cycle upon MeJA-elicitation have also been observed in synchronized tobacco BY-2 cell cultures (Swiatek et al. 2002).

5.3.5 MeJA represses a number of genes participating in cell cycle progression

Using a combination of deep sequencing technologies and Blast2GO annotation (see Experimental Methods for details), 149 cell cycle-associated contigs (referred to as cell cycle-associated genes from here onwards) were identified in the transcriptome of mRNA isolated from cultured *Taxus* cells (Additional information Table 5.5). A comparison of gene expression between mock-elicited and MeJA-elicited cultures was done at 18 hours

and 72 hours post-elicitation. At both 18 hours and 72 hours post-elicitation, none of the 149 cell cycle associated-genes were upregulated in MeJA-elicited cultures relative to the mock-elicited cultures. However, a total of 52 cell cycle genes were significantly downregulated (> 2-fold down regulation, $P < 0.05$) at 18 hours and 72 hours post-elicitation in MeJA-elicited cultures relative to mock-elicited cultures. Figure 5.6 shows the hierarchical clustering of the 52 cell cycle genes that were downregulated in MeJA-elicited cultures. At 18 hours post-elicitation, 49 genes that were homologous to genes involved in the G2/M and G1/S transition in other plant species were downregulated in MeJA-elicited cultures (Table 5.1). In particular, the gene representing E2F target protein 1 (ETG1), which is a component of the replisome complex and needed for DNA replication (Takahashi et al. 2008), was drastically downregulated (~160 fold). The transcription factor E2F, which in Arabidopsis governs expression of ETG1 and other cell cycle genes [about 70 target genes, (Vandepoele et al. 2005)] involved in the G1/S transition was also downregulated. Genes representing CDC6 (Castellano et al. 2001), CDC45 (Stevens et al. 2004), CDC48 and D-type cyclins (Meijer and Murray 2000), whose expression typically peaks during G1 or early S phase, and some of the genes representing B-type cyclins and other G2 and M phase-specific genes that facilitate progression through mitosis were also downregulated.

At 72 hours post-elicitation, about 20 cell cycle genes were significantly downregulated in MeJA-treated cultures (Table 5.2). Most of these genes (17 out of 20) were also downregulated at the 18 hour time point when compared to mock-elicited cultures. However, in contrast to the 18 hour time point, which had genes representing both the G1/S and G2/M transition, the majority of the downregulated genes at 72 hours

were those whose expression typically peaks during G2 and M phase. For example, Cyclin A1, B1, B2, cyclin dependent kinase B (CDKB) and -other G2/M specific cyclins, whose transcripts are known to accumulate during G2 and M phases (Inze and De Veylder 2006), were found to be the most downregulated (> 10-fold downregulation, Table 5.2). This result implies that in MeJA-elicited cultures, fewer cells are going through mitosis at the 72 hour time point as compared to mock-elicited cultures.

A comparison was made between the gene expression levels at 18 hours and 72 hours for both mock-elicited and MeJA-elicited cultures (18h mock-elicited vs. 72h mock-elicited and 18h MeJA-elicited vs 72h MeJA-elicited). There was no change in expression of cell cycle-related genes in the mock-elicited cultures. However, comparison between 18h MeJA-elicited and 72h MeJA-elicited cultures showed that genes that are usually expressed during G2 and M phase (e.g., cyclin dependent kinase B, cyclin A1, cyclin B2 and B3, etc.) were downregulated at 72 hours as compared to 18 hours (Table 5.3). Some G1 phase-specific genes (e.g., D-type cyclins and CDC 48 homologs) were upregulated at 72 hours as compared to 18 hours (Table 5.4).

Apart from the cell cycle-specific genes, genes representing the subclasses of core histones, H2A, H2B, H3 and H4, which are essential for cell proliferation and required for the packaging of DNA into chromatin (Yi et al. 2006; Gutierrez 2009) were also repressed in MeJA-elicited cultures at both 18 and 72 hours (Additional information, Tables 5.6 and 5.7).

5.4 Discussion

In the present study, we quantified the effect of MeJA, a widely used enhancer of plant secondary metabolism, on asynchronously dividing *T. cuspidata* cell cultures. Biomass measurements showed that MeJA repressed culture growth (Figure 5.1A). There was a time lag between growth inhibition and cell death, indicating that MeJA-mediated growth inhibition was not due to necrosis and/or rupturing of cell membranes (Figure 5.1C, D). Biotic (fungal derived) and abiotic (Cerium (Ce^{+4})) elicitors induce apoptotic cell death in *Taxus* cultures within a few hours to few days post-elicitation (Yuan et al. 2002; Qiao et al. 2003; Ge et al. 2002). Here, we observed DNA fragmentation, a hallmark of apoptotic cell death, only at a very late time point (day 30 of the culture period), implying that apoptosis is not directly linked to MeJA elicitation (Figure 5.2). Similar results have been reported for *T. cuspidata* P991 and *T. canadensi*s C093D cell lines upon MeJA elicitation (Kim et. al, 2005). One explanation for this anomalous behavior for MeJA is that MeJA elicitation in *Taxus* suspensions did not markedly increase the phosphatic acid (PA) levels, which is associated with regulating cell death response (Yang et al. 2008). Ce^{+4} caused both increased paclitaxel levels and increased PA levels, leading to cell death (Yang et al. 2008). Repression of growth without cell death and a delayed onset of apoptosis suggest that MeJA is repressing growth by altering cellular metabolism and/or affecting the cell cycle. We previously demonstrated that MeJA upregulates paclitaxel biosynthetic pathway genes (Patil et al. 2012; Nims et al. 2006; Lenka et al. 2012), and thus metabolism is shifted towards synthesis of paclitaxel. Here, the influence of MeJA on the *Taxus* cell cycle and the mechanism of growth inhibition have been elucidated.

MeJA addition to asynchronously dividing *Taxus* cultures resulted in four effects on the cell cycle, as revealed by flow cytometric analyses: i) transient increase in G2 phase cells, ii) transient decrease in S phase cells, iii) increase in G0/G1 phase cells at later stages post-elicitation, and iv) decreases in G2 and S phase cells at later stages post-elicitation (Figure 5.3 and 5.6). At a mechanistic level, the effect of jasmonates has been shown to be dependent on the phase of the cell cycle in synchronized tobacco BY-2 cells (Swiatek et al. 2002). When JA was applied before the G1/S transition it prevented DNA replication, keeping BY-2 cells in G1 phase. When JA was applied during S phase, it prevented cells from entering mitosis without directly affecting their DNA synthesis (Swiatek et al. 2002; Swiatek et al. 2004). Though our cultures were not synchronized, a similar effect was observed upon MeJA elicitation, with a drop in the percentage of cells in S phase and an increase in the percentage of cells in G2 phase immediately following elicitation. The decreased percentage of cells in G2 and S and increased percentage of cells in G0/G1 at 96 hours post-elicitation suggest that the cells were not permanently arrested in G2/M, but rather moving slowly. An EdU pulse label assay confirmed these data showing clearly that MeJA addition slowed progression through the cell cycle (Figure 5.4).

The transcription of several cell cycle genes at 18 hours and 72 hours post-elicitation with MeJA also correlated with the flow cytometric data trends. Concomitant with the decrease in S phase cells (Figure 5.3B), significant downregulation of expression of ETG1 and CDC6 genes at the 18 hour time point was observed. Expression of ETG1 and CDC6 genes has been shown to be necessary for the G1/S transition in Arabidopsis (Castellano et al. 2001; Takahashi et al. 2008). Genes representing CDC45 (Stevens et al.

2004) and CDC48 homologs (Feiler et al. 1995), which play a role in the G1/S transition were also downregulated. Plant cyclins are known to interact with cyclin-dependent kinases (CDKs), and these CDK-cyclin complexes regulate the key G1/S and G2/M transition points responsible for DNA replication and mitosis, respectively. Plant cyclins, especially the A and B types, show oscillatory behavior at the transcription level, where transcript levels peak during certain phases of the cell cycle. Generally, D-type cyclins are known to regulate the G1/S transition, A-type cyclins regulate the S/M transition, and B-type cyclins regulate both the G2/M transition and M phase control (Breyne and Zabeau 2001; Inze and De Veylder 2006); though a number of exceptions to these functional assignments have been reported (Inze and De Veylder 2006; Kawamura et al. 2006). Genes representing all these three classes of cyclins were downregulated at the 18 hour time point in MeJA-elicited cultures relative to mock-elicited cultures. Also, cyclin-dependent kinase B (CDKB) genes, which are regulated at the transcript level and are necessary for the G2/M transition (Inze and De Veylder 2006), were downregulated at 18 hours in MeJA-elicited cultures. The expression patterns of some of these cell cycle genes are thus consistent with the increase in G2 phase cells within 24 hours post-elicitation with MeJA (Figure 5.3C). At 72 hours post elicitation, the majority of downregulated genes were those for which expression peaked during G2 and M phases (e.g., cyclin A1, CDKB, cyclin B2, etc.). Some of the genes that are involved in G1/S transition (e.g., ETG1, CDC45, etc.) were also downregulated at the 72 hour time point (Table 5.2), indicating that cell proliferation and progression of cells from G1 for division is hindered.

Comparison of cultures at 18 and 72 hours post-elicitation with MeJA shows that G2/M-specific cell cycle genes (e.g., G2-mitotic specific cyclin, cyclin A1, CDKB, etc.) are downregulated at 72 hours as compared to 18 hours (Table 5.3). This result implies that the downregulation of genes required to drive cells through G2 and M phases causes more cells to remain in G2 phase. Some G1 phase genes (e.g., cyclin D (d2-4 type cyclin) and CDC 48, Table 5.4) are also upregulated at 72 hours as compared to 18 hours post-elicitation, implying that more cells are present in G0/G1 phase at 72 hours relative to 18 hours in MeJA-elicited cultures. These results correlate well with flow cytometric data (Figure 5.3), where both a decrease in G2 and S phase cells and an increase in G0/G1 phase cells were observed after 72 hours post-elicitation.

Moreover, along with the cell cycle-specific genes, histone-encoding genes were also downregulated upon MeJA elicitation. Histones are highly conserved across eukaryotic species and have been classified into four subcategories of core histones (H2A, H2B, H3, and H4) and linker histones (H1). For most species, each core histone protein is encoded by a multigene family (Piontkivska et al. 2002). Biotic and abiotic stresses can repress expression of histone genes in plants. For example, in cultured parsley cells, UV radiation and fungal elicitors repressed expression of several genes essential for cell cycle progression including histones H2A, H2B, H3, and H4 (Logemann et al. 1995), leading to growth inhibition. Similar results were observed here in MeJA-elicited *T. cuspidata* cultures, where all the genes representing histones were downregulated relative to mock-elicited cultures at both 18 and 72 hours post-elicitation. Thus, histone gene repression can be correlated to decreased cell division in *Taxus*, analogous to observations in parsley cells (Logemann et al. 1995).

The number of cells incorporating EdU was significantly lower in MeJA-elicited cultures when compared to mock-elicited cultures (Figure 5.5). This result suggests that over time the number of actively dividing cells (i.e., synthesizing DNA) decreased in MeJA-elicited cultures. This result is supported by the increase in G0/G1 phase cells observed in MeJA-elicited cultures (Figure 5.3A). One explanation is that cells remain in G0 phase and are specialized for accumulation of paclitaxel and potentially other secondary metabolites (Naill and Roberts 2005a). Total metabolic activity inferred from total cellular protein content is relatively uniform in MeJA-elicited cultures (Naill and Roberts 2005c), indicating that non-cycling cells are still metabolically active, but potentially redirect carbon flux away from primary metabolism towards secondary metabolism. Alkaloid accumulation increased in cultures of *Solanum aviculare* where cell cycle progression was inhibited using a cell cycle arrest agent, again suggesting that the metabolic flux may be directed towards secondary pathways in non-proliferating cells (Mak and Doran 1993). Research to date in plant systems has been able to identify a significant G0 population in culture and presents indirect evidence to suggest a function of this population, but has not been able to explicitly correlate the non-cycling cell population to other metabolic information. A multi-parametric flow cytometry study to simultaneously analyze non-cycling cells (G0 phase cells) and paclitaxel-accumulating cells can reveal this relationship in the *Taxus* cell culture system, and warrants further investigation.

In summary, the MeJA-mediated repression of cell growth in *Taxus* cultures was shown to correlate with inhibition of cell cycle progression as evident both at the culture level through flow cytometric analyses and at the transcriptional level by repression of

key cell cycle-associated genes. The newly annotated *Taxus* cell cycle-associated genes will provide an importance resource for future cell cycle studies of both *Taxus* and related gymnosperms. The cell cycle progression patterns in culture closely parallel the transcriptional regulation of cell cycle-associated genes in MeJA-elicited and mock-elicited *Taxus* cell cultures. The results from this study advance fundamental understanding of the mechanism of action of secondary metabolite elicitors such as MeJA on repression of plant cell division. This result is especially important for species such as *Taxus*, where most research has been focused on improving paclitaxel synthesis with less attention paid to the negative effect of MeJA on growth and implications on bioprocessing.

Table 5.1 Contigs expressed in *Taxus* cell cultures and annotated as cell cycle-related

genes downregulated in MeJA-elicited cultures relative to mock-elicited cultures at 18

hours post-elicitation.

Contig No.	Sequence description	Fold Change (Normalized)
140962	E2F target protein 1	-163.64
121259	cell division control protein 6 homolog	-143.52
65828	ccb22_orysj ame: G2 mitotic-specific cyclin-B2-2	-36.41
12355	probable G2 mitotic-specific cyclin	-33.23
10406	cyclin dependent kinase regulator	-26.23
11366	D2 4-type cyclin	-19.75
68975	G2 mitotic-specific cyclin S13-6	-14.18
61510	D3-type cyclin	-6.19
119383	cyclin dependent kinase B	-5.46
118076	cell division control protein 45 homolog	-5.21
19091	cell division cycle-associated 7-like isoform 2	-5.03
68106	B1-type cyclin dependent kinase	-5.00
66244	cyclin-dependent kinases regulatory subunit	-4.41
141136	cyclin A1	-4.35
18492	cyclin B 2	-4.17
62294	E2F protein	-3.49
142510	antagonist of E2F-DP complex	-3.26
9782	cyclin-dependent kinases regulatory subunit	-3.14
11005	cell division cycle protein	-3.05

12010	cyclin-dependent kinases regulatory subunit	-2.89
75242	cyclin B3-1	-2.88
108329	cell division cycle protein	-2.81
57179	cell division	-2.74
105427	cell division cycle protein 48 homolog	-2.72
91147	cell division cycle protein 48 homolog	-2.60
113240	cell division control protein	-2.57
134490	cell division cycle protein	-2.56
99133	cell division cycle protein 48 homolog	-2.55
100939	cell division cycle protein 48 homolog	-2.51
10476	transcription factor E2F	-2.50
103306	cell division cycle protein 48 homolog	-2.43
110709	cell division cycle protein 48 homolog	-2.41
97765	cell division control protein	-2.39
134513	cell division cycle protein	-2.37
127620	cell division cycle protein 48 homolog	-2.37
109918	cell division cycle protein 48 homolog	-2.35
112279	cell division cycle protein 48 homolog	-2.35
105698	cell division cycle protein 48 homolog	-2.34
106161	cell division control protein	-2.33
59549	D2 4-type cyclin	-2.31
116949	cell division cycle protein 48 homolog	-2.26
111055	cell division cycle protein 48 homolog	-2.18
107757	cell division cycle protein 48 homolog	-2.18
109405	cell division cycle protein 48 homolog	-2.11

102800	cell division cycle protein	-2.07
13227	cyclin dependent kinase A	-2.05
109272	cell division cycle protein 48 homolog	-2.03
18149	cyclin-dependent kinase F-1	-2.00
100185	cell division cycle protein 48 homolog	-2.00

Table 5.2 Contigs expressed in *Taxus* cell cultures and annotated as cell cycle-related genes downregulated in MeJA-elicited cultures relative to mock-elicited cultures at 72 hours post-elicitation.

Contig No.	Sequence description	Fold change (normalized values)
141136	cyclin A1	-49.32
119383	cyclin dependent kinase B	-44.40
65828	ccb22_orysj ame: G2 mitotic-specific cyclin-B2-2	-42.36
12355	probable G2 mitotic-specific cyclin	-40.96
142510	antagonist of E2F-DP complex	-40.53
68975	G2 mitotic-specific cyclin S13-6	-32.15
68106	B1-type cyclin dependent kinase	-27.65
118076	cell division control protein 45 homolog	-23.96
66244	cyclin-dependent kinases regulatory subunit	-23.03
11005	cell division cycle protein	-20.99
10406	cyclin dependent kinase regulator	-14.94
140962	E2F target protein 1	-12.52
75242	cyclin B3-1	-9.86
9782	cyclin-dependent kinases regulatory subunit	-8.81
79802	cell division cycle cofactor of APC complex	-6.64
10476	transcription factor E2F	-5.79
81095	anaphase-promoting complex subunit CDC20	-5.69
61510	D3-type cyclin	-3.68
12010	cyclin-dependent kinases regulatory subunit	-3.51

125598	cell division control protein	-3.25
19091	cell division cycle-associated 7-like isoform 2	-3.12
18492	cyclin B 2	-2.99

Table 5.3 Contigs expressed in *Taxus* cell cultures whose expression is downregulated 72 hours post-elicitation as compared to 18 hours post-elicitation in MeJA-elicited cultures.

Contig No.	Sequence Description	Fold Change (normalized values)
119383	cyclin dependent kinase B	-17.90
141136	cyclin A1	-13.62
66244	cyclin-dependent kinases regulatory subunit	-13.34
68975	G2 mitotic-specific cyclin S13-6	-8.09
68106	B1-type cyclin dependent kinase	-7.96
75242	cyclin B3-1	-6.74
12355	probable G2 mitotic-specific cyclin	-5.50
79802	cell division cycle cofactor of APC complex	-4.97
65828	ccb22_orysj ame: G2 mitotic-specific cyclin-B2-2	-4.79
81095	anaphase-promoting complex subunit CDC20	-4.06
9782	cyclin-dependent kinases regulatory subunit	-3.62

Table 5.4 Contigs expressed in *Taxus* cell cultures whose expression is upregulated 72 hours post-elicitation as compared to 18 hours post-elicitation in MeJA-elicited cultures.

Contig No.	Sequence Description	Fold Change (normalized values)
11366	D2 4-type cyclin	16.25
11041	cyclin-dependent protein	3.50
59549	D2 4-type cyclin	2.55
107757	cell division cycle protein 48 homolog	2.19
100185	cell division cycle protein 48 homolog	2.18
112647	cell division cycle protein 48 homolog	2.15
109272	cell division cycle protein 48 homolog	2.13
145394	cell division control protein	2.12
113719	cell division cycle protein 48 homolog	2.04
92332	cell division cycle protein 48 homolog	2.04
101973	cell division cycle protein 48 homolog	2.04
107852	cell division cycle protein 48 homolog	2.01
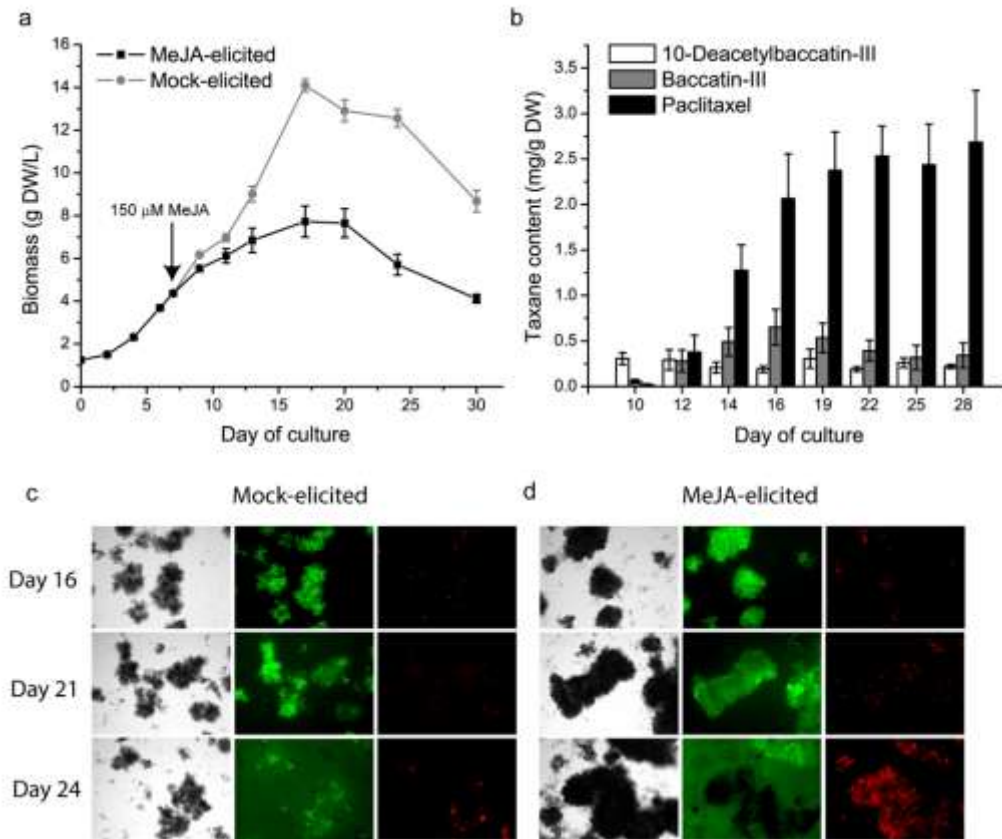
Figure 5.1 Effect of MeJA elicitation on *T. cuspidata* P93AF cultures growth, taxane production and viability. **(A)** Biomass concentrations in MeJA-elicited cultures as compared to mock-elicited cultures. Reported values are the average of three biological replicates and error bars represent standard error of the mean (SEM). **(B)** Taxane levels as determined by UPLC in MeJA-elicited cultures as compared to mock-elicited cultures. Mock-elicited cultures did not produce detectable levels of taxanes. Reported values are the average of three biological replicates and error bars represent SEM. **(C, D)** Viability of mock-elicited and MeJA-elicited cultures on day 16 (Row 1), day 21 (Row 2), and day 24 (Row 3) of the culture period. Columns indicate brightfield (Column 1), FDA-stained (Column 2) and PI-stained (Column 3) images. Cultures were either mock-elicited or elicited with 150 μM MeJA on day 7 of the culture period.
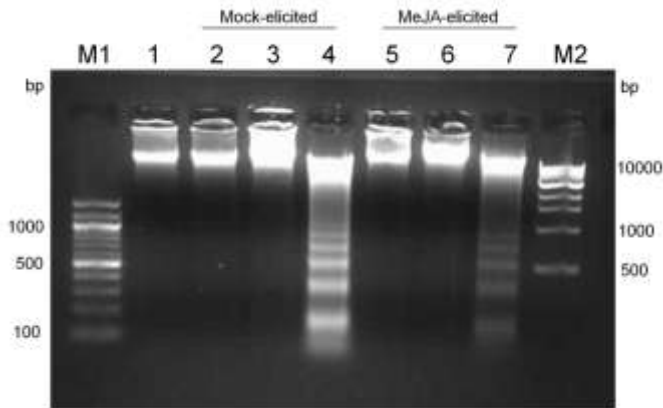
Figure 5.2 Effect of MeJA elicitation on induction of oligonucleosomal fragmentation in cultured *T. cuspidata* P93AF cells. The agarose gel shows DNA extracted from mock-elicited and MeJA-elicited cultures. M1, 100 bp marker; lane 1, mock-elicited (day 7); lanes 2, 3 and 4, mock-elicited cultures on day 11, 24 and 30 of culture period, respectively; lanes 5, 6, and 7, MeJA-elicited cultures on day 11, 24 and 30 of the culture period, respectively; M2, 1 kbp marker. Cultures were either mock-elicited or elicited with 150 μM MeJA on day 7 of the culture period.
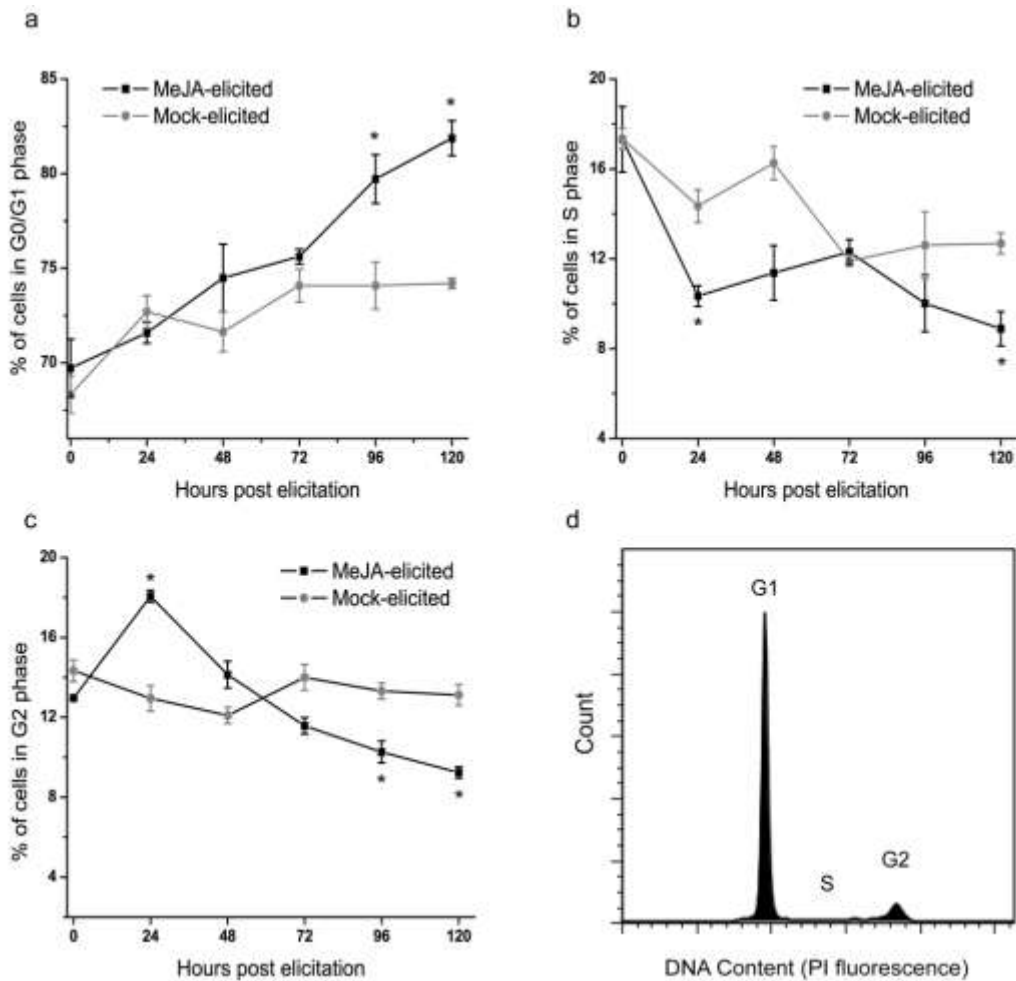
Figure 5.3 Cell cycle distribution in MeJA-elicited and mock-elicited *T. cuspidata* P93AF cultures. The percentage of cells in **(A)** G0/G1, **(B)** S, and **(C)** G2/M phases is shown. **(D)** Cell cycle analysis using the Watson Pragmatic Model of the FlowJo (v7.6) software. RNAse A (50 µg/mL) treatment, followed by staining with propidium iodide (PI) (50 µg/mL) was performed to obtain DNA histograms. Reported values are the average of three biological replicates and error bars represent SEM. The asterisk (*) indicates a statistically significant difference ($P < 0.05$; paired Student's t test) between MeJA-elicited and mock-elicited conditions. Cultures were either mock-elicited or elicited with 150 µM MeJA on day 7 of the culture period.

137
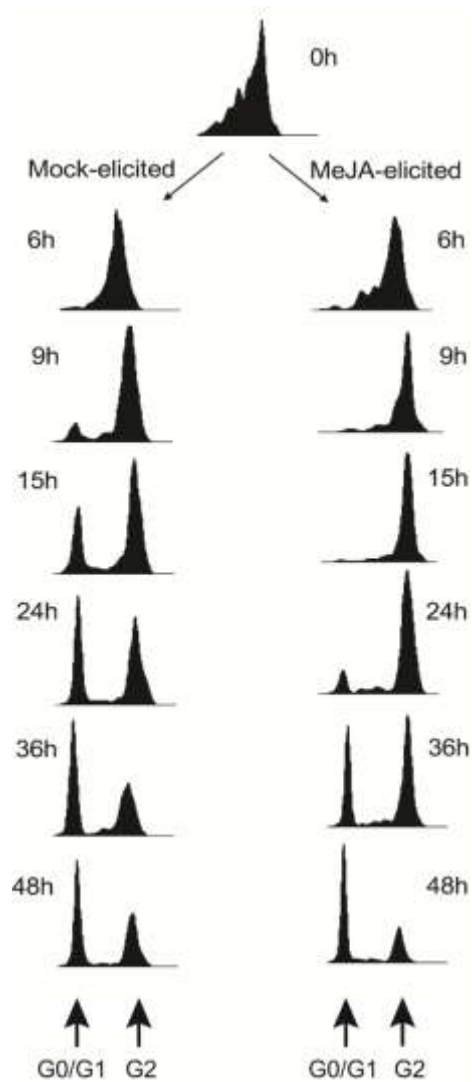
Figure 5.4 Progression of EdU pulse labeled cells in mock-elicited and MeJA-elicited cultures. Only EdU positive cells were selected from bivariate histograms of EdU/DNA content. Cultures were either mock-elicited or elicited with 150 μM MeJA on day 7 of the culture period. Four hours later 10 μM EdU was added to all cultures.
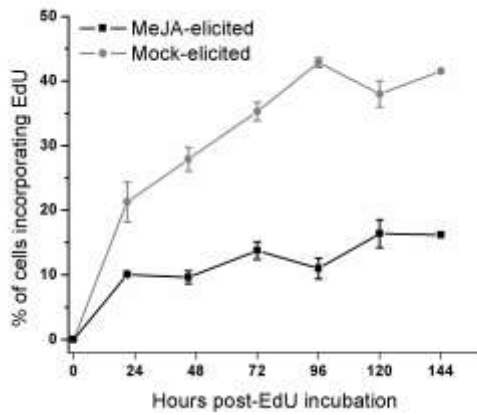
Figure 5.5 Total EdU incorporation in mock-elicited and MeJA-elicited cultures. Circles represent mock-elicited cultures. Squares represent MeJA-elicited cultures. Cultures were either mock-elicited or elicited with 150 μM MeJA on day 7 of the culture period. Four hours later 10 μM EdU was added to all cultures.
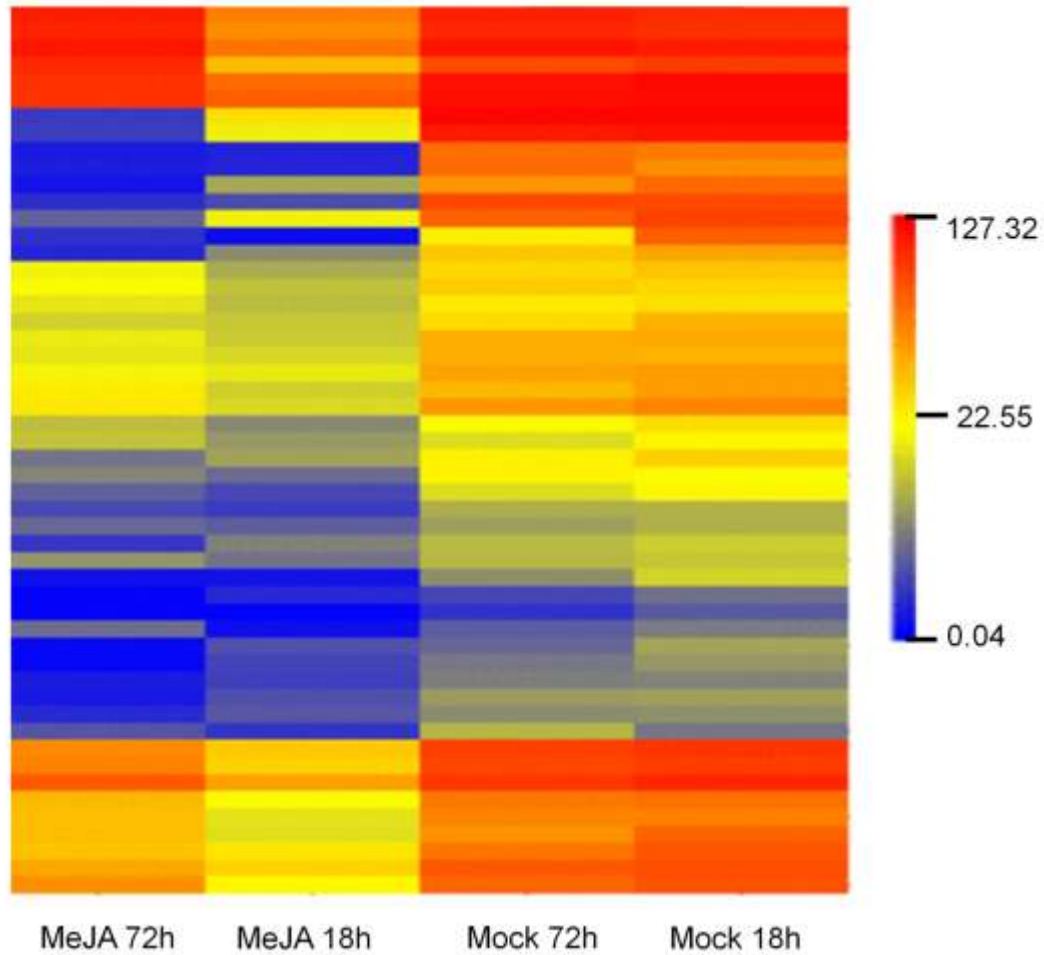
Figure 5.6 Heat map showing expression patterns of significantly downregulated cell cycle related-genes in MeJA-elicited cultures as compared to mock-elicited cultures. Hierarchical clustering was performed using average linkage and Euclidean distance as a measurement of similarity. Changes in gene expression were calculated based on the RPKM values of corresponding genes.

5.5 Additional information (not included in chapter)

i) Development of EdU-based proliferation assay

A widely used technique for monitoring cell cycle activity and for direct measurement of new DNA synthesis is by incorporation of a thymidine analog such as bromodeoxyuridine (BrdU) into DNA, followed by immunodetection with a specific antibody raised against the thymidine analog. This technique was successfully used in *Taxus* cell cultures in our lab (Naill and Roberts 2005a). However, the DNA denaturation process required to expose BrDU to the antibody is lengthy, difficult to perform and can affect the culture morphology (Kotogany et al. 2010). To alleviate these issues, EdU (5-ethynyl-2'-deoxyuridine), a terminal alkyne-containing nucleoside analog of thymidine, can be used. The EdU detection method is based on simple click chemistry, which consists of an azide-conjugated fluorochrome (such as Alexa Fluor 488) and copper (I) as the catalyzer of the click reaction. As EdU detection does not rely on high molecular size antibodies, DNA denaturation steps can be omitted, which provides a more rapid analysis and better preservation of cellular structures.

Based on existing protocols for BrDU detection (Naill and Roberts 2005a; Yanpaisan et al. 1998), *Taxus* cells were cultured in medium containing 10 mM EdU (Invitrogen) for the required incubation period. Nuclei were isolated from EdU-incubated cultures and control cultures (not incubated with EdU), as mentioned in 2.2.3. Several steps were changed from the manufacturer's protocols (Click-iT EdU Alexa Fluor 488 Flow Cytometry Assay kit, cat no: C35002, Invitrogen, Carlsbad, CA) for successful staining and flow cytometric analysis of EdU-stained nuclei. The optimization steps for

successful EdU and DNA staining and their subsequent flow cytometric analysis were: i) use of Galbraith's nuclei isolation buffer instead of water for determining the optimal working concentration (using dilution) of Click-iT Reaction buffer (Component G) and buffer additive (component I), ii) use of Galbraith's nuclei isolation buffer instead of water to dissolve paraformaldehyde for fixing the nuclei, and iii) choosing the optimal forward and side scatter settings on LSRII flow cytometer to differentiate between nuclei and debris. The optimal conditions are described in Materials and Methods (Section 5.2). This EdU-based technique reduced the time for cell cycle analysis to approximately three hours, as compared to 7-8 hours for the analogous BrDU technique, which necessitates BrDU detection by both primary and secondary antibodies and includes multiple washing steps. This protocol can potentially be translated to intact single cells and protoplasts in the future for multi-parameter flow cytometric studies (Section 6.2.2)
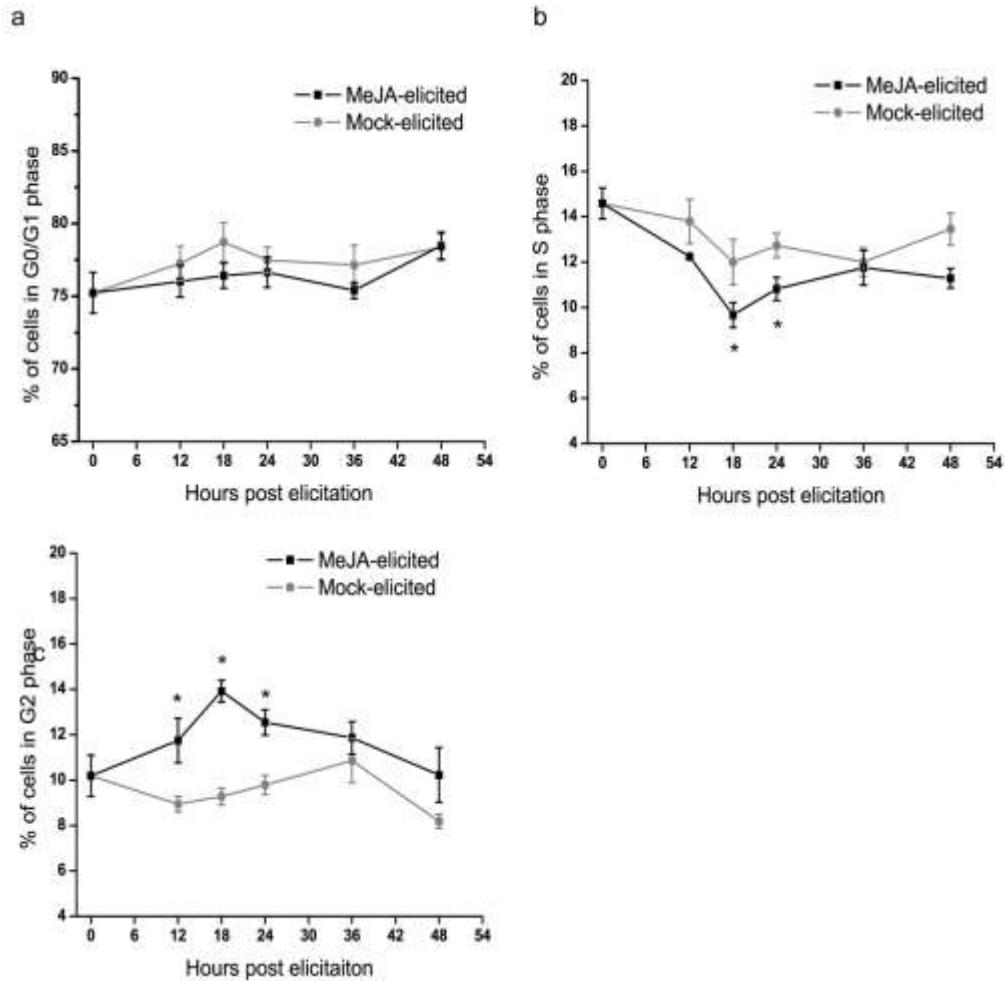
Figure 5.7 Cell cycle distribution in MeJA-elicited and mock-elicited *T. cuspidata* P93AF cultures within 48 hours post elicitation. The percentage of cells in **(A)** G0/G1, **(B)** S, and **(C)** G2/M phases is shown. Cell cycle analysis was done using the Watson Pragmatic Model of the FlowJo (v7.6) software. RNAse A (50 µg/mL) treatment, followed by staining with propidium iodide (PI) (50 µg/mL) was performed to obtain DNA histograms. Reported values are the average of three biological replicates and error bars represent SEM. The asterisk (*) indicates a statistically significant difference ($P < 0.05$; paired Student's t test) between MeJA-elicited and mock-elicited conditions.

Cultures were either mock-elicited or elicited with 150 µM MeJA on day 7 of the culture period.

Table 5.5 Complete list of 149 contigs expressed in *Taxus* cell cultures that are predicted to be cell cycle-related.

Contig No.	Specific function
10110	low quality protein: cyclin-dependent kinase D-1-like
10406	cyclin dependent kinase regulator
10743	cyclin T1
10765	cyclin dependent kinase inhibitor
11041	cyclin-dependent protein
11341	cyclin-dependent kinase C-1-like
11366	D2 4-type cyclin
117445	cyclin BRF1-like TBP-binding protein
117583	cyclin-related protein
117875	cyclin family protein
119004	B-type cyclin
119383	cyclin dependent kinase B
119769	cyclin-dependent kinase G-2-like
12010	cyclin-dependent kinases regulatory subunit
12269	cyclin delta-3
12355	probable G2 mitotic-specific cyclin
12531	cyclin-L1-1
13227	cyclin dependent kinase A
140080	cyclin H-1
141136	cyclin A1
18077	CCC11_orysj ame: full=cyclin-C1-1 short= 1 1

18149	cyclin-dependent kinase F-1
18354	cyclin-dependent kinase G-2-like
18492	cyclin B 2
18814	cyclin-T1-5-like isoform 1
19788	cyclin family expressed
22178	cyclin-D-binding myb-like transcription factor
22860	cyclin-dependent protein kinase
439	CKB11_orysj ame: full=cyclin-dependent kinase B1-1 short=CDKB1 1 short=CDKB 1
46333	cyclin M
57438	cyclin family expressed
57795	cyclin-dependent kinase C-1-like
58809	cyclin dependent kinase inhibitor
59549	D2 4-type cyclin
59726	cyclin-dependent kinase F-4-like
60181	cyclin-dependent kinase G-2-like
61510	D3-type cyclin
62310	cyclin-dependent kinase F-4-like
64817	calcyclin binding protein
65153	cyclin-dependent kinase E-1
65828	CCB22_orysj ame: full=cyclin-B2-2
66244	cyclin-dependent kinases regulatory subunit
67880	D2 4-type cyclin
68106	B1-type cyclin dependent kinase
68643	cyclin-dependent kinase E-1

68975	G2 mitotic-specific cyclin S13-6
75100	cyclin family expressed
75242	cyclin B3-1
76658	cyclin-dependent kinase E-1
90048	calcyclin binding protein
9782	cyclin-dependent kinases regulatory subunit
100185	cell division cycle protein 48 homolog
100939	cell division cycle protein 48 homolog
10134	plastid division2 protein
101973	cell division cycle protein 48 homolog
102800	cell division cycle protein
103306	cell division cycle protein 48 homolog
103776	cell division cycle protein 48 homolog
103991	cell division cycle protein 48 homolog
104612	cell division cycle protein 48 homolog
105427	cell division cycle protein 48 homolog
105698	cell division cycle protein 48 homolog
106161	cell division control protein
107757	cell division cycle protein 48 homolog
107852	cell division cycle protein 48 homolog
108329	cell division cycle protein
109017	cell division cycle protein 48 homolog
109272	cell division cycle protein 48 homolog
109405	cell division cycle protein 48 homolog
109610	cell division cycle protein 48 homolog

109918	cell division cycle protein 48 homolog
11005	cell division cycle protein
110200	cell division control protein
110559	cell division cycle protein
110709	cell division cycle protein 48 homolog
110863	cell division cycle protein 48 homolog
111055	cell division cycle protein 48 homolog
111300	cell division cycle protein 48 homolog
112008	cell division cycle protein
112279	cell division cycle protein 48 homolog
112647	cell division cycle protein 48 homolog
113240	cell division control protein
113719	cell division cycle protein 48 homolog
114075	cell division control protein
116949	cell division cycle protein 48 homolog
117777	cell division control protein 48 homolog B-like
118076	cell division control protein 45 homolog
11868	plastid division protein chloroplastic-like
119196	nuclear division RFT1-like protein
12019	cell division control
121259	cell division control protein 6 homolog
124695	cell division cycle and apoptosis regulator protein
125598	cell division control protein
127620	cell division cycle protein 48 homolog
128286	cell division control protein

148

12900	cell division
129444	cell division control protein 6 homolog
134490	cell division cycle protein
134513	cell division cycle protein
13564	plastid division protein chloroplastic-like
140234	plastid division protein PDV1-like
141017	cell division control
141711	cell division
141752	cell division control protein 48 homolog C-like
145394	cell division control protein
145766	nuclear division RFT1-like protein
146264	cell division cycle cofactor of APC complex
18555	cell division protein FtsY homolog
18658	cell division-associated protein BIMB-like
19091	cell division cycle-associated 7-like isoform 2
23923	meiotic nuclear division protein 1 homolog
57179	cell division
58621	plastid division regulator
62766	cell division protein
65384	cell division control protein 48 homolog C-like
65772	cell division cycle protein 48 homolog
67851	cell division cycle 5-like
68799	cell division cycle protein 48 homolog
74520	cell division control
75212	cell division protein

76811	cell division control protein 48 homolog C-like
77042	cell division protease FTSH-like protein
79802	cell division cycle cofactor of APC complex
80228	cell division cycle cofactor of APC complex
80940	cell division cycle protein
82001	cell division cycle cofactor of APC complex
87666	cell division protein
91147	cell division cycle protein 48 homolog
92263	cell division cycle protein 48 homolog
92332	cell division cycle protein 48 homolog
92539	cell division cycle protein 48 homolog
96454	cell division control protein 48 homolog E-like
97765	cell division control protein
98625	cell division cycle protein 48 homolog
99133	cell division cycle protein 48 homolog
99223	cell division cycle protein 48 homolog
119534	dual specificity phosphatase CDC25
119826	AAA family ATPase CDC48 subfamily
21530	AAA family ATPase CDC48 subfamily
22931	PCDC2 rp-
69905	RNA polymerase ii assessory factor CDC73P
81095	anaphase-promoting complex subunit CDC20
10476	transcription factor E2F
140962	E2F target protein 1
142510	antagonist of E2F-DP complex

146585	E2F -associated phospho
19706	E2F-associated phospho
62294	E2F protein
74429	protein kinase wee1

Table 5.6 Contigs expressed in *Taxus* cell cultures that are predicted to encode histones and which are downregulated in MeJA-elicited cultures relative to mock-elicited cultures at 18 hours post-elicitation.

Contig No.	Seq. Description	Fold Change (normalized values)
75207	histone chaperone	-602.2
96097	histone H2B	-16.56
21437	histone H2A	-15.37
129999	histone H2BN	-15.31
127298	histone H2B	-12.13
23029	histone H3	-10.77
93181	histone H3-like	-10.35
120251	H2B5_wheat ame: full=histone ame: full=WCH2B-6	-9.51
65215	histone H2A	-8.47
133736	histone H3	-8.16
99292	histone H2B	-7.70
105777	histone H4	-7.58
125916	histone H2A	-7.34
97023	histone H3	-7.30
145388	histone H3	-7.09
89365	H2B5_wheat ame: full=histone ame: full=WCH2B-6	-6.93
103001	histone H3	-6.53
92399	histone H3	-6.27

90765	histone -like isoform 1	-6.24
125880	histone H4	-6.17
65477	histone H2B like protein	-6.09
126700	histone H4	-5.73
138300	histone	-5.50
89314	histone H2B	-5.47
96814	histone H3	-5.40
92302	histone H2A	-5.17
93891	histone H3	-5.14
142011	histone H2A	-5.13
121465	histone H1-like protein	-5.07
88085	histone H4	-5.01
112797	histone H4	-5.00
112244	histone H3	-4.92
91339	histone H3	-4.88
79833	histone H2B	-4.86
128757	histone H4	-4.82
125318	histone H2A	-4.49
28497	histone H2A	-4.42
92425	histone H3	-4.37
45090	histone-lysine n-methyltransferase ATXR4-like	-4.34
18499	histone H2A variant	-4.33
141827	probable histone H2A variant 3	-4.29
21433	histone H2A variant	-4.28

126269	histone -like	-4.28
141835	histone-like protein	-4.24
125453	histone H4	-4.10
110266	histone H3	-4.08
68567	histone gene transcript 5 hairpin-binding protein	-3.86
125786	histone H2B	-3.85
57733	histone acetyltransferase	-3.82
101758	histone H3	-3.75
89296	histone H4	-3.74
124694	histone H4	-3.63
60238	histone-lysine n-methyltransferase ASHR3	-3.57
138148	histone H2A-like protein	-3.54
126658	histone H4	-3.43
102145	histone H2A-like	-3.42
90623	histone H4	-3.36
95231	histone H2A-like protein	-3.30
87786	histone H4	-3.29
97564	histone H4	-3.24
104335	histone 2	-3.23
120016	histone H3	-3.23
147310	histone RNA hairpin-binding protein	-3.13
109265	histone H2B	-3.12
145669	histone H4	-3.08

27108	histone H4	-3.07
145507	histone H4	-3.03
125121	histone H4	-3.01
147353	histone H3	-2.98
111922	histone 2	-2.94
108403	histone H2B	-2.91
37028	histone-lysine n-methyltransferase SUVR3	-2.89
57220	histone acetyltransferase type B catalytic	-2.82
91392	histone H4	-2.78
59833	histone H3	-2.75
61107	histone H4	-2.73
91166	histone H2B	-2.68
61146	histone H2B	-2.66
40540	H2B5_wheat ame: full=histone ame: full=WCH2B-6	-2.62
10241	histone-lysine n-methyltransferase SUVR4	-2.59
75030	histone	-2.56
136283	histone H3	-2.52
125003	histone H3	-2.51
65860	histone-lysine n-methyltransferase MLL5	-2.46
77267	histone H2B	-2.45
147393	histone H4	-2.44
141233	histone-like protein	-2.40
59456	histone chaperone ASF1B	-2.25

18845	histone-arginine methyltransferase CARM1	-2.21
18640	histone H2B	-2.21
128784	histone H2B	-2.19
20988	histone-lysine n-methyltransferase SETD1B	-2.17
69186	histone-lysine n-methyltransferase ASHH3-like	-2.15
21973	histone H3	-2.14
139810	histone-lysine n-methyltransferase-like protein	-2.12
11058	histone deacetylase	-2.07
96821	histone H3	-2.04
77046	histone deacetylase	-2.03
141984	histone	-2.02
125733	histone H2B	-2.01
125492	histone H4	-2.01

Table 5.7 Contigs expressed in *Taxus* cell cultures that are predicted to encode histones and which are downregulated in MeJA-elicited cultures relative to mock-elicited cultures at 72 hours post-elicitation.

Contig No.	Seq. Description	Fold Change (normalized values)
93181	histone H3-like	-384.00
92399	histone H3	-265.58
141984	histone	-245.67
97023	histone H3	-215.60
102145	histone H2A-like	-201.15
133736	histone H3	-187.98
103001	histone H3	-143.25
96814	histone H3	-137.91
92425	histone H3	-129.39
65215	histone H2A	-120.02
21973	histone H3	-87.63
93891	histone H3	-87.45
125916	histone H2A	-79.72
127298	histone H2B	-78.48
21437	histone H2A	-56.09
142011	histone H2A	-48.65
68567	histone gene transcript 5 hairpin-binding protein	-47.12
120251	H2B5_wheat ame: full=histone ame: full=WCH2B-6	-46.42

135558	histone H4	-43.99
19008	histone H4	-43.84
59456	histone chaperone ASF1B	-40.88
147310	histone RNA hairpin-binding protein	-36.94
110266	histone H3	-36.93
79833	histone H2B	-34.76
61107	histone H4	-31.67
145388	histone H3	-25.72
59833	histone H3	-24.78
40540	H2B5_wheat ame: full=histone ame: full=WCH2B-6	-24.07
125003	histone H3	-23.49
91339	histone H3	-20.41
121465	histone H1-like protein	-17.74
12499	histone H3	-17.57
141835	histone-like protein	-16.25
125453	histone H4	-16.06
128757	histone H4	-15.62
105777	histone H4	-15.24
96097	histone H2B	-14.23
129999	histone H2BN	-13.49
89365	H2B5_wheat ame: full=histone ame: full=WCH2B-6	-11.65
23029	histone H3	-11.33
125318	histone H2A	-10.77

65477	histone H2B like protein	-10.28
112244	histone H3	-9.79
21433	histone H2A variant	-9.19
138148	histone H2A-like protein	-8.16
41101	histone H2A	-7.85
103567	histone H1-like protein	-7.82
95231	histone H2A-like protein	-7.64
91392	histone H4	-7.43
18499	histone H2A variant	-7.20
104335	histone 2	-7.18
90765	histone -like isoform 1	-7.13
111922	histone 2	-6.44
125880	histone H4	-6.41
134675	histone H1-like protein	-6.30
99292	histone H2B	-6.13
126700	histone H4	-5.79
126658	histone H4	-5.40
77377	histone H1-like protein	-5.36
105385	histone H1-like protein	-5.17
112797	histone H4	-5.15
89296	histone H4	-5.11
90728	histone H1	-4.73
97564	histone H4	-4.61
138300	histone	-4.46
90623	histone H4	-4.35

75030	histone	-4.21
28497	histone H2A	-3.98
124753	histone deacetylase HD2	-3.52
145632	HD2 type histone deacetylase	-3.35
87786	histone H4	-3.34
124694	histone H4	-3.30
145669	histone H4	-3.27
141233	histone-like protein	-3.26
101531	histone H4	-3.25
145507	histone H4	-3.07
65000	histone H1-like protein	-3.05
120016	histone H3	-3.04
27108	histone H4	-2.92
110798	histone H4	-2.62
126269	histone -like	-2.47
91166	histone H2B	-2.24
134849	histone 2	-2.21
60923	histone Z	-2.13
136329	histone H2A-like protein	-2.08
124714	histone H2A	-2.04
97372	histone H2A-like protein	-2.03
77046	histone deacetylase	-2.01
125786	histone H2B	-2.01

CHAPTER 6
IMPACT AND FUTURE WORK

6.1 Impact

The overarching goal of the work presented in this dissertation is to optimize processes for production of pharmaceuticals in plant-based systems, in particular for plant cell suspension cultures. The basic emphasis is on understanding cellular metabolic control and culture heterogeneity in *Taxus* suspension cultures, which produce the pharmaceutically relevant anti-cancer drug paclitaxel. Instability in product yields over multiple subculture periods has hampered the efficient and sustainable use of plant cell culture technology for production of paclitaxel. In Chapter 2, paclitaxel accumulation in *Taxus* cell suspension culture was quantified over multiple subculture periods and correlated to mean aggregate size. Paclitaxel levels varied approximately 6.9-fold over the six-month timeframe investigated and were negatively correlated to the mean aggregate size of the cultures. These results not only extend the previous work on aggregation done in our laboratory (Kolewe 2011), but also demonstrate the relevance of measuring, and potentially controlling aggregate size during long term subculture, particularly for plant suspensions where industrially relevant secondary metabolites are not pigmented to enable rapid culture selection.

Understanding regulation of gene expression is critical to the design of targeted metabolic engineering approaches. In Chapter 3, expression patterns of known paclitaxel biosynthetic pathway genes were quantified from different culture phenotypes to understand the role of biosynthetic pathway gene expression in the creation of specific culture states. This work represents one of the first molecular studies to gain a

mechanistic understanding of paclitaxel accumulation variability in *Taxus* cell cultures, which could provide rational engineering strategies to control variability and optimize performance of *Taxus* cell cultures. While this study collectively showed that some degree of variability in paclitaxel accumulation can be directly linked to changes in biosynthetic pathway gene expression, there were clearly contributions from other factors. To fully understand the factors that regulate paclitaxel accumulation, a systems-wide genomics approach was conducted using 454 and Illumina sequencing methods, as described in Chapter 4. A comprehensive, annotated transcriptome of cultured *T. cuspidata* cells was generated. Several pathways outside of paclitaxel biosynthesis were found active upon MeJA elicitation, and such complementary and competing pathways can ultimately affect final paclitaxel levels within the culture. Though, a complete analysis of the transcriptome data to understand all the active pathways in the cultures is still ongoing, the results thus far have been exciting and have the potential to rapidly accelerate genetic engineering efforts in *Taxus* cell cultures.

In Chapter 5, MeJA was shown to affect the growth of *Taxus* cell cultures at the level of the cell cycle. A number of genes annotated as "cell cycle" genes were found to be downregulated in the MeJA-elicited state. The results from this study provide valuable insight into the relatively unknown mechanisms governing MeJA perception and subsequent events leading to repression of cell growth in *Taxus*. Apart from improving our fundamental understanding about MeJA's mechanism of action in *Taxus* cell cultures, these data also demonstrate a successful example of application of the recently annotated transcriptome. In the future, this annotated base transcriptome can serve as a scaffold to understand gene expression, which could: i) improve our understanding of global

transcriptional control of paclitaxel biosynthesis, and ii) act as a valuable resource for genomic studies in *Taxus* and other non-model medicinal plant species..

6.2. Recommendations for future work

In addition to the suggestions already provided in the previous chapters, it is anticipated that the work presented in this thesis will provide a foundation for future work on the process engineering and population- and genetic-level characterization of *Taxus* cell cultures.

6.2.1 Process engineering strategies to control aggregate size

The work in this thesis emphasizes the importance of controlling aggregate size, which could help minimize variability in paclitaxel yields over long term subculture. Some of the efforts to investigate the effect of process parameters, such as inoculation density and time of inoculation on aggregation, have already been initiated. Results indicate that cultures inoculated at higher densities showed consistently smaller aggregates and cultures inoculated earlier showed slightly decreased aggregate size and biomass accumulation (Section 2.5 and Kathryn Geldart, Senior thesis 2012). Further studies need to be undertaken to fully understand the relationship amongst these parameters and paclitaxel accumulation. Studies to understand the effect of operating parameters such as agitation rate on aggregation have also been initiated (Kathryn Geldart, Senior thesis 2012). In order to control aggregate size, turbulent shear forces can be used to promote aggregate dissociation. Shearing forces to dissociate aggregates can be achieved either by manually passing the aggregates back and forth through smaller diameter pipettes or by using higher agitation rates. However, care should be taken that excessive shearing does

not cause cell damage and/or cell death, which would negatively affect cell health and paclitaxel production. For manipulating agitation rates controlled bioreactors could be used, as they can also allow for better control of other operating parameters such as pH and temperature. Recently, a population balance equation framework to describe *Taxus* cell aggregates as a particulate system was developed and utilized in our laboratory to quantitatively predict changes in total biomass, mean aggregate size, and aggregate size distributions (Kolewe et al. 2012). Results obtained from shearing experiments and the relationship to paclitaxel accumulation can be included in this model to further improve its predictability, which can be used to optimize operating conditions and culture performance. Ultimately identification of optimal conditions to control aggregate size will improve both paclitaxel production and reliability of achievable yields.

6.2.2 Multiparameter flow cytometry to determine the relationship between paclitaxel-accumulating and noncycling cells in *Taxus* cell culture

The proportion of cells accumulating secondary metabolites in a culture can significantly change the overall productivity, resulting in variable culture yields over time. For example, in *C. roseus*, the proportion of cells accumulating anthocyanin was approximately 10% of the total population, and the variation in total anthocyanin content was attributed primarily to a change in the proportion of cells accumulating anthocyanin (Hall and Yeoman 1987). Certain cells in culture can differentiate and have specialized roles for metabolite storage, such as in *Macleaya microcarpa* for the storage of alkaloids (Franke and Bohm 1982). It is speculated that G0 cells may play a significant role in secondary metabolism (Yanpaisan et al. 1998; Naill and Roberts 2005a). Results have indicated an increase in the percentage of G0/G1 cells in the *T. cuspidata* P93AF cell line

164

upon MeJA elicitation. Similar results were obtained with another *T. cuspidata* cell line (P991) in our laboratory, where BrdU staining was used to calculate the percentage of noncycling (G0) cells in the culture. About 65% of the *Taxus* cells (P991 cell line) were identified as noncycling in mid-exponential phase (Naill and Roberts 2005a), however the role of these cells in suspension cultures was not characterized. Total metabolic activity inferred via total cellular protein content was relatively uniform in MeJA-elicited cultures (Naill and Roberts 2005c) indicating that noncycling cells are still metabolically active, but potentially redirecting carbon flux away from primary metabolism towards secondary metabolism. In another study, alkaloid accumulation increased in cultures of *Solanum aviculare* where cell cycle progression was inhibited using a cell cycle arrest agent, again suggesting that the metabolic flux may be directed towards secondary pathways in nonproliferating cells (Mak and Doran 1993). To this point, investigators have only been able to identify a significant G0 population in culture or present indirect evidence to suggest a function of this population, but have not been able to explicitly correlate the noncycling cells to other cellular metabolic information.

One way to test the hypothesis that noncycling cells are more active in accumulating paclitaxel is by using a multi-parametric flow cytometric staining approach to simultaneously identify noncycling cells and paclitaxel-accumulating cells. Cultures should be elicited with MeJA, followed by digestion of aggregated cultures into single cells (Naill and Roberts 2004) and then dual stained for paclitaxel and EdU based on the methods described in this dissertation. One primary difficulty is that intact single cells must be used for this type of analysis, rather than nuclei, which were used in this dissertation for DNA content and EdU analysis. Hence experiments will have to be

165

conducted to establish a reproducible method to analyze DNA and EdU in single cells. Another complication will be design of these experiments with respect to specifically identifying the precise timing of addition of MeJA and EdU. For efficient EdU incorporation, early exponential phase cells (day 4 to day 7) should be used as the cells are actively dividing in this phase, allowing cycling and noncycling cells to be distinguished. For paclitaxel staining, cells must have accumulated a sufficient amount of paclitaxel for detection, which typical begins after 4 to 5 days post MeJA-elicitation (as measured by HPLC/UPLC). However, continuous incubation with EdU can affect the distribution of cells in the cell cycle, and can also result in cell toxicity. Such effects have been observed with BrDU (Yanpaisan et al. 1998), which is an analog of EdU. Hence, experiments will have to be performed to figure out the precise timing of MeJA and EdU addition. To account for the issues of spectral overlap of dyes, singly-stained samples (as well as an unstained sample) should be analyzed in parallel, followed by the generation of a compensation matrix using the FlowJO software. Simultaneous analysis of more than one parameter along with cell proliferation (BrDU incorporation) has been used previously in other cell systems (Rosato et al. 2001; Pechhold et al. 2009). The information gained from this study will provide insight into regulation of paclitaxel metabolism in specific cell populations.

6.2.3 Metabolic engineering of *Taxus* cell cultures

6.2.3.1 Further characterization of global molecular-genetic regulatory networks to enable metabolic engineering

Though initial efforts to compare gene expression profiles using Illumina sequencing amongst cultures with different bulk paclitaxel/taxane accumulation patterns have been initiated, a detailed characterization of pathways still needs to be established before the best targets for metabolic engineering can be selected. Once targets are identified, experiments can be designed to either overexpress or silence the target genes, and effects on taxane accumulation can be assessed.

Aggregate size has been shown to be an important parameter which can affect the levels of secondary metabolite accumulated in several plant cell culture systems (Edahiro and Seki 2006; Bolta et al. 2003; Zhao et al. 2003), including paclitaxel accumulation in *Taxus* suspension cultures (Kolewe et al. 2011). As cell aggregate size is governed by cohesiveness of cell wall, genes involved in cell wall biosynthesis likely contribute to presence of different sized aggregates within a culture. The recent transcriptome data obtained can be grouped based on molecular function, e.g., cell cycle progression or cell wall biosynthesis. Grouping the genes based on cell wall biosynthesis can potentially provide a list of genes that are differentially expressed in small and large aggregate cultures. These results can be used to identify genes/pathways responsible for morphological differences in the cultures, and potentially for differential paclitaxel accumulation. Genes that are shown to be involved in aggregation would be a target for gene silencing approaches, to allow for smaller aggregate sizes. Overall, further analysis

167

of the available transcriptome data will provide a superior understanding of *Taxus* metabolism and its regulation at the level of transcription.

6.2.3.2 *Agrobacterium*-mediated stable transformation method

The targeted metabolic engineering of *Taxus* cells in culture requires a method for stable transformation. *Agrobacterium tumefaciens* provides an ideal method of stable transformation in *Taxus* cell culture (Ketchum et al. 2007). A single paper describes the *Agrobacterium*-mediated transformation of *Taxus* (Ketchum et al. 2007); however, this method was not reproducible in our lab due to possible somaclonal variation of *Taxus* cell lines derived from the same original stock (Vongpaseuth 2011). To facilitate the development of the transformation protocol, we collaborated with the Van Eck group at the Boyce Thompson Institute for Plant Research. The Van Eck group has successfully established *Agrobacterium*-mediated transformation protocols for other plant species (Ganapathi et al. 2001; Eck et al. 2006), and were able to develop a successful working protocol for our *Taxus* cell cultures. Now that *Agrobacterium*-mediated transformation has been demonstrated with our cell lines, future work will focus on developing superior cell lines with enhanced performance characteristics (e.g., higher yields of paclitaxel). A combination of overexpression or RNAi strategies can be used to divert flux towards paclitaxel synthesis. Ultra performance liquid chromatography (UPLC) can be utilized to investigate the effect of overexpression or knockout of target genes on the accumulation of paclitaxel and other taxanes in both MeJA-elicited and mock-elicited cells.

BIBLIOGRAPHY

Abdala G, Castro G, Kraus T (1999) Endogenous jasmonic acid and radial cell expansion in buds of potato tubers. Journal of Plant Physiology 155 (6):706-710.

Abe M, Shibaoka H, Yamane H, Takahashi N (1990) Cell cycle-dependent disruption of microtubules by methyl jasmonate in tobacco BY-2 cells. Protoplasma 156 (1):1-8.

Ajikumar PK, Xiao WH, Tyo KEJ, Wang Y, Simeon F, Leonard E, Mucha O, Phon TH, Pfeifer B, Stephanopoulos G (2010) Isoprenoid pathway optimization for Taxol precursor overproduction in Escherichia coli. Science 330 (6000):70-74.

Alper H, Miyaoku K, Stephanopoulos G (2005) Construction of lycopene-overproducing E-coli strains by combining systematic and combinatorial gene knockout targets. Nat Biotechnol 23 (5):612-616.

Ananta I, Subroto MA, Doran PM (1995) Oxygen-transfer and culture characteristics of self-immobilized solanum aviculare aggregates. Biotechnol Bioeng 47 (5):541-549.

Aoyagi H, DiCosmo F, Tanaka H. 2002. Efficient paclitaxel production using protoplasts isolated from cultured cells of Taxus cuspidata. Planta Medica 68(5):420-424.

Baebler S, Hren M, Camloh M, Ravnikar M, Bohanec B, Plaper I, Ucman R, Zel J (2005) Establishment of cell suspension cultures of yew (*Taxus* x media rehd.) and assessment of their genomic stability. In Vitro Cell Dev Biol Plant 41 (3):338-343.

Becker H (1970) Studies on the formation of volatile substances in plant tissue cultures. Biochem Physiolo Pflanzen 161:425-441.

Bergounioux C, Brown SC, Petit PX (1992) Flow-cytometry and plant protoplast cell biology. Physiologia Plantarum 85 (2):374-386.

Bergounioux C, Perennes C, Brown SC, Gadal P (1988) Nuclear-RNA quantification in protoplast cell-cycle phases. Cytometry 9 (1):84-87.

Boisson AM, Gout E, Bligny R, Rivasseau C (2012) A simple and efficient method for the long-term preservation of plant cell suspension cultures. Plant Methods 8:4.

Bolta Z, Baricevic D, Raspor P (2003) Biomass segregation in sage cell suspension culture. Biotechnol Lett 25 (1):61-65.

Bonfill M, Bentebibel S, Moyano E, Palazon J, Cusido R, Eibl R, Pinol M (2007) Paclitaxel and baccatin III production induced by methyl jasmonate in free and immobilized cells of *Taxus* baccata. Biologia Plantarum 51 (4):647-652.

Bonfill M, Exposito O, Moyano E, Cusido RM, Palazon J, Pinol MT (2006) Manipulation by culture mixing and elicitation of paclitaxel and baccatin III production in *Taxus* baccata suspension cultures. In Vitro Cellular & Developmental Biology-Plant 42 (5):422-426.

Borman S (1994) Total synthesis of the anticancer agent Taxol achieved by two different routes. Chem Eng News 72:32-34.

Bourgaud F, Gravot A, Milesi S, Gontier E (2001) Production of plant secondary metabolites: a historical perspective. Plant Sci 161(5):839-851

Breyne P, Zabeau M (2001) Genome-wide expression analysis of plant cell cycle modulated genes. Current Opinion in Plant Biology 4 (2):136-142.

Bringi V, Kadkade PG, Prince CL, Roach B (2007) Enhanced production of taxol and taxanes by cell cultures of *Taxus* species. US Patent 7264954 B1.

Callebaut A, Terahara N, Haan M, Decleire M (1997) Stability of anthocyanin composition in Ajuga reptans callus and cell suspension cultures. Plant Cell Tissue Organ Cult 50 (3):195-201.

Campbell MM, Ellis BE (1992) Fungal elicitor-mediated responses in pine cell cultures: cell wall-bound phenolics. Phytochemistry 31 (3):737-742.

Capataz-Tafur J, Trejo-Tapia G, Rodriguez-Monroy M, Sepulveda-Jimenez G (2011) Arabinogalactan proteins are involved in cell aggregation of cell suspension cultures of Beta vulgaris L. Plant Cell Tissue Organ Cult 106 (1):169-177.

Cassells A, Curry R (2001) Oxidative stress and physiological, epigenetic and genetic variability in plant tissue culture: implications for micropropagators and genetic engineers. Plant Cell Tiss Org 64(2):145-157

Castellano MM, del Pozo JC, Ramirez-Parra E, Brown S, Gutierrez C (2001) Expression and stability of Arabidopsis CDC6 are associated with endoreplication. Plant Cell 13 (12):2671-2686.

Chemler JA, Koffas MAG (2008) Metabolic engineering for plant natural product biosynthesis in microbes. Curr Opin Biotechnol 19 (6):597-605.

Cheung F, Haas B, Goldberg S, May G, Xiao Y, Town C (2006) Sequencing Medicago truncatula expressed sequenced tags using 454 Life Sciences technology. BMC Genomics 7 (1):272.

Cho K, Agrawal GK, Shibato J, Jung Y-H, Kim YK, Nahm BH, Jwa NS, Tamogami S, Han O, Kohda K, Iwahashi H, Rakwal R (2007) Survey of differentially expressed proteins and genes in jasmonic acid treated rice seedling shoot and root at the proteomics and transcriptomics Levels. Journal of Proteome Research 6 (9):3581-3603.

Citterio S, Sgorbati S, Levi M, Colombo BM, Sparvoli E (1992) Pcna and total nuclear-protein content as markers of cell-proliferation in pea tissue. Journal of Cell Science 102:71-78.

Colegate SM, Molyneux RJ (eds) (2008) Bioactive natural products: detection, isolation, and structural determination. 2nd edn. CRC Press, USA.

Conesa A, Gotz S, Garcia-Gomez JM, Terol J, Talon M, Robles M (2005) Blast2GO: a universal tool for annotation, visualization and analysis in functional genomics research. Bioinformatics 21 (18):3674-3676.

Cragg GM, Grothaus PG, Newman DJ (2009) Impact of natural products on developing new anti-cancer agents. Chem Rev 109 (7):3012-3043.

Creemers-Molenaar J, Loeffen JPM, van Rossum M, Colijn-Hooymans CM (1992) The effect of genotype, cold storage and ploidy level on the morphogenic response of perennial ryegrass (Lolium perenne L.) suspension cultures. Plant Science 83 (1):87-94.

Croteau R, Ketchum R, Long R, Kaspera R, Wildung M (2006) Taxol biosynthesis and molecular genetics. Phytochemistry Reviews 5 (1):75-97.

Curtis WR, Tuerk AL (2006) Oxygen transport in plant tissue culture systems. In: Gupta SD, Ibaraki Y (eds) Plan Tissue Culture Engineering, vol 6. Focus on Biotechnology. Springer Netherlands, pp 173-186.

de O. Buanafina MM (2009) Feruloylation in Grasses: Current and Future Perspectives. Molecular Plant 2 (5):861-872.

DellaPenna D (2001) Plant metabolic engineering. Plant Physiology 125 (1):160-163.

Deusneumann B, Zenk MH (1984) Instability of indole alkaloid production in Catharanthus roseus cell suspension cultures. Planta Medica 50 (5):427-431.

Dolezel J, Greilhuber J, Suda J (2007) Estimation of nuclear DNA content in plants using flow cytometry. Nat Protocols 2 (9):2233-2244.

Doran PM (1999) Design of mixing systems for plant cell suspensions in stirred reactors. Biotechnol Progr 15 (3):319-335.

Dornenburg H, Knorr D (1995) Strategies for the improvement of secondary metabolite production in plant-cell cultures. Enzyme Microb Technol 17(8):674-684

Dubuis B, Kut OM, Prenosil JE (1995) Pilot-scale culture of Coffea arabica in a novel loop fluidised bed reactor. Plant Cell Tissue and Organ Culture 43 (2):171-183.

Eberhardt TL, Bernards MA, He L, Davin LB, Wooten JB, Lewis NG (1993) Lignification in cell suspension cultures of Pinus taeda. In situ characterization of a gymnosperm lignin. Journal of Biological Chemistry 268 (28):21088-21096.

Eck JV, Kirk DD, Walmsley AM (2006) Tomato (Lycopersicum esculentum). In, Wang K (ed) Agrobacterium Protocols. vol 343. Humana Press, Totowa, New Jersey pp 459-474

Edahiro J, Seki M (2006) Phenylpropanoid metabolite supports cell aggregate formation in strawberry cell suspension culture. J Biosci Bioeng 102 (1):8-13.

Eibl R, Eibl D (2002) Bioreactors for plant cell and tissue cultures. In: Oksman-Caldentey KM BW (ed) Plant biotechnology and transgenic plants. Marcel Dekker, New York, pp 163-199

Ellis DD, Zeldin EL, Brodhagen M, Russin WA, McCown BH (1996) Taxol production in nodule cultures of *Taxus*. J Nat Prod 59 (3):246-250.

Evans DE, Coleman JOD, Kearns A (2003) Plant cell culture. Basics. BIOS Scientific, London ; New York.

Exposito O, Syklowska-Baranek K, Moyano E, Onrubia M, Bonfill M, Palazon J, Cusido RM (2010) Metabolic responses of *Taxus* media transformed cell cultures to the addition of methyl jasmonate. Biotechnol Progr 26 (4):1145-1153.

171

Farmer EE, Ryan CA (1990) Interplant communication - airborne methyl jasmonate induces synthesis of proteinase-inhibitors in plant leaves. Proc Natl Acad Sci U S A 87 (19):7713-7716.

Feiler HS, Desprez T, Santoni V, Kronenberger J, Caboche M, Traas J (1995) The higher-plant Arabidopsis thaliana encodes a functional cdc48 homolog which is highly expressed in dividing and expanding cells. Embo Journal 14 (22):5626-5637.

Fett-Neto AG, DiCosmo F, Reynolds WF, Sakata K (1992) Cell culture of *Taxus* as a source of the antineoplastic drug taxol and related taxanes. Nat Biotechnol 10 (12):1572-1575.

Fett-Neto AG, Melanson SJ, Nicholson SA, Pennington JJ, Dicosmo F (1994) Improved taxol yield by aromatic carboxylic acid and amino acid feeding to cell cultures of *Taxus* cuspidata. Biotechnol Bioeng 44 (8):967-971.

Foster CE, Martin TM, Pauly M (2010) Comprehensive compositional analysis of plant cell walls (Lignocellulosic biomass) part I: lignin. J Vis Exp (37).

Franke J, Bohm H (1982) Accumulation and excretion of alkaloids by Macleaya-microcarpa cell cultures 2. Experiments in liquid medium. Biochemie Und Physiologie Der Pflanzen 177 (6):501-507.

Fujita Y, Tabata M, Nishi A, Yamada Y (1982) New medium and production of secondary compounds with the two-staged culture method. In: Fujiwara A (ed) Plant tissue culture. The Japanese Association for Plant Tissue Culture, Maruzen Co. Ltd., Tokyo, pp 399-400

Fukushima RS, Hatfield RD (2001) Extraction and isolation of lignin for utilization as a standard to determine lignin concentration using the acetyl bromide spectrophotometric method. Journal of Agricultural and Food Chemistry 49 (7):3133-3139.

Galbraith DW, Harkins KR, Maddox JM, Ayres NM, Sharma DP, Firoozabady E (1983) Rapid flow cytometric analysis of the cell-cycle in intact plant-tissues. Science 220 (4601):1049-1051.

Galis I, Simek P, Narisawa T, Sasaki M, Horiguchi T, Fukuda H, Matsuoka K (2006) A novel R2R3 MYB transcription factor NtMYBJS1 is a methyl jasmonate-dependent regulator of phenylpropanoid-conjugate biosynthesis in tobacco. Plant Journal 46 (4):573-592.

Ganapathi TR, Higgs NS, Balint-Kurti PJ, Arntzen CJ, May GD, Van Eck JM (2001) Agrobacterium- mediated transformation of embryogenic cell suspensions of the banana cultivar Rasthali (AAB). Plant Cell Rep 20 (2):157-162.

Gao M, Zhang W, Li X, Ruan C, Fan S (2011) Expression profiling of genes involved in Taxuyunnanine C biosynthesis in cell suspension cultures of *Taxus* chinensis by repeated elicitation with a newly synthesized jasmonate and sucrose feeding. Sheng Wu Gong Cheng Xue Bao 27 (1):101-107.

Garg R, Patel RK, Tyagi AK, Jain M (2011) De novo assembly of chickpea transcriptome using short reads for gene discovery and marker identification. DNA Research 18(1):53-63.

Gaurav V (2011) Flow cytometry of cultured plant cells for characterization of culture heterogeneity and cell sorting applications. Open Access Dissertations. Paper 370.

Gaurav V, Kolewe ME, Roberts SC (2010) Flow cytometric methods to investigate culture heterogeneities for plant metabolic engineering. Methods Mol Biol 643:243-262.

Ge ZQ, Yuan YJ, Wang YD, Ma ZY, Hu ZD (2002) Ce4+-Induced apoptosis of *Taxus* cuspidata cells in suspension culture. Journal of Rare Earths 20 (2):139-144.

Georgiev MI, Pavlov AI, Bley T (2007) Hairy root type plant in vitro systems as sources of bioactive substances. Applied Microbiology and Biotechnology 74 (6):1175-1185.

Gibson D, Ketchum R, Vance N, Christen A (1993) Initiation and growth of cell lines of *Taxus* brevifolia (Pacific yew). Plant Cell Rep 12 (9):479-482.

Gigolashvili T, Berger B, Mock H-P, Müller C, Weisshaar B, Flügge U-I (2007) The transcription factor HIG1/MYB51 regulates indolic glucosinolate biosynthesis in Arabidopsis thaliana. The Plant Journal 50 (5):886-901.

Gomez-Galera S, Pelacho AM, Gene A, Capell T, Christou P (2007) The genetic manipulation of medicinal and aromatic plants. Plant Cell Rep 26 (10):1689-1715.

Goossens A, Hakkinen ST, Laakso I, Seppanen-Laakso T, Biondi S, De Sutter V, Lammertyn F, Nuutila AM, Soderlund H, Zabeau M, Inze D, Oksman-Caldentey KM (2003) A functional genomics approach toward the understanding of secondary metabolism in plant cells. Proc Natl Acad Sci U S A 100 (14):8595-8600.

Gundlach H, Muller MJ, Kutchan TM, Zenk MH (1992) Jasmonic acid is a signal transducer in elicitor induced plant cell cultures. Proc Natl Acad Sci U S A 89 (6):2389-2393.

Gutierrez C (2009) The Arabidopsis cell division cycle. Arabidopsis Book 7:e0120.

Hall RD, Yeoman MM (1986) Factors determining anthocyanin yield in cell cultures of Catharanthus roseus (L.) G. Don. New Phytologist 103 (1):33-43.

Hall RD, Yeoman MM (1987) Intercellular and intercultural heterogeneity in secondary metabolite accumulation in cultures of Catharanthus roseus following cell line selection. J Exp Bot 38 (193):1391-1398.

Hanagata N, Ito A, Uehara H, Asari F, Takeuchi T, Karube I (1993) Behavior of cell aggregate of Carthamus tinctorius L cultured cells and correlation with red pigment formation. Journal of Biotechnology 30 (3):259-269.

Hao DC, Ge GB, Xiao PG, Zhang YY, Yang L (2011) The first insight into the tissue specific *Taxus* transcriptome via illumina second generation sequencing. PLoS ONE 6 (6).

Harvey AL (2008) Natural products in drug discovery. Drug Discov Today 13 (19-20):894-901.

Hawkins B (2008) Plants for life: Medicinal plant conservation and botanic gardens. Botanic Gardens Conservation International, Richmond, UK

Hefner J, Ketchum RE, Croteau R (1998) Cloning and functional expression of a cDNA encoding geranylgeranyl diphosphate synthase from *Taxus* canadensis and assessment of the role of this prenyltransferase in cells induced for taxol production. Arch Biochem Biophys 360 (1):62-74.

Hellwig S, Drossard J, Twyman RM, Fischer R (2004) Plant cell cultures for the production of recombinant proteins. Nat Biotechnol 22 (11):1415-1422.

Hirasuna TJ, Shuler ML, Lackney VK, Spanswick RM (1991) Enhanced anthocyanin production in grape cell cultures. Plant Science 78 (1):107-120.

Hoekstra SS, Harkes PAA, Verpoorte R, Libbenga KR (1990) Effect of auxin on cytodifferentiation and production of quinoline alkaloids in compact globular structures of Cinchona-Ledgeriana. Plant Cell Rep 8 (10):571-574.

Horwitz SB (2004) Personal recollections on the early development of taxol. J Nat Prod 67 (2):136-138.

Hsu JP, Hsu WC, Tsao HK (1993) Diffusion-enhanced bioreactions - a hypothetical mechanism for plant-cell aggregation. bulletin of mathematical biology 55 (5):869-889.

Hu FX, Huang JH, Xu YF, Gian XH, Zhong JJ (2006) Responses of defense signals, biosynthetic gene transcription and taxoid biosynthesis to elicitation by a novel synthetic jasmonate in cell cultures of *Taxus* chinensis. Biotechnol Bioeng 94 (6):1064-1071.

Huang SY, Chou CJ (2000) Effect of gaseous composition on cell growth and secondary metabolite production in suspension culture of Stizolobium hassjoo cells. Bioprocess and Biosystems Engineering 23 (6):585-593.

Hudgins JW, Franceschi VR (2004) Methyl Jasmonate-Induced Ethylene Production Is Responsible for Conifer Phloem Defense Responses and Reprogramming of Stem Cambial Zone for Traumatic Resin Duct Formation. Plant Physiology 135 (4):2134-2149.

Hulst AC, Meyer MMT, Breteler H, Tramper J (1989) Effect of aggregate size in cell cultures of Tagetes patula on thiophene production and cell growth. Appl Microbiol Biotechnol 30 (1989) 18-25.

Inze D, De Veylder L (2006) Cell cycle regulation in plant development. Annual Review of Genetics 40:77-105.

Ishikawa M, Suzuki M, Nakamura T, Kishimoto T, Robertson AJ, Gusta LV (2006) Effect of growth phase on survival of bromegrass suspension cells following cryopreservation and abiotic stresses. Annals of Botany 97 (3):453-459.

Zhang J (2003) Overexpression analysis of plant transcription factors. Current Opinion in Plant Biology 6 (5):430-440.

Jennewein S, Wildung MR, Chau M, Walker K, Croteau R (2004) Random sequencing of an induced *Taxus* cell cDNA library for identification of clones involved in Taxol biosynthesis. Proc Natl Acad Sci U S A 101 (24):9149-9154.

Kai G, Zhao L, Zhang L, Li Z, Guo B, Zhao D, Sun X, Miao Z, Tang K (2005) Characterization and expression profile analysis of a new cDNA encoding taxadiene synthase from *Taxus* media. J Biochem Mol Biol 38 (6):668-675.

Kal AJ, van Zonneveld AJ, Benes V, van den Berg M, Koerkamp MG, Albermann K, Strack N, Ruijter JM, Richter A, Dujon B, Ansorge W, Tabak HF (1999) Dynamics of gene expression revealed by comparison of serial analysis of gene expression transcript profiles from yeast grown on two different carbon sources. Mol Biol Cell 10 (6):1859-1872.

Kamath KR, Barry JJ, Miller KM (2006) The *Taxus* (TM) drug-eluting stent: A new paradigm in controlled drug delivery. Advanced Drug Delivery Reviews 58 (3):412-436.

Kathryn Geldart (2012) Controlling Aggregate Size in *Taxus* Cell Suspension Cultures Senior Thesis, Department of Chemical Engineering.

Kato A, Kawazoe S, Soh Y (1978) Biomass production of tobacco cells .4. Viscosity of broth of tobacco cells in suspension culture. Journal of Fermentation Technology 56 (3):224-228.

Kawamura K, Murray JAH, Shinmyo A, Sekine M (2006) Cell cycle regulated D3-type cyclins form active complexes with plant-specific B-type cyclin-dependent kinase in vitro. Plant Molecular Biology 61 (1-2):311-327.

Kessler M, ten Hoopen HJG, Furusaki S (1999) The effect of the aggregate size on the production of ajmalicine and tryptamine in Catharanthus roseus suspension culture. Enzyme Microb Technol 24 (5-6):308-315.

Ketchum REB, Gibson DM (1996) Paclitaxel production in suspension cell cultures of *Taxus*. Plant Cell Tissue and Organ Culture 46 (1):9-16.

Ketchum REB, Gibson DM, Croteau RB, Shuler ML (1999) The kinetics of taxoid accumulation in cell suspension cultures of *Taxus* following elicitation with methyl jasmonate. Biotechnol Bioeng 62 (1):97-105.

Ketchum REB, Tandon M, Begley TP, Gibson DM, Croteau R, Shuler ML (1997) The production of paclitaxel and other taxanes in *Taxus* canadensis suspension cell cultures elicited with methyl jasmonate. Plant Physiology 114 (3):1182-1182.

Ketchum REB, Wherland L, Croteau RB (2007) Stable transformation and long-term maintenance of transgenic *Taxus* cell suspension cultures. Plant Cell Rep 26 (7):1025-1033.

Kieran PM, MacLoughlin PF, Malone DM (1997) Plant cell suspension cultures: some engineering considerations. J Biotechnol 59 (1-2):39-52.

Kim BJ, Gibson DM, Shuler ML (2004) Effect of subculture and elicitation on instability of Taxol production in *Taxus* sp suspension cultures. Biotechnology Progress 20 (6):1666-1673.

Kim BJ, Gibson DM, Shuler ML (2005) Relationship of viability and apoptosis to taxol production in *Taxus* sp suspension cultures elicited with methyl jasmonate. Biotechnol Progr 21 (3):700-707.

King PJ, Mansfiel.Kj, Street HE (1973) Control of growth and cell-division in plant cell suspension cultures. Canadian Journal of Botany-Revue Canadienne De Botanique 51 (10):1807-1823.

Kinnersley AM, Dougall DK (1980) Increase in anthocyanin yield from wild carrot cell cultures by a selection system based on cell aggregate size. Planta 149 (2):200-204.

Kobayashi Y, Fukui H, Tabata M (1989) Effect of oxygen-supply on berberine production in cell-suspension cultures and immobilized cells of thalictrum-minus. Plant Cell Rep 8 (4):255-258.

Kolewe ME (2011) Development of plant cell culture processes to produce natural product pharmaceuticals: Characterization, analysis, and modeling of plant cell aggregation. Electronic Doctoral Dissertations for UMass Amherst. Paper AAI3482636,

Kolewe ME, Gaurav V, Roberts SC (2008) Pharmaceutically active natural product synthesis and supply via plant cell culture technology. Mol Pharm 5 (2):243-256.

Kolewe ME, Henson MA, Roberts SC (2010) Characterization of aggregate size in *Taxus* suspension cell culture. Plant Cell Rep 29 (5):485-494.

Kolewe ME, Henson MA, Roberts SC (2011) Analysis of aggregate size as a process variable affecting paclitaxel accumulation in *Taxus* suspension cultures. Biotechnol Progr 27 (5):1365-1372.

Kolewe ME, Roberts SC, Henson MA (2012) A population balance equation model of aggregation dynamics in *Taxus* suspension cell cultures. Biotechnol Bioeng 109 (2):472-482.

Kotogany E, Dudits D, Horvath GV, Ayaydin F (2010) A rapid and robust assay for detection of S-phase cell cycle progression in plant cells and tissues by using ethynyl deoxyuridine. Plant Methods 6.

Kuboi T, Yamada Y (1978) Changing cell aggregations and lignification in tobacco suspension cultures. Plant and Cell Physiology 19 (3):437-443.

Kumagai-Sano F, Hayashi T, Sano T, Hasezawa S (2006) Cell cycle synchronization of tobacco BY-2 cells. Nature Protocols 1 (6):2621-2627.

Kumar J, Gupta PK (2008) Molecular approaches for improvement of medicinal and aromatic plants. Plant Biotechnology Reports 2 (2):93-112.

Lange BM, Lapierre C, Sandermann H (1995) Elicitor-Induced Spruce Stress Lignin - Structural Similarity to Early Developmental Lignins. Plant Physiology 108 (3):1277-1287.

Laskaris G, Bounkhay M, Theodoridis G, van der Heijden R, Verpoorte R, Jaziri M (1999) Induction of geranylgeranyl diphosphate synthase activity and taxane accumulation in *Taxus* baccata cell cultures after elicitation by methyl jasmonate. Plant Science 147 (1):1-8.

Lee EK, Jin YW, Park JH, Yoo YM, Hong SM, Amir R, Yan Z, Kwon E, Elfick A, Tomlinson S, Halbritter F, Waibel T, Yun BW, Loake GJ (2010) Cultured cambial meristematic cells as a source of plant natural products. Nat biotech 28 (11):1213-1217.

Lenka SK, Boutaoui N, Paulose B, Vongpaseuth K, Normanly J, Roberts SC, Walker EL (2012) Identification and expression analysis of methyl jasmonate responsive ESTs in paclitaxel producing *Taxus* cuspidata suspension culture cells. BMC Genomics 13 (1):148.

Leple JC, Dauwe R, Morreel K, Storme V, Lapierre C, Pollet B, Naumann A, Kang KY, Kim H, Ruel K, Lefebvre A, Joseleau JP, Grima-Pettenati J, De Rycke R, Andersson-Gunneras S, Erban A, Fehrle I, Petit-Conil M, Kopka J, Polle A, Messens E, Sundberg B, Mansfield SD, Ralph J, Pilate G, Boerjan W (2007) Downregulation of cinnamoyl-coenzyme a reductase in poplar: Multiple-level phenotyping reveals effects on cell wall polymer metabolism and structure. Plant Cell 19 (11):3669-3691.

Li J, Ou D, Zheng L, Gan N, Song L (2011) Applicability of the fluorescein diacetate assay for metabolic activity measurement of Microcystis aeruginosa (Chroococcales, Cyanobacteria). Phycological Research 59 (3):200-207.

Li JWH, Vederas JC (2009) Drug Discovery and Natural Products: End of an Era or an Endless Frontier? Science 325 (5937):161-165.

Li SY, Yuan W, Yang PY, Antoun MD, Balick MJ, Cragg GM (2010) Pharmaceutical Crops: an overview. Pharmaceutical Crops 1:1-17.

Libourel IG, Shachar-Hill Y (2008) Metabolic flux analysis in plants: from intelligent design to rational engineering. Annu Rev Plant Biol 59:625-650.

Lijavetzky D, Almagro L, Belchi-Navarro S, Martinez-Zapater J, Bru R, Pedreno M (2008) Synergistic effect of methyljasmonate and cyclodextrin on stilbene biosynthesis pathway gene expression and resveratrol production in Monastrell grapevine cell cultures. BMC Research Notes 1 (1):132.

Linden JC, Haigh JR, Mirjalili N, Phisaphalong M (2001) Gas concentration effects on secondary metabolite production by plant cell cultures. Adv Biochem Eng Biotechnol 72:27-62.

Lindsey K, Yeoman MM (1983) The relationship between growth-rate, differentiation and alkaloid accumulation in cell-cultures. J Exp Bot 34 (145):1055-1065.

Logemann E, Wu SC, Schroder J, Schmelzer E, Somssich IE, Hahlbrock K (1995) Gene activation by UV light, fungal elicitor or fungal infection in Petroselinum crispum is correlated with repression of cell cycle-related genes. Plant Journal 8 (6):865-876.

Madhusudhan R, Ravishankar GA (1996) Gradient of anthocyanin in cell aggregates of Daucus carota in suspension cultures. Biotechnol Lett 18 (11):1253-1256.

Mak YX, Doran PM (1993) Effect of cell-cycle inhibition on synthesis of steroidal alkaloids by solanum aviculare plant cells. Biotechnol Lett 15 (10):1031-1034.

Martin VJJ, Pitera DJ, Withers ST, Newman JD, Keasling JD (2003) Engineering a mevalonate pathway in Escherichia coli for production of terpenoids. Nat Biotechnol 21 (7):796-802.

Matkowski A (2008) Plant in vitro culture for the production of antioxidants--a review. Biotechnol Adv 26 (6):548-560.

Matsuki T, Tazaki H, Fujimori T, Hogetsu T (1992) The Influences of Jasmonic Acid Methyl-Ester on Microtubules in Potato Cells and Formation of Potato-Tubers. Bioscience Biotechnology and Biochemistry 56 (8):1329-1330.

Mavituna F, Park JM (1987) Size distribution of plant-cell aggregates in batch culture. The Chemical Engineering Journal 35 (1):B9-B14.

McChesney JD, Venkataraman SK, Henri JT (2007) Plant natural products: Back to the future or into extinction? Phytochemistry 68 (14):2015-2022.

McCoy E, O'Connor SE (2008) Natural products from plant cell cultures. Prog Drug Res 65:329, 331-370.

Meijer M, Murray JAH (2000) The role and regulation of D-type cyclins in the plant cell cycle. Plant Molecular Biology 43 (5-6):621-633.

Menges M, Hennig L, Gruissem W, Murray JAH (2002) Cell cycle-regulated gene expression in arabidopsis. Journal of Biological Chemistry 277 (44):41987-42002.

Mirjalili N, Linden JC (1996) Methyl jasmonate induced production of taxol in suspension cultures of *Taxus* cuspidata: Ethylene interaction and induction models. Biotechnology Progress 12 (1):110-118.

Mishiba KI, Okamoto T, Mii M (2001) Increasing ploidy level in cell suspension cultures of Doritaenopsis by exogenous application of 2,4-dichlorophenoxyacetic acid. Physiologia Plantarum 112 (1):142-148.

Mishra BN, Ranjan R (2008) Growth of hairy-root cultures in various bioreactors for the production of secondary metabolites. Biotechnology and Applied Biochemistry 49:1-10.

Morozova O, Hirst M, Marra MA (2009) Applications of new sequencing technologies for transcriptome analysis. Annual Review of Genomics and Human Genetics 10 (1):135-151.

Morris P (1986) Long term stability of alkaloid productivity in cell suspension cultures of Catharanthus roseus. In: Morris P, Scragg AH, Stafford A, Fowler MW (eds) Secondary metabolism in plant cell cultures. University Press, Cambridge, pp 257-262.

Morris P, Rudge K, Cresswell R, Fowler MW (1989) Regulation of product synthesis in cell cultures of Catharanthus roseus .5. Long term maintenance of cells on a production medium. Plant Cell Tissue and Organ Culture 17 (2):79-90.

Mortazavi A, Williams BA, McCue K, Schaeffer L, Wold B (2008) Mapping and quantifying mammalian transcriptomes by RNA-Seq. Nat Methods 5 (7):621-628.

Muir WH, Hildebrandt AC, Riker AJ (1954) Plant tissue cultures produced from single isolated cells. Science 119 (3103):877-878.

Mustafa NR, de Winter W, van Iren F, Verpoorte R (2011) Initiation, growth and cryopreservation of plant cell suspension cultures. Nat Protocols 6 (6):715-742.

Naill MC, Roberts SC (2004) Preparation of single cells from aggregated *Taxus* suspension cultures for population analysis. Biotechnol Bioeng 86 (7):817-826.

Naill MC, Roberts SC (2005a) Cell cycle analysis of *Taxus* suspension cultures at the single cell level as an indicator of culture heterogeneity. Biotechnol Bioeng 90 (4):491-500.

Naill MC, Roberts SC (2005b) Culture of isolated single cells from *Taxus* suspensions for the propagation of superior cell populations. Biotechnol Lett 27 (21):1725-1730.

Naill MC, Roberts SC (2005c) Flow cytometric analysis of protein content in *Taxus* protoplasts and single cells as compared to aggregated suspension cultures. Plant Cell Rep 23 (8):528-533.

Neumann K-H, Kumar A, Imani J (2009) cell division, cell growth, cell differentiation. plant cell and tissue culture - a tool in biotechnology. In. Principles and practice. Springer Berlin Heidelberg, pp 235-247. doi:10.1007/978-3-540-93883-5_12

Nims E, Dubois CP, Roberts SC, Walker EL (2006) Expression profiling of genes involved in paclitaxel biosynthesis for targeted metabolic engineering. Metab Eng 8 (5):385-394.

Ogino T, Hiraoka N, Tabata M (1978) Selection of high nicotine-producing cell lines of tobacco callus by single-cell cloning. Phytochem 17(11):1907-1910

Ono NN, Tian L (2011) The multiplicity of hairy Root cultures: Prolific possibilities. Plant Science 180 (3):439-446.

Parchman T, Geist K, Grahnen J, Benkman C, Buerkle CA (2010) Transcriptome sequencing in an ecologically important tree species: assembly, annotation, and marker discovery. BMC Genomics 11 (1):180.

Patil RA, Kolewe ME, Normanly J, Walker EL, Roberts SC (2012) Contribution of taxane biosynthetic pathway gene expression to observed variability in paclitaxel accumulation in *Taxus* suspension cultures. Biotechnology Journal 7 (3):418-427.

Pauwels L, Inzé D, Goossens A (2009) Jasmonate-inducible gene: what does it mean? Trends in Plant Science 14 (2):87-91.

Pauwels L, Morreel K, Witte ED, Lammertyn F, Montagu MV, Boerjan W, Inzé D, Goossens A (2008) Mapping methyl jasmonate-mediated transcriptional reprogramming of metabolism and cell cycle progression in cultured Arabidopsis cells. Proc Natl Acad Sci U S A 105 (4):1380-1385.

Pechhold K, Koczwara K, Zhu X, Harrison VS, Walker G, Lee J, Harlan DM (2009) Blood glucose levels regulate pancreatic β-cell proliferation during experimentally-induced and spontaneous autoimmune diabetes in mice. PLoS ONE 4 (3):e4827.

Pepin MF, Smith MAL, Reid JF (1999) Application of imaging tools to plant cell culture: Relationship between plant cell aggregation and flavonoid production. In Vitro Cellular & Developmental Biology-Plant 35 (4):290-295.

Pfaffl MW, Horgan GW, Dempfle L (2002) Relative expression software tool (REST (C)) for group-wise comparison and statistical analysis of relative expression results in real-time PCR. Nucleic Acids Research 30 (9).

Phillips RL, Kaeppler SM, P. O (1994) Genetic instability of plant tissue cultures: breakdown of normal controls. Proc Nati Acad Sci 91:5222-5226

Pierre B (2004) Transcription factors as tools for metabolic engineering in plants. Current Opinion in Plant Biology 7 (2):202-209.

Piontkivska H, Rooney AP, Nei M (2002) Purifying selection and birth-and-death evolution in the histone H4 gene family. Mol Biol Evol 19 (5):689-697.

Qiao JJ, Yuan YJ, Zhao H, Wu JC, Zeng AP (2003) Apoptotic cell death in suspension cultures of *Taxus* cuspidata co-treated with salicylic acid and hydrogen peroxide. Biotechnol Lett 25 (5):387-390.

Qu JG, Zhang W, Hu QL, Jin MF (2006) Impact of subculture cycles and inoculum sizes on suspension cultures of Vitis vinifera. Chinese Journal of Biotechnology 22 (6):984-989.

Qu JG, Zhang W, Yu XJ, Jin MF (2005) Instability of anthocyanin accumulation in Vitis vinifera L. var. Gamay Freaux suspension cultures. Biotechnology and Bioprocess Engineering 10 (2):155-161.

Ramakers C, Ruijter JM, Deprez RHL, Moorman AFM (2003) Assumption-free analysis of quantitative real-time polymerase chain reaction (PCR) data. Neuroscience Letters 339 (1):62-66.

Ranch JP, Giles KL (1980) Factors affecting growth and aggregate dissociation in batch suspension-cultures of datura-innoxia (Miller). Annals of Botany 46 (6):667-683.

Rao SR, Ravishankar GA (2002) Plant cell cultures: Chemical factories of secondary metabolites. Biotechnology Advances 20 (2):101-153.

Reinhoud PJ, Schrijnemakers EWM, Iren F, Kijne JW (1995) Vitrification and a heat-shock treatment improve cryopreservation of tobacco cell suspensions compared to two-step freezing. Plant Cell Tissue Organ Cult 42 (3):261-267.

Reymond P, Farmer EE (1998) Jasmonate and salicylate as global signals for defense gene expression. Current Opinion in Plant Biology 1 (5):404-411.

Rischer H, Orešič M, Seppänen-Laakso T, Katajamaa M, Lammertyn F, Ardiles-Diaz W, Van Montagu MCE, Inzé D, Oksman-Caldentey K-M, Goossens A (2006) Gene-to-metabolite networks for terpenoid indole alkaloid biosynthesis in Catharanthus roseus cells. Proceedings of the National Academy of Sciences 103 (14):5614-5619.

Ro DK, Paradise EM, Ouellet M, Fisher KJ, Newman KL, Ndungu JM, Ho KA, Eachus RA, Ham TS, Kirby J, Chang MCY, Withers ST, Shiba Y, Sarpong R, Keasling JD (2006) Production of the antimalarial drug precursor artemisinic acid in engineered yeast. Nature 440 (7086):940-943.

Roberts MF, Wink M (1998) Alkaloids : biochemistry, ecology, and medicinal applications. Language of science. Plenum Press, New York.

Roberts SC, Naill M, Gibson DM, Shuler ML. 2003. A simple method for enhancing paclitaxel release from Taxus canadensis cell suspension cultures utilizing cell wall digesting enzymes. Plant Cell Reports 21:1217-1220.

Roberts SC (2007) Production and engineering of terpenoids in plant cell culture. Nat Chem Biol 3 (7):387-395.

Rosato MT, Jabbour AJ, Ponce RA, Kavanagh TJ, Takaro TK, Hill JP, Poot M, Rabinovitch PS, Faustman EM (2001) Simultaneous analysis of surface marker expression and cell cycle progression in human peripheral blood mononuclear cells. Journal of Immunological Methods 256 (1-2):35-46.

Ruiz-May E, De-la-Peña C, Galaz-Ávalos RM, Lei Z, Watson BS, Sumner LW, Loyola-Vargas VM (2011) methyl jasmonate induces atp biosynthesis deficiency and accumulation of proteins related to secondary metabolism in catharanthus roseus (l.) g. hairy roots. Plant and Cell Physiology 52 (8):1401-1421.

Ryerson DE, Heath MC (1996) Cleavage of nuclear DNA into oligonucleosomal fragments during cell death induced by fungal infection or by abiotic treatments. Plant Cell 8 (3):393-402.

Saito K, Mizukami H (2002) Plant cell cultures as producers of secondary compounds. In: Oksman-Caldentey, Kirsi-Marja, Barz W (eds) Plant Biotechnology and Transgenic Plants. Marcel Dekker, New York,

Sato F, Yamada Y (1984) High berberine-producing cultures of coptis japonica cells. Phytochemistry 23 (2):281-285.

Schlatmann JE, Vinke JL, Tenhoopen HJG, Heijnen JJ (1995) Relation between dissolved-oxygen concentration and ajmalicine production-rate in high-density cultures of catharanthus-roseus. Biotechnol Bioeng 45 (5):435-439.

Schoendorf A, Rithner CD, Williams RM, Croteau RB (2001) Molecular cloning of a cytochrome P450 taxane 10 beta-hydroxylase cDNA from *Taxus* and functional expression in yeast. Proc Natl Acad Sci U S A 98 (4):1501-1506.

Scragg AH, Bond P, Leckie F, Cresswell R, Fowler MW, Allan E.J. (eds) (1987) Growth and product formation by plant cell suspensions cultivated in bioreactors. Bioreactors and Biotransformations. Elsevier Applied Science Publications, New York.

Seo HS, Song JT, Cheong JJ, Lee YH, Lee YW, Hwang I, Lee JS, Choi YD (2001) Jasmonic acid carboxyl methyltransferase: A key enzyme for jasmonate-regulated plant responses. Proc Natl Acad Sci U S A 98 (8):4788-4793.

Shuler ML (1999) Overview of yield improvement strategies for secondary metabolite production in plant cell culture. In: Fu TJ, Sing G, Curtis WR (eds) Proceedings of the Symposium on Plant Cell and Tissue Culture for the Production of Food Ingredients. Kluwer Academic/Plenum Publishing, New York. 75-83.

Siegler D (1998) Plant Secondary Metabolism. Kluwer Academic Publisher, Boston.

Skehan P. (2002) Cell growth and cytotoxicity assays. In: Studzinski GP (ed) Cell Growth, differentiation and senescence. A practical approach. Oxford University Press, New York.

Smetanska I (2008) Production of secondary metabolites using plant cell cultures. Food Biotechnol 187-228.

Srinivasan V, Pestchanker L, Moser S, Hirasuna TJ, Taticek RA, Shuler ML (1995) Taxol production in bioreactors: Kinetics of biomass accumulation, nutrient uptake, and taxol production by cell suspensions of *Taxus* baccata. Biotechnol Bioeng 47 (6):666-676.

Srivastava S, Srivastava AK (2007) Hairy root culture for mass-production of high-value secondary metabolites. Critical Reviews in Biotechnology 27 (1):29-43.

Stevens R, Grelon M, Vezon D, Oh JS, Meyer P, Perennes C, Domenichini S, Bergounioux C (2004) A CDC45 homolog in Arabidopsis is essential for meiosis, as shown by RNA interference-induced gene silencing. Plant Cell 16 (1):99-113.

Suzuki H, Reddy MSS, Naoumkina M, Aziz N, May GD, Huhman DV, Sumner LW, Blount JW, Mendes P, Dixon RA (2005) Methyl jasmonate and yeast elicitor induce differential transcriptional and metabolic re-programming in cell suspension cultures of the model legume Medicago truncatula. Planta 220 (5):696-707.

Swiatek A, Lenjou M, Van Bockstaele D, Inze D, Van Onckelen H (2002) Differential Effect of Jasmonic Acid and Abscisic Acid on Cell Cycle Progression in Tobacco BY-2 Cells. Plant Physiology 128 (1):201-211.

Swiatek A, Van Dongen W, Esmans EL, Van Onckelen H (2004) Metabolic fate of jasmonates in tobacco bright yellow-2 cells. Plant Physiology 135 (1):161-172.

Syklowska-Baranek K, Pietrosiuk A, Kokoszka A, Furmanowa M (2009) Enhancement of taxane production in hairy root culture of *Taxus* x media var. Hicksii. Journal of Plant Physiology 166 (17):1950-1954.

Tabata H (2004) Paclitaxel production by plant-cell-culture technology. In: Biomanufacturing, vol 87. Advances in Biochemical Engineering/Biotechnology. Springer Berlin / Heidelberg, pp 1-23.

Takahashi K, Fujino K, Kikuta Y, Koda Y (1994) Expansion of potato cells in response to jasmonic acid. Plant Science 100 (1):3-8.

Takahashi K, Fujino K, Kikuta Y, Koda Y (1995) Involvement of the accumulation of sucrose and the synthesis of cell wall polysaccharides in the expansion of potato cells in response to jasmonic acid. Plant Science 111 (1):11-18.

Takahashi N, Lammens T, Boudolf V, Maes S, Yoshizumi T, De Jaeger G, Witters E, Inze D, De Veylder L (2008) The DNA replication checkpoint aids survival of plants deficient in the novel replisome factor ETG1. EMBO J 27 (13):1840-1851.

Takebe I, Otsuki Y, Aoki S (1968) Isolation of tobacco mesophyll cells in an intact and active state. Plant Cell Physiol. 9:115-124

Taticek RA, Mooyoung M, Legge RL (1990) Effect of bioreactor configuration on substrate uptake by cell-suspension cultures of the plant eschscholtzia-californica. Applied Microbiology and Biotechnology 33 (3):280-286.

Thanh NT, Murthy HN, Yu KW, Hahn EJ, Paek KY (2005) Methyl jasmonate elicitation enhanced synthesis of ginsenoside by cell suspension cultures of Panax ginseng in 5-l balloon type bubble bioreactors. Appl Microbiol Biotechnol 67 (2):197-201.

Ushiyama K (1991) Large-scale culture of ginseng. In: Komamine A, Misawa M, DiCosmo F (eds) Plant Cell Culture in Japan: Progress in production of useful plant metabolites by japanese enterprises using plant cell culture technology. CMC, pp 92-98

van der Fits L, Memelink J (2000) ORCA3, a Jasmonate-responsive transcriptional regulator of plant primary and secondary metabolism. Science 289 (5477):295-297.

Vandepoele K, Vlieghe K, Florquin K, Hennig L, Beemster GTS, Gruissem W, Van De Peer Y, Inze D, De Veylder L (2005) Genome-wide identification of potential plant E2F target genes. Plant Physiology 139 (1):316-328.

Verma D, Van Huystee R (1970) Relationship between peroxidase, catalase and protein synthesis during cellular development in cell cultures of peanut. Can J Biochem 48:444-449.

Verpoorte R, van der Heijden R, ten Hoopen HJG, Memelink J (1999) Metabolic engineering of plant secondary metabolite pathways for the production of fine chemicals. Biotechnol Lett 21(6):467-479

Verpoorte R, Memelink J (2002) Engineering secondary metabolite production in plants. Curr Opin Biotechnol 13 (2):181-187.

Vongpaseuth K (2011) Novel systems for the functional characterization of genes related to paclitaxel metabolism in *Taxus* cell cultures. Electronic Doctoral Dissertations for UMass Amherst. Paper AAI3465233. ,

Vongpaseuth K, Roberts SC (2007) Advancements in the understanding of Paclitaxel metabolism in tissue culture. Curr Pharm Biotechnol 8 (4):219-236.

Wallner SJ, Nevins DJ (1973) Formation and Dissociation of Cell Aggregates in Suspension Cultures of Pauls Scarlet Rose. American Journal of Botany 60 (3):255-261.

Wani MC, Taylor HL, Wall ME, Coggon P, Mcphail AT (1971) Plant antitumor agents .6. isolation and structure of taxol, a novel antileukemic and antitumor agent from *Taxus*-brevifolia. Journal of the American Chemical Society 93 (9):2325-&.

Wasternack C (2007) Jasmonates: An update on biosynthesis, signal transduction and action in plant stress response, growth and development. Annals of Botany 100 (4):681-697.

Watts MJ, Galpin IJ, Collin HA (1984) The effect of growth regulators, light and temperature on flavor production in celery tissue cultures. New Phytologist 98 (4):583-591.

Weber APM, Weber KL, Carr K, Wilkerson C, Ohlrogge JB (2007) Sampling the arabidopsis transcriptome with massively parallel pyrosequencing. Plant Physiology 144 (1):32-42.

Wheeler AL, Long RM, Ketchum REB, Rithner CD, Williams RM, Croteau R (2001) Taxol biosynthesis: differential transformations of taxadien-5[small alpha]-ol and its acetate ester by cytochrome P450 hydroxylases from *Taxus* suspension cells. Arch Biochem Biophys 390 (2):265-278.

Wickremesinhe ERM, Arteca RN (1994) *Taxus* cell-suspension cultures - optimizing growth and production of taxol. Journal of Plant Physiology 144 (2):183-188.

Widholm JM (1972) Use of fluorescein diacetate and phenosafranine for determining viability of cultured plant cells. Stain Technology 47 (4):189-194.

Wilson SA, Roberts SC (2011) Recent advances towards development and commercialization of plant cell culture processes for the synthesis of biomolecules. Plant Biotechnol J.

Wink M, Alfermann AW, Franke R, Wetterauer B, Distl M, Windhövel J, Krohn O, Fuss E, Garden H, Mohagheghzadeh A, Wildi E, Ripplinger P (2005) Sustainable bioproduction of phytochemicals by plant in vitro cultures: anticancer agents. Plant Genetic Resources 3 (02):90-100.

Wu J, Lin L (2003) Enhancement of taxol production and release in *Taxus* chinensis cell cultures by ultrasound, methyl jasmonate and in situ solvent extraction. Applied Microbiology and Biotechnology 62 (2-3):151-155.

Wu Q, Sun C, Luo HM, Li Y, Niu YY, Sun YZ, Lu AP, Chen SL (2011) Transcriptome analysis of *Taxus* cuspidata needles based on 454 pyrosequencing. Planta Medica 77 (4):394-400.

Wu SQ, Schalk M, Clark A, Miles RB, Coates R, Chappell J (2006) Redirection of cytosolic or plastidic isoprenoid precursors elevates terpene production in plants. Nat Biotechnol 24 (11):1441-1447.

Xu JF, Xie J, Han AM, Feng PS, Su ZG (1998) Kinetic and technical studies on large-scale culture of Rhodiola sachalinensis compact callus aggregates with air-lift reactors. Journal of Chemical Technology and Biotechnology 72 (3):227-234.

Yamada Y, Hashimoto T (1990) Possibilities for improving yield of secondary metabolites in plant cell cultures. In: Nijkamp HJ, Van der Plas L, Van Aartrijk J (eds) Current Plant Science and Biotechnology in Agriculture. Progress in Plant Cellular and Molecular Biology. Kluwer, The Netherlands, pp 547-556

Yang S, Lu SH, Yuan YJ (2008) Lipidomic analysis reveals differential defense responses of *Taxus* cuspidata cells to two elicitors, methyl jasmonate and cerium (Ce4+). Biochimica Et Biophysica Acta-Molecular and Cell Biology of Lipids 1781 (3):123-134.

Yang YM, He DG, Scott KJJ (1994) Cell aggregates in wheat suspension cultures and their effects on isolation and culture of protoplasts. Plant Cell Rep 13 (3):176-179.

Yanpaisan W, King NJC, Doran PM (1998) Analysis of cell cycle activity and population dynamics in heterogeneous plant cell suspensions using flow cytometry. Biotechnol Bioeng 58 (5):515-528.

Yanpaisan W, King NJC, Doran PM (1999) Flow cytometry of plant cells with applications in large-scale bioprocessing. Biotechnology Advances 17 (1):3-27.

Yazaki K, Takeda K, Tabata M (1997) Effects of methyl jasmonate on shikonin and dihydroechinofuran production in Lithospermum cell cultures. Plant and Cell Physiology 38 (7):776-782.

Yeoman MM, Yeoman CL (1996) Manipulating secondary metabolism in cultured plant cells. New Phytologist 134 (4):553-569.

Yesilirmak F, Sayers Z (2009) Heterelogous expression of plant genes. Int J Plant Genomics 2009:296482.

Yi H, Sardesai N, Fujinuma T, Chan CW, Veena, Gelvin SB (2006) Constitutive expression exposes functional redundancy between the Arabidopsis histone H2A gene HTA1 and other H2A gene family members. Plant Cell 18 (7):1575-1589.

Yuan Y-J, Li C, Hu Z-D, Wu J-C, Zeng A-P (2002) Fungal elicitor-induced cell apoptosis in suspension cultures of *Taxus* chinensis var. mairei for taxol production. Process Biochemistry 38 (2):193-198.

Yukimune Y, Tabata H, Higashi Y, Hara Y (1996) Methyl jasmonate-induced overproduction of paclitaxel and baccatin III in *Taxus* cell suspension cultures. Nat Biotechnol 14 (9):1129-1132.

Zeliang PK, Pattanayak A, Iangrai B, Khongwir EA, Sarma BK (2010) Fertile plant regeneration from cryopreserved calli of Oryza rufipogon Griff. and assessment of variation in the progeny of regenerated plants. Plant Cell Rep 29 (12):1423-1433.

Zenk MH, El-Shagi H, Ulbrich B (1977) Production of rosmarinic acid by cell-suspension cultures of Coleus blumei. Naturwissenschaften 64 (11):585-586.

Zerbino D, Birney E (2008) Velvet: Algorithms for de novo short read assembly using de bruijn graphs. Genome Research.

Zhang CH, Xu HB (2001) Improved paclitaxel production by in situ extraction and elicitation in cell suspension cultures of *Taxus* chinensis. Biotechnology Letters 23 (3):189-193.

Zhang W, Curtin C, Franco C (2002) Towards manipulation of post-biosynthetic events in secondary metabolism of plant cell cultures. Enzyme Microb Technol 30 (6):688-696.

Zhang Y, Turner JG (2008) Wound-induced endogenous jasmonates stunt plant growth by inhibiting mitosis. PLoS ONE 3 (11):e3699.

Zhao D, Huang Y, Jin Z, Qu W, Lu D (2003) Effect of aggregate size in cell cultures of Saussurea medusa on cell growth and jaceosidin production. Plant Cell Rep 21 (11):1129-1133.

Zhao J, Verpoorte R (2007) Manipulating indole alkaloid production by Catharanthus roseus cell cultures in bioreactors: from biochemical processing to metabolic engineering. Phytochemistry Reviews 6 (2):435-457.

Zhao J, Zhu WH, Hu Q, Guo YQ (2001) Compact callus cluster suspension cultures of Catharanthus roseus with enhanced indole alkaloid biosynthesis. In Vitro Cellular & Developmental Biology-Plant 37 (1):68-72.

Zhishen J, Mengcheng T, Jianming W (1999) The determination of flavonoid contents in mulberry and their scavenging effects on superoxide radicals. Food Chemistry 64 (4):555-559.

Zhong J, Yoshida M, Yoshida T (1995) Effects of biological factors on cell growth and anthocyanin formation by suspended cultures of Perilla frutescens cells. Chin J Biotechnol 11 (2):143-147.